universität wien

DISSERTATION

Titel der Dissertation

Analysis Of Molecular Mechanisms Responsible For The Assembly And Regulation Of Effector Complexes In RNA Silencing

angestrebter akademischer Grad

Doktor der Naturwissenschaften (Dr. rer.nat.)

Verfasser:	Philipp Johannes Franz Leuschner
Matrikel-Nummer:	9804196
Dissertationsgebiet (lt. Studienblatt):	Molekulare Biologie
Betreuer:	Dr. Javier Martinez

Wien, am 21. November 2007

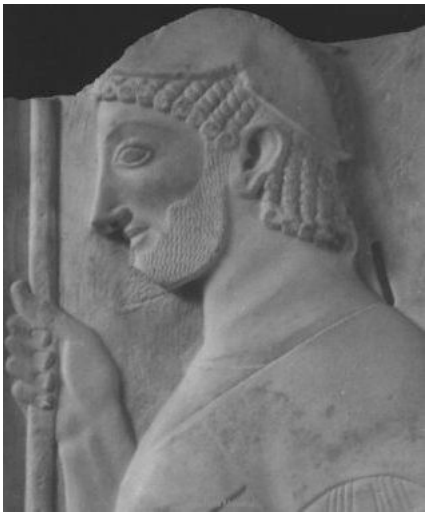

Κλῦτε, Πανελλήνων προφερέστατοι, εἰ ἐτεὸν δὴ
οἵδ' ὑμεῖς, οὓς δή κρυερῇ βασιλῆος ἐφετμῇ
Ἀργῴης ἐπὶ νηὸς ἄγει μετὰ κῶας Ἰήσων.

Apollonius of Rhodes, *The Argonautica 2, 209–211*

Listen, bravest of all the Hellenes, if it be truly ye, whom by a king's ruthless command Jason is leading on the ship Argo in quest of the fleece.

Table Of Contents

1. Summary

The core of all small RNA silencing phenomena resides in a ribonucleoprotein (RNP) complex that minimally consists of a short, single-stranded RNA molecule and an Argonaute protein. In the case of short interfering RNAs (siRNAs) and microRNAs (miRNAs), the functional effector complex is called RNA Induced Silencing Complex, or RISC for short. In this work, I have analyzed (a) how this complex is assembled and (b) how such assembly cascades that ultimately lead to a functional RNP can be regulated.

I could show that Argonaute becomes loaded with an siRNA, when it is still double-stranded. Furthermore, Argonaute has to cleave the passenger strand, which is bound to the guide strand, to efficiently release it and convert RISC into its active, functional configuration. This irreversible cleavage step enforces siRNA asymmetry. Thus, it may play an important role for the future design of potent siRNAs to mimimize off-target effects. If the passenger strand cannot be cleaved, it becomes removed intact by a bypass pathway, albeit at a greatly reduced speed. This is of relevance for miRNA duplexes displaying internal bulges or for Argonaute proteins lacking endonucleolytic cleavage activity, where in both cases passenger strand cleavage cannot occur.

I could also demonstrate that the miRNA production cascade is not a rigid program that is being executed by default whenever a miRNA gene is transcribed. In the case of miR-138, the processing of its precursor transcript is regulated by the action of an inhibitory protein. This factor recognizes the precursor RNA hairpin and blocks the final cleavage step in all tissues with the exception of specific neuronal cells and fetal liver cells. These findings have contributed to a better understanding of how miRNA expression can be regulated. Differential processing of a precursor miRNA may allow the uncoupling of miRNA function from the transcriptional status of its genomic locus. We envision that such regulation enables tight but also dynamic control of miRNA expression and could be a more general way of regulating miRNA function.

2. Zusammenfassung

Das Herzstück aller *RNA silencing* Phänomene, hervorgerufen durch kleine RNA-Stränge, ist ein Ribonukleoproteinkomplex (RNP), der in der Minimalvariante aus einem kurzen, einzelsträngigen RNA-Molekül und einem Argonaute Protein besteht. Im Falle von *short interfering* RNAs (siRNAs) und microRNAs (miRNAs) wird dieser funktionelle Effektorkomplex *RNA Induced Silencing Complex* (RNA-induzierter *Silencing* Komplex), kurz RISC, genannt. In dieser Arbeit habe ich analysiert, (a) wie dieser Komplex zusammengefügt wird und (b) wie derartige Assemblierungskaskaden, die letztendlich zu einem funktionellen RNP führen, reguliert werden können.

Ich konnte zeigen, dass Argonaute mit einer siRNA beladen wird, die noch doppelsträngig ist. Zudem muss Argonaute den *passenger*-Strang schneiden, der am *guide*-Strang gebunden ist, um ihn effizient freizugeben und um RISC in die aktive und funktionelle Konfiguration umzuwandeln. Dieser irreversible Vorgang verstärkt die Asymmetrie einer siRNA, weshalb dies eine wichtige Rolle bei der zukünftigen Konzeption von wirksamen siRNAs spielen könnte, um unspezifische Nebeneffekte zu vermeiden. Kann der *passenger*-Strang nicht geschnitten werden, wird er durch einen Umgehungsmechanismus intakt freigegeben, allerdings mit einer in hohem Maße reduzierten Geschwindigkeit. Diese Resultate haben Relevanz für miRNA-Duplexe, die interne Wölbungen aufweisen, und für Argonaute Proteine, die keine endonukleolytische Schneideaktivität aufweisen, wo in beiden Fällen der *passenger*-Strang nicht geschnitten werden kann.

Ich konnte auch zeigen, dass die miRNA-Prozessierungskaskade keine starres Standardprogramm ist, das ausgeführt wird, sobald ein miRNA-Gen transkribiert wird. Im Falle von miR-138 wird die Prozessierung des Vorläufertranskripts von einem Inhibitorprotein gesteuert. Dieser Faktor erkennt die Vorläufer-RNA-Haarnadelstruktur und blockiert die finale Prozessierung in allen Geweben mit der Ausnahme von spezifischen neuronalen Zellen und Zellen der fötalen Leber. Diese Resultate haben zu einem besseren Verständnis der miRNA-Genexpression geführt, wo differenzielles Prozessieren einer Vorläufer-miRNA die Funktion der miRNA von ihrem transkriptionellen Status am genomischen Lokus entkoppeln könnte. Wir glauben, dass eine derartige Regulation eine straffe, aber gleichzeitig dynamische Kontolle der miRNA-Genexpression erlaubt und dass dies eine etwas mehr verbreitetere Möglichkeit darstellen könnte, wie die Funktion von miRNAs reguliert wird.

3. Introduction to RNA silencing

3.1. History

In the year 1998, the concepts of regulation and control of gene expression were shaken by the seminal discovery of Andrew Fire, Craig Mello and colleagues, who conclusively demonstrated that injecting double-stranded ribonucleic acid (dsRNA) into *C. elegans* worms causes silencing of the cognate genes (Fire et al., 1998). All of a sudden, scientists were confronted with the alluring possibility to silence their favorite genes *in vivo* simply by introducing complementary dsRNA.

However, first hints of such silencing already surfaced in the late 1980s and early 1990s, where plant biologists observed that introducing extra copies of a gene responsible for the purple color of petunia flowers had the exact opposite effect as expected: instead of a much deeper color, the flower leaves became white or patchy, and it seemed as if both the transgenes and the endogenous gene were silenced (Napoli et al., 1990; van der Krol et al., 1990). A similar phenomenon was observed for plants infected with an RNA virus harboring fragments of an endogenous plant gene: its expression was silenced (Wassenegger et al., 1994).

The observations were there, but only after the publication of Fire, Mello and colleagues the pieces of this puzzle fell into place. RNA interference (RNAi), as this phenomenon was named, is hypothesized to have evolved in ancient times as a defense system against rogue genetic elements, such as transposons or retro-viruses, who replicate and proliferate in the cell via dsRNA-intermediates (Hannon, 2002; Hannon and Rossi, 2004; Novina and Sharp, 2004). Obviously, eukaryotic cells consider dsRNA as a potential threat to their genomes and employ the RNAi machinery in an effort to eliminate such mobile, parasitic nucleic acids. The scientist can easily exploit this system to specifically silence any gene of interest, simply by introducing exogenous dsRNA molecules bearing sequence complementarity to a particular protein-coding messenger RNA (mRNA), which in turn is treated like a parasitic element: it is recognized, cleaved and degraded. RNAi can thus be used as a straightforward, reverse genetic approach in order to link gene sequence to biological function.

Today, it is widely accepted that the discovery of RNAi has been the most important achievement in molecular biology since the invention of the polymerase chain

reaction (PCR). In 2006—only eight years after their groundbreaking publication—Andrew Fire and Craig Mello were awarded the Nobel Prize in Physiology or Medicine, underscoring the relevance of their work. RNAi is now known to operate in plants and metazoan species and is extensively used as a genetic inactivation tool (Elbashir et al., 2001a). Both biochemical and genetic analyses have contributed to our current mechanistic understanding of RNAi. Many key concepts, however, are still not fully understood.

3.2. The mechanism of RNAi

The trigger of RNAi is long dsRNA; it is recognized in the cell as foreign and a potential threat. Long dsRNA can emerge from various sources such as simultaneous sense and antisense transcription of specific genomic loci or viral replication intermediates (Peters and Meister, 2007). The actions the cell takes during the RNAi response can be divided into two distinct phases (Figure 1). In the initiation phase, the long dsRNA duplex is recognized and processed into short dsRNA molecules termed short interfering RNAs (siRNAs) (Bernstein et al., 2001; Hamilton and Baulcombe, 1999). In entering the effector phase, siRNAs are unwound and one strand assembles into the RNA-induced silencing complex (RISC), a ribonucleoprotein (RNP) complex, where the small RNA operates as a template for the recognition and cleavage of cognate RNA molecules (Hammond et al., 2001; Martinez et al., 2002a). Here, the single stranded siRNAs are tightly associated with members of the Argonaute (Ago) family of proteins. They are named after the *argonaute* (AGO) phenotype in *A. thaliana,* which itself was named after its resemblance to argonauts, a group of pelagic octopuses (Bohmert et al., 1998).

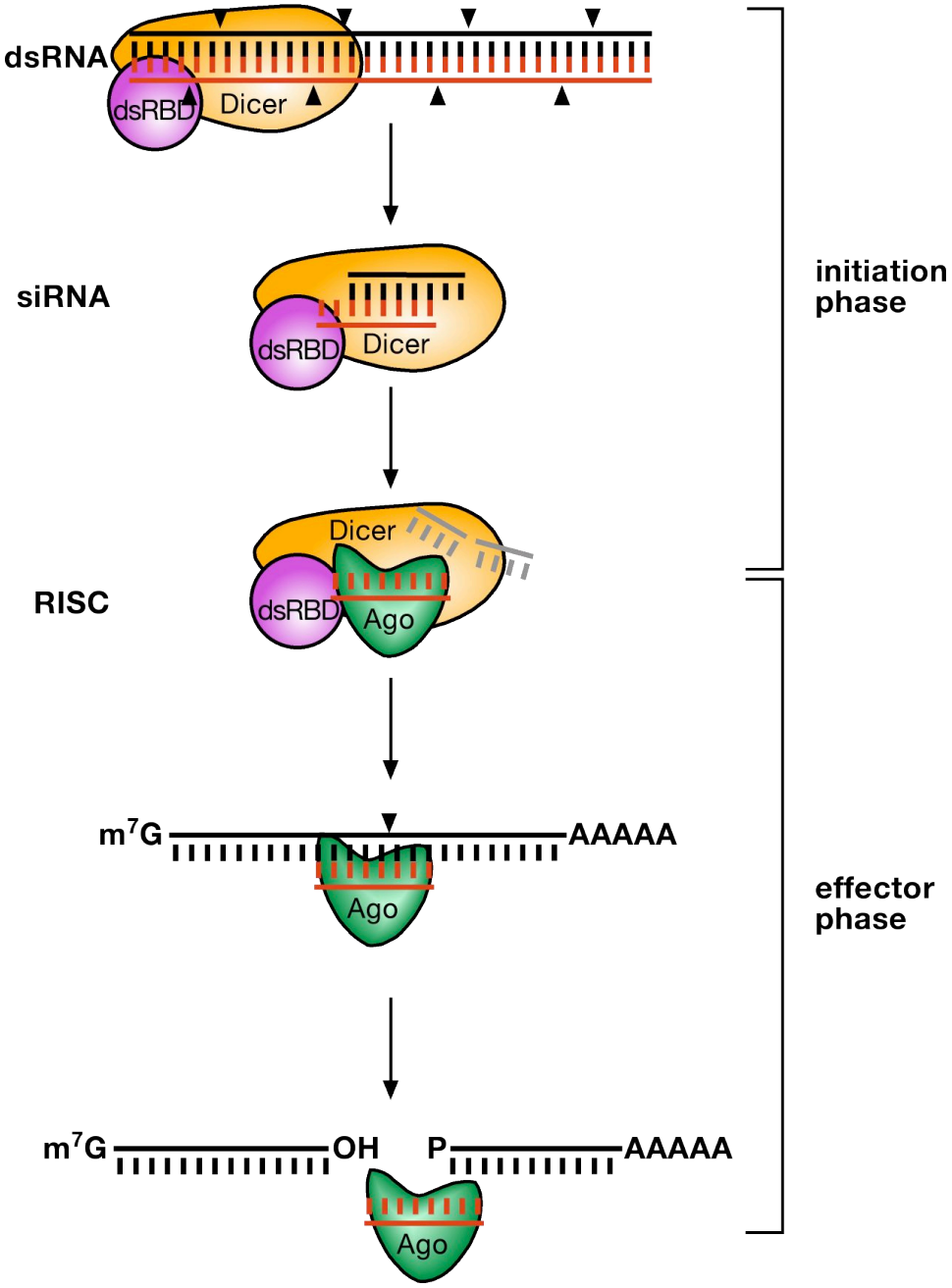

Figure 1. The mechanism of RNAi.
Long dsRNA is recognized by the RNase III like enzyme Dicer and chopped into ~21 nt small interfering RNA (siRNAs). With the help of a dsRNA binding domain (dsRBD) protein these are loaded into Argonaute (Ago) proteins and serve as a guiding cue to target the RNA induced silencing complex (RISC) to complementary RNAs for their endonucleolytic cleavage and subsequent degradation.

3.2.1. The initiation phase

The elegance of RNAi consists in converting the actual trigger of the response—long dsRNA—into small and versatile signaling units called siRNAs. These are, in turn, employed by the cellular machinery to act against the source of the long dsRNA by taking advantage of base complementarity and base pairing.

3.2.1.1. Dicing the long dsRNA

A crucial player in this step is the RNase III like enzyme Dicer that recognizes the dsRNA and processes it into ~21 nucleotide (nt) siRNA duplexes (Bernstein et al., 2001; Elbashir et al., 2001a; Elbashir et al., 2001b; Filipowicz, 2005; Ketting et al., 2001; Knight and Bass, 2001; Provost et al., 2002). Dicer has a molecular weight of approximately 200 kDa and features a DExH RNA helicase/ATPase domain, DUF283 and PAZ domains, two neighboring RNase III-like domains (RIIIa and RIIIb) and a C-terminal dsRNA binding domain (dsRBD). The two RIIIa and RIIIb domains of the same Dicer molecule interact with each other, so that Dicer acts as a pseudodimer/intramolecular dimer. Dicer contains a single processing center, where dsRNA substrates are cleaved at approximately 20 bp from the 3′ terminus bound by the PAZ domain (Kolb et al., 2005; Zhang et al., 2004). As a consequence of Dicer-mediated cleavage, siRNAs bear characteristic and functionally important 5′-phosphate groups and 2-nt 3′-overhangs featuring 3′-hydroxyl groups.

3.2.1.2. RISC assembly and siRNA asymmetry

In metazoan species, Dicer functions in complex with a dsRBD protein. In *D. melanogaster,* Dicer-1 is associated with Loquacious (Forstemann et al., 2005; Jiang et al., 2005) and Dicer-2 with R2D2 (Tomari et al., 2004). Mammalian Dicer cooperates with TRBP (the human immunodeficiency virus transactivating response RNA-binding protein) (Chendrimada et al., 2005; Haase et al., 2005), the ortholog of Loquacious. These dsRBD proteins are hypothesized to assist Dicer in the crucial step of RISC loading, where the siRNA is partially unwound and passed to Argonaute proteins. This process is very well studied in *D. melanogaster,* where the assembly process can be monitored by native gel electrophoresis (Pham et al., 2004). Apparently, the siRNA is not simply handed over by Dicer, but has to go through a series of intermediate complexes, termed pre-RISC and holo-RISC to finally become the mature RISC (Kim et al., 2007). In mammals, the picture is less clear. Results indicate that Dicer, TRBP and Ago2 are

sufficient to assemble on and unwind an siRNA duplex (Gregory et al., 2005; Maniataki and Mourelatos, 2005).

An important concept during RISC loading and siRNA unwinding is siRNA asymmetry (Khvorova et al., 2003). siRNAs can be considered asymmetric according to the binding energy of the two 5′-ends. The greater the GC-content the more energy is required to unwind the respective 5′-end. In *D. melanogaster,* the dsRBD protein R2D2 associated with Dicer-2 is able to sense this asymmetry. As a consequence, the strand, whose 5′-end is less stable according to the binding energy, is loaded into RISC (Tomari et al., 2004). It is less evident, how siRNA asymmetry is determined in mammals, however the binding energy of the 5′-ends plays a crucial role as well.

3.2.1.3. Passenger strand removal

Since an siRNA is typically asymmetric, the RNAi machinery is able distinguish the two siRNA strands. The strand, that will function in RISC, is called the "guide strand," as it will serve as a guide to direct RISC to its target RNAs. The second strand is called "passenger strand," as it just accompanies the guide strand in the siRNA duplex and is degraded after RISC assembly. A crucial question is, how is the passenger strand removed from the duplex? Does this process require an RNA helicase? Is the passenger strand removed intact or is it the "first target" of the assembling RISC? This process was scrutinized in four publications within three months using mammalian cells and *D. melanogaster* (Leuschner et al., 2006; Matranga et al., 2005; Miyoshi et al., 2005; Rand et al., 2005). It is now well established that RISC cleaves the passenger strand during assembly and that this event is crucial for its fast and efficient removal. However, if a passenger strand cannot be cleaved by assembling RISC, it is removed intact by a so-called bypass pathway, which operates substantially slower. Only recently, first evidence of an RNA helicase acting during RISC assembly surfaced. Robb and Rana demonstrated that RNA helicase A interacts with the siRNA, Dicer, TRBP and Ago2 and show evidence for its activity during siRNA loading (Robb and Rana, 2007). However, this involvment requires further study and more experiments to obtain a clearer picture.

3.2.2. The effector phase

3.2.2.1. Target RNA clevage

Once an siRNA has been assembled into RISC, it serves as a molecular guide to target complementary RNAs. A single stranded RNA (ssRNA) associated with a protein of the Argonaute protein family is considered the hallmark of RNA silencing. This silencing is achieved by the action of the protein component of RISC, Ago (see 3.2.2.2), an endonuclease that—upon binding with a high degree of complementarity—cleaves or "slices" the target (Martinez et al., 2002a; Martinez and Tuschl, 2004; Schwarz et al., 2004; Tomari and Zamore, 2005).

RISC displays a weak affinity for ssRNA and is thereby able to promote the annealing of the siRNA to the target RNA. Since RISC is unable to open structured RNA, efficient binding is dependent on the secondary structure and the resulting accessibility of the target sequence. Here, the 5′ part of the siRNA plays a very important role in establishing first contact to the target (Ameres et al., 2007).

However, the siRNA in RISC does not only guide Ago to the target RNA but, once fully bound, it also acts as a "molecular ruler". Counting from the 5′-end of the siRNA, Ago cleaves the phosphodiester bond across nucleotides 10 and 11 (Elbashir et al., 2001b; Elbashir et al., 2001c; Haley and Zamore, 2004; Martinez et al., 2002b). The cleavage products feature 5′-phosphate and 3′-hydroxyl termini, and Mg^{2+} is required for catalysis (Martinez and Tuschl, 2004; Schwarz et al., 2004). Furthermore, for cleavage to occur, only bases 2 to 12 need to be paired to the substrate RNA, corresponding to one full turn of an RNA:RNA helix (Chiu and Rana, 2003; Doench and Sharp, 2004; Haley and Zamore, 2004).

After cleavage, the target RNA is released enabling RISC to start multiple series of catalysis (Haley and Zamore, 2004; Hutvágner and Zamore, 2002; Martinez and Tuschl, 2004). While RISC does not require ATP-hydrolysis for target RNA cleavage in single-turnover conditions, the presence of ATP has been shown to increase the rate of cleavage in multiple turnover conditions (Haley and Zamore, 2004).

3.2.2.2. The family of Argonaute proteins

The central mediators of RNA silencing are Argonaute proteins. These proteins come in different flavors, but all display a common domain structure (Figure 2). Argonautes belong to PAZ-PIWI-domain (PPD) proteins. They typically feature an N-

terminal PAZ (PIWI-Argonaute-Zwille) and a C-terminal PIWI (P-element Induced Wimpy Testes) domain (Carmell et al., 2002; Cerutti et al., 2000). The PAZ domain can also be found in Dicer and is known to function as an RNA binding domain (Bernstein et al., 2001). The PIWI domain is involved in protein–protein interactions (Tahbaz et al., 2004). Most importantly, the PIWI domain was also shown to adopt an RNase H like fold (Parker et al., 2004; Song et al., 2004). This result plus the findings that target RNA cleavage requires Mg^{2+} and leaves 5′-phosphates as well as 3′-hydoxy groups (Wintersberger, 1990) led to the conclusion that the PIWI domain harbors the elusive slicer activity. In mammals, however, Ago2 is the only paralog to display slicer activity in its PIWI domain (Liu et al., 2004; Meister et al., 2004; Song et al., 2004).

Phylogenetically, the Argonaute family of proteins can be divided into three subfamilies: (a) the Argonaute subfamily, (b) the Piwi subfamily and (c) a subfamily only present in *C. elegans* (Yigit et al., 2006). In *D. melanogaster*, Ago1 and Ago2 represent the Argonaute subfamily, whereas Ago3, Aubergine and Piwi belong to the Piwi-subfamily. In vertebrates, "Ago"-proteins embody the Argonaute subfamily (Ago-1–4 in human, Ago 1–5 in mouse) with proteins from the Piwi-subfamily being denoted HIWI/HILI (HIWI-like) for human, MIWI/MILI for mouse, ZIWI for Zebrafish.

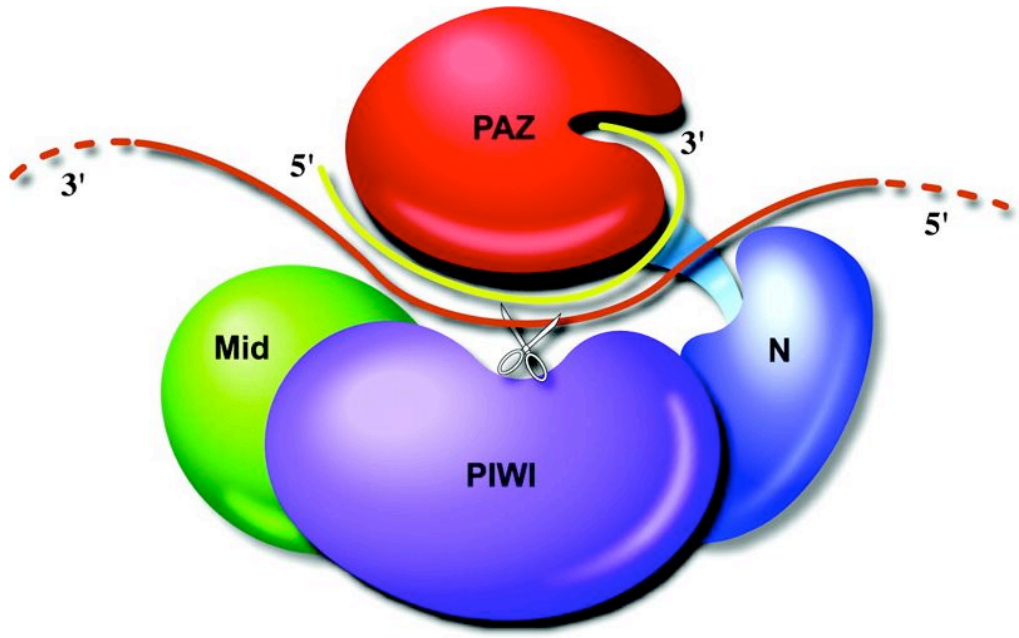

Figure 2. Illustration of RISC bound to a target RNA as proposed by (Song et al., 2004)
The PAZ domain (red) anchors the 3′ end of the siRNA (yellow) inside its cleft and the 5′ end on the distal end of the domain. The target mRNA (brown) bound by the siRNA reaches through the protein domains. The active site in the PIWI domain (shown as scissors) is positioned across the middle of the siRNA guide strand to cleave the target mRNA.

3.2.3. RNAi as a reverse genetic tool

In an era, where the genomes of all important model organisms are sequenced and publicly available, it became evident that RNAi would allow easy and practicable loss-of-function studies for virtually all known genes. Instead of the tedious work to generate mutants, dsRNA bearing the sequence of the gene of interest has to be introduced. In *C. elegans,* feeding the worms with *E. coli* producing the desired dsRNA is enough to silence the gene of interest (Fire et al., 1998). In *D. melanogaster*, inverted repeats can be introduced into the fly genome, that feature a promoter, which can be put under tight transcriptional control (Dietzl et al., 2007). In higher eukaryotes such as mammals, long dsRNA cannot be used for efficient RNAi, since these organisms have developed an unspecific interferon-based, antiviral response to this trigger (Manche et al., 1992; Stark et al., 1998). Here, dsRNA is recognized by the dsRNA-dependent protein kinase (PKR), a serine-threonine kinase that undergoes autophoshphorylation and then causes phosphorylation of downstream substrates. As a consequence, translation is shut down very rapidly leading to a pleiotropic effect of the dsRNA. To circumvent this problem, Dicer-like pre-processed siRNAs are used, since they are small enough to evade the interferon response (Elbashir et al., 2001a).

3.3. microRNAs

3.3.1. Discovery of microRNAs

As mentioned above, RNAi is hypothesized to have evolved as a defense system against rogue genetic elements that replicate via long dsRNA intermediates. A major discovery, however, was the finding that higher eukaryotic cells harness the mechanisms of RNAi to regulate the expression of endogenous genes. Just as in the canonical RNAi pathway (Figure 1), short ssRNA molecules that are stably encoded in the genome serve as sequence specific guides to target RISC to cognate sequences typically present in the 3′-untranslated region (UTR) of messenger RNAs (mRNAs). These RNAs are called microRNAs (miRNAs) (Ambros, 2004). First reports of small RNAs regulating the expression of protein coding genes with complementary regions in the 3′-UTR of mRNAs were published before the "RNAi revolution" in 1998 (Lee et al., 1993). At that time, miRNAs were called small temporal RNAs (stRNAs), since they were discovered as regulators in the developmental timing of *C. elegans* larval development (Grosshans et al., 2005; Lee et al., 1993; Reinhart et al., 2000). The

discovery of siRNAs encouraged scientists to look for endogenous small RNAs and to eventually decribe the class of miRNAs (Lagos-Quintana et al., 2001; Lagos-Quintana et al., 2003; Lagos-Quintana et al., 2002; Lau et al., 2001; Lim et al., 2003a; Lim et al., 2003b; Reinhart et al., 2002).

3.3.2. Biology of microRNAs

Today, miRNAs are defined as a growing family of ~22 nt small, endogenous, non-coding RNAs (ncRNAs) that specifically regulate expression of complementary mRNAs (Kloosterman and Plasterk, 2006). While siRNAs can be derived from any part of long dsRNA molecules, miRNAs have a defined, unique sequence and are liberated in a non-random fashion from precursor dsRNA transcripts that fold into a typical stem-loop structure. miRNAs act post-transcriptionally by binding complementary sequences in the 3′-UTR of particular mRNAs, causing translational repression or target mRNA cleavage.

3.3.2.1. microRNA genomics

miRNAs have been described in many organisms of both animal and plant kingdoms (Ambros, 2004; Kim and Nam, 2006), but they also exist in viruses (Baulcombe, 2004; Cullen, 2006; Pfeffer et al., 2004). Current estimates expect a few thousand miRNAs (Berezikov et al., 2005; Carthew, 2006; Lim et al., 2003a) that regulate approximately 20–30% of all genes (Brennecke and Cohen, 2003; Lewis et al., 2005). Such predictions are generated by sophisticated computer algorithms that scan genomes for sequences, which—upon transcription—fold into hairpin-like structures that are substrates for RNase III mediated cleavage. Employing secondary structure comparison, features could be defined that distinguish genuine RNase III substrate hairpins from other non-precursor hairpins (Ritchie et al., 2007). Another important criterion for miRNA prediction programs is evolutionary conservation at the sites of the potential hairpins. However, recent findings in *eutherians* indicate that in addition to strongly conserved miRNA families, such as the *let-7* family, rapidly evolving miRNA genes exist that are only present in distinct classes of the animal kingdom (Houbaviy et al., 2005).

miRNA genes are encoded in the genome in various fashions (Bartel, 2004; Kim, 2005). First, miRNAs can exist as individual, monocistronic transcription units where the miRNA is excised from a ncRNA transcript. Such loci are also termed "intergenic miRNAs", since the neighboring genes are >1 kb away. Second, miRNAs can be embedded in introns as well as exons of protein coding or non-coding transcripts.

Here, miRNAs can reside in both the sense or the anti-sense orientation (Lagos-Quintana et al., 2001; Lau et al., 2001). Third, miRNAs can also exist in so-called miRNA-clusters, where multiple miRNAs are serially encoded in a polycistronic transcript (Lee et al., 2002). Such a cluster, in turn, can reside in an autonomous transcription unit, or in an exon or intron of a host gene. It appears that the vast majority of miRNAs is transcribed by RNA polymerase II (Cai et al., 2004; Lee et al., 2004a). The human miR-19-cluster, which resides between Alu-repeats, is transcribed by RNA polymerase III, but this seems to be an exception rather than a common rule (Borchert et al., 2006). The use of RNA polymerase II promoters provides miRNAs with access to all the associated regulatory factors that allow tight transcriptional control both in space and time. Indeed, many miRNAs show specific expression patterns during developmental stages as well as under specific conditions and in certain cell types (Lagos-Quintana et al., 2003; Lagos-Quintana et al., 2002).

3.3.2.2. microRNA biogenesis

The biogenesis of miRNAs (Figure 3) is similar in all organisms ranging from plants to animals (Murchison and Hannon, 2004) and shares many features with the canonical RNAi pathway (Figure 1). miRNAs are expressed as long, primary transcripts in the nucleus (pri-miRNAs), which are processed by the Microprocessor complex—consisting of the dsRBD Pasha/DGCR8 and the RNase III like enzyme Drosha—into miRNA precursors (pre-miRNAs) (Kim, 2005). pre-miRNA hairpins show a 2-nt 3′-overhang characteristic of RNase III cleavage, which is recognized by Exportin-5, a Ran–GTP-dependent nuclear export factor (Bohnsack et al., 2004; Lund et al., 2004). Once translocated to the cytoplasm, pre-miRNA precursors are recognized by the Dicer–Loquacious/TRBP complex, which liberates a ~22 nt duplex RNA. According to the asymmetry rules (see above) the duplex is unwound, the passenger or miRNA* strand removed and the mature miRNA loaded into RISC. The differences between mammalian RISC loaded with an siRNA or a miRNA are not yet fully understood (Meister et al., 2004). However, both siRNAs, and miRNAs have been shown to guide target RNA cleavage for substrates with perfect complementarity, arguing that not the history of the short RNA molecules, but the degree of complementarity balances target cleavage versus translational repression (Doench et al., 2003). Consequently, siRNAs can act in a miRNA-manner when binding imperfectly to an RNA.

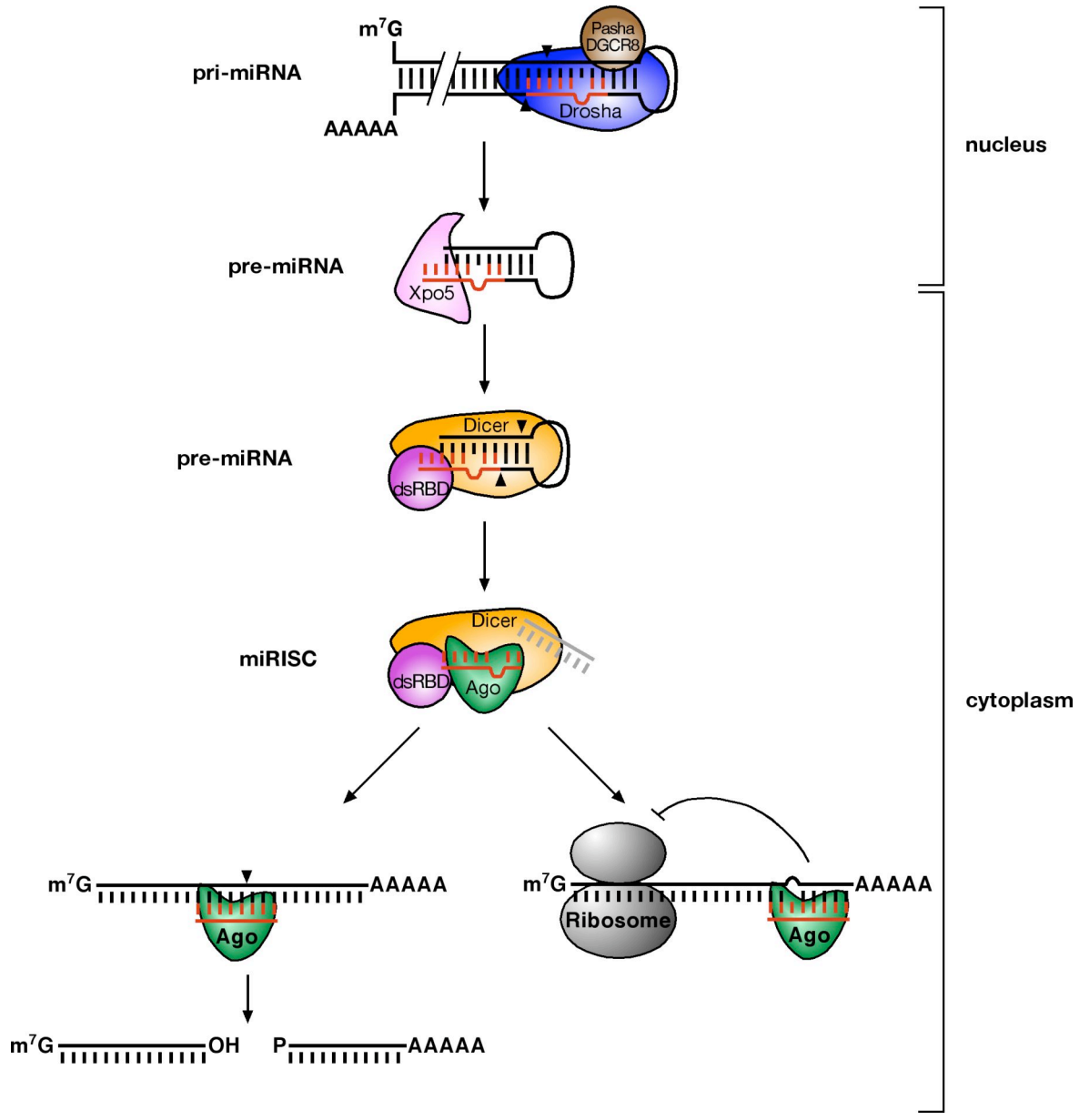

Figure 3. The miRNA pathway.
miRNA primary transcripts that are generated by RNA polymerase II feature a 7-methyl-guanosine cap and a poly-A tail. They fold into a hairpin shaped structure that is recognized by the Microprocessor complex, consisting of the nuclear RNase III like enzyme Drosha and the dsRBD DGCR8/Pasha. The pri-miRNAs are cropped to pre-miRNAs, which in turn are recognized by Exportin-5 and transferred to the cytoplasm. The cytoplasmic RNase III like enzyme Dicer in complex with the dsRBD TRBP/Loquacious cleaves off the terminal loop, thereby generating the ~22 nt miRNA duplex. This duplex is loaded into Ago proteins, unwound and—as in the RNAi-pathway—serves as a molecular guide to target the miRNA-associated RISC (miRISC) to complementary RNAs. In case of target RNAs displaying perfect complementarity, miRNAs loaded into Ago2 proteins are able to cleave the target. However, the main function of miRNAs appears to be translational repression by imperfect binding to target RNAs.

In *D. melanogaster,* the siRNA and miRNA pathways are separated. The Dicer-1–Loquacious complex cleaves pre-miRNAs and loads the miRNA into Ago1, whereas the Dicer-2–R2D2 complex cleaves long dsRNA into siRNAs that are shuttled to Ago2 (Lee et al., 2002; Pham et al., 2004). Two recent publications introduced the idea that the different intrinsic structures of siRNA/siRNA* and miRNA/miRNA* duplexes determine, where the small RNA will be loaded into (Forstemann et al., 2007; Tomari et al., 2007). Since the dsRNA–siRNA pathway does not seem to exist in mammals, only one Dicer paralog is present that functions in miRNA biogenesis and that is more closely related to *Drosophila's* Dicer-1.

Very recently, a novel class of miRNA-type regulatory RNAs were discovered (Okamura et al., 2007). These "miRNAs" are derived from short intronic hairpins termed mirtrons. Here, the requirement of Drosha-mediated cleavage is bypassed since mirtrons are generated by the splicing machinery and lariat-debranching enzyme. The resulting pre-miRNA-like hairpins are then channeled into the miRNA pathway downstream of Drosha and fed into the pool of functional miRNAs.

3.3.2.3. Regulation of microRNA expression

As mentioned above, the great majority of miRNAs is under the control of RNA polymerase II promoters (Cai et al., 2004; Lee et al., 2004a) explaining how miRNAs can display such distinct expression patterns. However, a detailed description of core miRNA promoters is still missing. Recently, a computational approach was able to uncover few basic motifs that are very similar to the already known *cis*-acting elements for the initiation of transcription (Zhou et al., 2007). In the past year, more and more evidence accumulated that the expression of miRNAs is not only regulated at the promoter but also post-transcriptionally in various modes. We demonstrated that the brain-specific miRNA *miR-138* is ubiquitously transcribed but processing is inhibited in all tissues other than neurons of the neo-cortex, the hippocampus and the cerebellum, as well as cells of the fetal liver (Obernosterer et al., 2006) (see section 4.2). Shortly thereafter, Thompson and colleagues found that the expression of miRNAs can be extensively regulated by altering the levels of the RNase III like enzyme Drosha that initiates the miRNA–processing cascade (Thomson et al., 2006). These publications were followed by additional results confirming differential ratios between precursor and mature miRNAs indicative of post-transcriptional regulation (van Rooij et al., 2006). Just

recently, adenosine to inosine RNA editing was also found to affect the processing of pre-miR-151 by Dicer–TRBP (Kawahara et al., 2007).

3.3.2.4. Silencing by microRNAs

While plant miRNAs bind their cognate sequences with perfect complementarity leading to target cleavage, animal miRNAs almost exclusively show imperfect binding followed by a plethora of silencing phenomena (Pillai et al., 2007; Valencia-Sanchez et al., 2006). Despite these considerable differences in the regulatory output, the mechanism, how a miRNA finds and binds its target, appears to be conserved in all species. Genuine miRNA target sites contain a stretch of nucleotides that display perfect Watson–Crick complementarity to the 5′ part of the miRNA, namely the bases 2–8 (Lewis et al., 2003). This heptamer is also called the miRNA "seed" and is absolutely essential for the binding of the miRNA. Indeed, perfect binding of the miRNA seed to a target site with all the other miRNA bases being unpaired is enough to yield functional silencing (Brennecke et al., 2005). However, minor flaws within the seed—such as a G:U wobble pair that would abrogate silencing—can be compensated by a strong binding of the 3′ end of the miRNA. The requirement of seed-binding was already indicated earlier, at a time when miRNAs were not yet known (Lai et al., 1998). Here, a conserved sequence motif termed K-box was discovered in the 3′ UTRs of Enhancer of split Complex genes that is essential for regulation of these genes by Notch receptor activity.

The effect of seed-only regulation has to be taken into consideration whenever siRNAs are designed to target a specific mRNA. While the siRNA will silence the gene of interest via the RNAi pathway and target RNA cleavage, the same RISC can also act like a RISC loaded with a miRNA by binding to other mRNAs harboring accessible sequence motifs complementary to bases 2–8 of the siRNA. These messages are silenced via the miRNA-pathway and will of course contribute to the phenotype that is observed (Jackson et al., 2006). Such an unwanted result is called an "off target effect" and it is usually overcome by blasting the "siRNA seed" against the genome to check for any possible matches (Reynolds et al., 2004).

But which mechanisms do miRNAs use to regulate their targets? The most prominent silencing mode of miRNAs appears to be translational repression (Bartel, 2004; Olsen and Ambros, 1999). Whether RISC bound to the target site interferes with the initiation or elongation of translation is still a matter of debate, owing to the fact that

these experiments were performed using different systems (Jackson and Standart, 2007; Pillai et al., 2007). Repression can be observed directly at the initiation phase (Humphreys et al., 2005; Pillai et al., 2005), as well as at post-initiation phases (Maroney et al., 2006; Nottrott et al., 2006; Petersen et al., 2006). Very recently, a study implied the anti-association factor eIF6, that prevents assembly of the 80S ribosome, to associate with miRNA-associated RISC (miRISC) (Chendrimada et al., 2007). Furthermore, human Ago2 was found to contain a motif similar to the m(7)G cap-binding domain of eIF4E, an important translation initiation factor (Kiriakidou et al., 2007). This motif is essential for silencing by translational repression, potentially by binding the cap and thus preventing the recruitment of eIF4E.

To allow efficient long-term silencing, miRISC has to be recycled. This occurs in the so-called processing bodies (p-bodies), where bound target RNAs are transported, decapped and subsequently degraded rapidly by exonucleases (Jakymiw et al., 2005; Liu et al., 2005; Sen and Blau, 2005). However, p-bodies have also been shown to act as storage facilities, from where repressed target RNAs can be recruited back to the cytoplasm for translation (Bhattacharyya et al., 2006).

A different mode of silencing can be observed in the zebrafish *D. rerio*, where miRNAs were shown to affect the stability of the poly-A tail of mRNAs. The miRNA family miR-430 is required for the deadenylation of maternal mRNAs in the developing fish embryo (Giraldez et al., 2005), clearing the translation machinery for embryonic mRNAs.

Finally, miRNAs displaying perfect complementarity to target sites can also lead to target RNA cleavage (Yekta et al., 2004), highlighting the functional equivalence of miRNA-associated RISC (miRISC) and siRNA-associated RISC (siRISC) in mammals.

3.3.2.5. microRNA function

In mammals, more than 200 miRNAs have been defined and annotated (Bartel, 2004), but only very few target genes are known, because animal miRNAs bind cognate sequences imperfectly, thereby creating complex secondary structures. As a consequence, refined computational tools and elaborate algorithms need to be employed, in order to assign target genes to known miRNA sequences (Enright et al., 2003; Krek et al., 2005; Lewis et al., 2003; Rehmsmeier et al., 2004). So far the overlap between the various prediction programs has been very small, probably owing to differential ranking of parameters such as phylogenetic conservation of the target site, especially the seed,

folding energy and of course statistics. As a consequence, *in silico* predicted miRNA targets have to be validated *in vivo*.

miRNAs regulate important biological and pathological processes, including cell differentiation, apoptosis, and cellular transformation [reviewed in (Ambros, 2004; Bartel, 2004; Hagan and Croce, 2007; He and Hannon, 2004; Kloosterman and Plasterk, 2006)]. It is clear that miRNAs are absolutely essential for early animal development. Dicer knock-out mice die around embryonic day 7.5 as a consequence of stem cell depletion (Bernstein et al., 2003). A *D. melanogaster* mutant for *Dicer-1* also displays problems with germ-line stem cell maintenance (Lee et al., 2004b). Zebrafish embryos lacking zygotic as well as maternally provided Dicer are able to differentiate into several cell types but display abnormalities during gastrulation, somitogenesis, brain and heart development (Giraldez et al., 2005). Later in animal development, miRNAs have been found to play a role during developmental timing. In *C. elegans,* lin-4 and let-7—the first miRNAs that were discovered—warrant proper transition of the larval stages by regulating heterochronic genes (Abrahante et al., 2003; Grosshans et al., 2005; Lee et al., 1993; Lin et al., 2003; Pasquinelli et al., 2000; Wightman et al., 1993). Also, signaling pathways that are important in animal development are subjected to miRNA-mediated regulation. In particular, target genes of the Notch pathway in *D. melanogaster* are regulated by miRNAs (Lai et al., 2005).

Concerning cellular functions and metabolism, miRNAs have been shown to affect apoptosis and energy homeostasis both in flies and vertebrates (Brennecke et al., 2003; Poy et al., 2004; Teleman et al., 2006). During organogenesis, muscle and heart development is regulated by miRNAs with high phylogenetic conservation (Aboobaker et al., 2005; Chen et al., 2006; Naguibneva et al., 2006; Sokol and Ambros, 2005; Tuddenham et al., 2006; Zhao et al., 2005). Probably the most interesting organ that shows extensive regulation by miRNAs is the brain. The functions of miRNAs range from differentiation of neuronal progenitor cells (Conaco et al., 2006) over neuronal outgrowth and morphogenesis (Vo et al., 2005) to synaptic plasticity (Schratt et al., 2006).

Over the past few years, more and more evidence was put forth that aberrant expression of miRNAs also contributes to the oncogenic potential of tumorigenic cells, providing a link between miRNAs and cancer (Calin and Croce, 2006; Calin et al., 2004a; Calin et al., 2004b; Ciafre et al., 2005; Volinia et al., 2006; Yanaihara et al., 2006). Interestingly, most miRNAs show a lower level of expression in tumor tissue leading to a

loss of cellular differentiation (Lu et al., 2005; Thomson et al., 2006) underlining the role of miRNA in promoting cellular differentiation.

3.4. Other small RNA silencing pathways

3.4.1. piRNAs

The cloning and sequencing of small RNA populations from *D. melanogaster* led to the identification of 24 to 29-nt-long RNAs next to the expected 22-nt miRNAs (Aravin et al., 2003). These longer RNA molecules were found to associate with Argonaute proteins from the Piwi subfamily (Aravin et al., 2006; Brennecke et al., 2007; Carmell et al., 2007; Girard et al., 2006; Grivna et al., 2006a; Grivna et al., 2006b; Gunawardane et al., 2007; Saito et al., 2006; Vagin et al., 2006; Watanabe et al., 2007). Hence, these RNA molecules were named piRNAs, short for Piwi-associated RNAs. Interestingly, piRNAs are not encoded as hairpins (Betel et al., 2007). Thus, their biogenesis is completely different from miRNAs. piRNAs are generated in an amplification loop, where—in *D. melanogaster*—sense piRNAs associated with Ago3 cleave long antisense RNA thereby setting the 5′-end of the antisense piRNAs that associate with a different Argonaute protein, called Aubergine. The antisense piRNA in Aubergine cleaves long sense RNAs forming the 5′-end of sense piRNAs. This process is called the "ping-pong model" (Brennecke et al., 2007; Gunawardane et al., 2007). The formation of the 3′-end is still unknown. In *D. melanogaster*, piRNAs are enriched for sequences from transposons and repeats, whereas in the mouse and rat, only 17% of all piRNAs map to repetitive elements (Hartig et al., 2007). Nonetheless, genetic analysis of Piwi-mutants suggests a conserved function of piRNAs in transposon control (Aravin et al., 2007; Carmell et al., 2007; Kalmykova et al., 2005; Sarot et al., 2004).

3.4.2. RNA silencing and epigenetics

3.4.2.1. Transcriptional gene silencing

In plants, small RNAs do not only function on the post-transcriptional level but they can also lead to transcriptional gene silencing (Matzke and Birchler, 2005). This phenomenon is induced by dsRNA via *de-novo* DNA methylation followed by heterochromain formation (Mette et al., 2000; Wassenegger et al., 1994). A similar pathway exists in the fission yeast *S. pombe,* where dsRNA leads to the formation of repressive heterochromatin that silences gene expression (Volpe et al., 2002). The

effector complex is termed RITS (RNA-Induced Initiation of Transcriptional gene Silencing) and contains a short siRNA and an Argonaute protein (Motamedi et al., 2004; Verdel et al., 2004). RITS binds to nascent transcripts, interacts with modified histones and recruits chromatin-remodeling factors (Buhler et al., 2006; Motamedi et al., 2004; Noma et al., 2004). There is evidence that small RNA can mediate transcriptional gene silencing in animals, too (Fukagawa et al., 2004; Kanellopoulou et al., 2005; Kawasaki and Taira, 2004), but the detailed mechanisms and functions still remain obscure.

3.4.2.2. Targeted DNA elimination

During the sexual process of conjugation of ciliated protozoa such as *Tetrahymena*, the genome becomes extensively reorganized. This programmed deletion of DNA is mediated by an RNAi-related pathway (Mochizuki and Gorovsky, 2004, 2005), where sequences become marked for subsequent excision (Chalker and Yao, 2001; Mochizuki et al., 2002; Taverna et al., 2002; Yao et al., 2003).

3.4.2.3. RNA silencing and Polycomb proteins

Finally, RNAi components were found to play a role in silencing via Polycomb group proteins. In *D. melanogaster,* Dicer-2, PIWI and Argonaute1 appear to be required for long-distance physical interactions between chromosomes, indicating an involvement in higher-order nuclear organization (Grimaud et al., 2006; Lei and Corces, 2006).

3.5. Aim of this thesis

During my doctoral studies, I was focusing on upstream events in RNA silencing. This thesis can be divided into two parts. First, I was analyzing the process of RISC assembly. Much is known about this process, yet what happens exactly to the siRNA, when it is finally loaded into the Argonaute protein, was still elusive. The aim here was to characterize crucial steps during this process and the potential impact on silencing efficiency. Secondly, I was interested if miRNA-processing can be regulated, a hitherto completely unknown field, since it was generally accepted that differential expression of miRNA genes is exclusively achieved via transcriptional control. I envision that insights into this phenomenon will certainly lead to a more complete understanding of miRNA expression and target regulation.

4. Results

4.1. Cleavage of the siRNA passenger strand during RISC assembly in human cells

Cleavage of the siRNA passenger strand during RISC assembly in human cells

Philipp J.F. Leuschner[1], Stefan L. Ameres[2], Stephanie Kueng[3] & Javier Martinez[1+]

[1]Institute of Molecular Biotechnology of the Austrian Academy of Sciences, IMBA, Vienna, Austria, [2]Max F. Perutz Laboratories, Department of Biochemistry, University of Vienna, Vienna, Austria, and [3]Institute of Molecular Pathology, IMP, Vienna, Austria

A crucial step in the RNA interference (RNAi) pathway involves the assembly of RISC, the RNA-induced silencing complex. RISC initially recognizes a double-stranded short interfering RNA (siRNA), but only one strand is finally retained in the functional ribonucleoprotein complex. The non-incorporated strand, or 'passenger' strand, is removed during the assembly process and most probably degraded thereafter. In this report, we show that the passenger strand is cleaved during the course of RISC assembly following the same rules established for the siRNA-guided cleavage of a target RNA. Chemical modifications impairing the cleavage of the passenger strand also impair the cleavage of a target RNA *in vitro* as well as the silencing of a reporter gene *in vivo*, suggesting that passenger strand removal is facilitated by its cleavage during RISC assembly. Interestingly, target RNA cleavage can be rescued if an otherwise non-cleavable passenger strand shows a nick at the scissile phosphodiester bond, which further indicates that the cleavage event *per se* is not essential.

Keywords: passenger strand; RNAi; Argonaute; RISC

EMBO reports (2006) 7, 314–320. doi:10.1038/sj.embor.7400637

INTRODUCTION

RNA interference (RNAi) is a post-transcriptional gene-silencing phenomenon that occurs in many eukaryotic organisms following stimulation by double-stranded RNA (dsRNA; Fire *et al*, 1998). In general, the RNAi response (reviewed by Filipowicz, 2005) can be divided into two distinct steps. The first step, called the assembly phase, comprises the recognition of a dsRNA molecule and its processing into ~21-nucleotide (nt) RNA molecules, termed short interfering RNAs (siRNAs), by the RNase III-like enzyme Dicer (Hammond *et al*, 2000; Zamore *et al*, 2000; Bernstein *et al*, 2001). siRNAs are then shuttled into the RNA-induced silencing complex (RISC), a ribonucleoprotein complex composed of an Argonaute protein (Elbashir *et al*, 2001a; Lee *et al*, 2004; Pham *et al*, 2004; Tomari *et al*, 2004a, b) and a single-stranded guide RNA. The selection of the RNA strand to be incorporated is governed by the thermodynamic profile of the siRNA duplex termini (Khvorova *et al*, 2003; Schwarz *et al*, 2003). In the second phase, also known as the effector phase, RISC uses this single-stranded RNA molecule as a guide to endonucleolytically cleave complementary RNAs (Hammond *et al*, 2000; Nykänen *et al*, 2001; Elbashir *et al*, 2001a; Martinez *et al*, 2002). Although RISC-mediated target RNA cleavage is very well studied (Haley & Zamore, 2004; Liu *et al*, 2004; Martinez & Tuschl, 2004; Meister *et al*, 2004; Schwarz *et al*, 2004; Song *et al*, 2004), the final steps of the assembly process of RISC are still a matter of debate, especially how the 'guide' strand is separated from the passenger strand.

Whereas in mammalian cells only few studies exist on the assembly of RISC (Pham & Sontheimer, 2005), this process has been extensively studied in *Drosophila melanogaster* (Okamura *et al*, 2004; Tomari *et al*, 2004a, b), in which the unwinding of the siRNA has been shown to depend on the presence of Ago2 (Okamura *et al*, 2004; Tomari *et al*, 2004b). Such studies have so far focused on the siRNA strand that is incorporated into RISC, referred to as the 'guide strand'. In contrast, the fate of the non-incorporated strand, or 'passenger strand', has mostly been neglected. In this report, we investigate the role and fate of the passenger strand during RISC assembly in HeLa cells both *in vitro* and *in vivo*, and focus on its implications on silencing. We show that for its efficient removal, the passenger strand has to be cleavable at its 'natural' site, that is, at 10 nt from the 5′-phosphate of the guide strand. If this cleavage step is blocked, the siRNA duplex still becomes loaded into RISC, but target RNA cleavage is severely impaired owing to the non-efficient removal of the passenger strand.

RESULTS AND DISCUSSION

Modified passenger strands impair target RNA cleavage

It was previously shown that affinity-purified human RISC is able to cleave synthetic, short, non-capped RNAs (Martinez & Tuschl, 2004). Interestingly, a short target RNA containing a 2′-*O*-methyl ribose at guanosine 9 (G_9, the nucleotide immediately upstream of

[1]Institute of Molecular Biotechnology of the Austrian Academy of Sciences, IMBA, Dr-Bohr-Gasse 3-5, 1030 Vienna, Austria
[2]Max F. Perutz Laboratories, Department of Biochemistry, University of Vienna, Dr-Bohr-Gasse 9/5, 1030 Vienna, Austria
[3]Institute of Molecular Pathology, IMP, Dr-Bohr-Gasse 7, 1030 Vienna, Austria
[+]Corresponding author. Tel: +43 1 79044 4860;
E-mail: javier.martinez@imba.oeaw.ac.at

Received 3 November 2005; revised 12 December 2005; accepted 21 December 2005; published online 20 January 2006

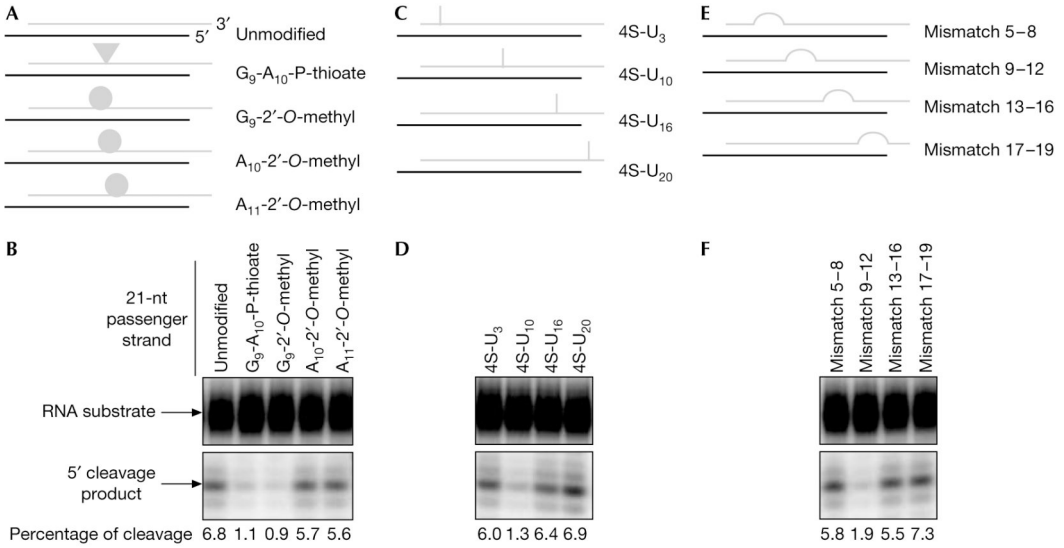

Fig 1 | Chemical modifications on the passenger strand impair cleavage of a target RNA. (**A**) Graphical representation of short interfering RNAs (siRNAs) containing unmodified or chemically modified passenger strands. Passenger strands are shown in grey and guide strands in black in this report. 2′-*O*-methyl modifications are depicted as circles and phosphorothioates as triangles. (**B**) Phosphorimaging of cleavage reactions using siRNAs depicted in (**A**) resolved on a 6% denaturing polyacrylamide gel. Arrows point to the RNA substrate and the labelled 5′-cleavage product. The percentage of cleaved target RNA is indicated at the bottom of the gel. (**C**) Graphical representation of siRNAs containing 4S-U substitutions (indicated as bars) at different positions on the passenger strand. (**D**) Phosphorimaging of cleavage reactions using siRNAs depicted in (**C**). (**E**) Graphical representation of siRNAs containing 4-nt mismatches at different positions on the passenger strand. (**F**) Phosphorimaging of cleavage reactions using siRNAs depicted in (**E**).

the cleavage site) was poorly cleaved, probably owing to steric hindrance caused by the bulky methyl group. A deoxyribose at G_9 and 2′-*O*-methyl ribose groups 1 and 2 nt downstream of the cleavage site were, however, well tolerated.

We reasoned that RISC, during its assembly on the guide strand, might regard a passenger strand as its first RNA target, in a similar manner as affinity-purified RISC recognizes and cleaves a short target RNA. In this model, a chemically modified short RNA that cannot be cleaved by affinity-purified RISC should also not be cleaved when present as a passenger strand in an siRNA. We used HeLa cytoplasmic extracts and monitored the effect of these and other modifications on target RNA cleavage when present on the passenger strand of an siRNA duplex.

We observed a greater than sixfold reduction in the cleavage of a complementary target RNA when the passenger strand contained a phosphorothioate bond between G_9 and A_{10}, a modification that was shown to impair cleavage of a substrate RNA (Schwarz *et al*, 2004), or featured a 2′-*O*-methyl ribose at G_9 (Fig 1A, and Fig 1B, lanes 2,3). However, 2′-*O*-methyl ribose groups positioned 1 or 2 nt downstream of the cleavage site (A_{10} and A_{11}) did not impair target RNA cleavage, as was the case for an unmodified siRNA (Fig 1A, and Fig 1B, lanes 1,4,5). A similar, ~6-fold reduction in target RNA cleavage was obtained with a passenger strand, in which the adenine residue downstream of the predicted cleavage site (A_{10}) was substituted by a 4-thio-uridine (4S-U; Fig 1C, and Fig 1D, lane 2). This modification, when present in a short target RNA, abolished cleavage by affinity-purified RISC, most probably owing to a geometrical distortion in base pairing (supplementary Fig S1 online). 4S-U residues at non-central positions did not severely interfere with the cleavage of the target RNA (Fig 1C, and Fig 1D, lanes 1,3,4). Finally, we tested the effect of passenger strands featuring mismatches at different positions on the cleavage of a guide-complementary target RNA. A central 4-nt mismatch reduced the cleavage efficiency by a factor of 3 when compared with a full complementary siRNA (Fig 1E, and Fig 1F, lane 2), whereas non-central mismatches did not significantly affect the efficiency of cleavage (Fig 1E, and Fig 1F, lanes 1,3,4). These results indicate that modifications at the putative cleavage site on the passenger strand severely impair the assembly of functional RISC. Interestingly, 2′-*O*-methyl modifications at central positions on the guide strand had no effect on target RNA cleavage (data not shown), underlining that the impairment of target RNA cleavage is due to the passenger strand being rendered non-cleavable.

The passenger strand is cleaved during RISC assembly

As (i) RISC properly recognizes siRNAs featuring non-cleavable passenger strands (supplementary Fig S2A,B online), and (ii) Ago2 interacts with both strands of the duplex (supplementary Fig S2C,D online), we reasoned that the inhibition of target RNA cleavage might be explained by RISC being unable to effectively remove a passenger strand that cannot be cleaved, rather than failing to assemble on a modified siRNA. In principle, it could also be the case that a non-cleavable passenger strand acted as a suicide target on re-binding functional RISC. We can, however, rule out this possibility, as a non-cleavable passenger strand is not

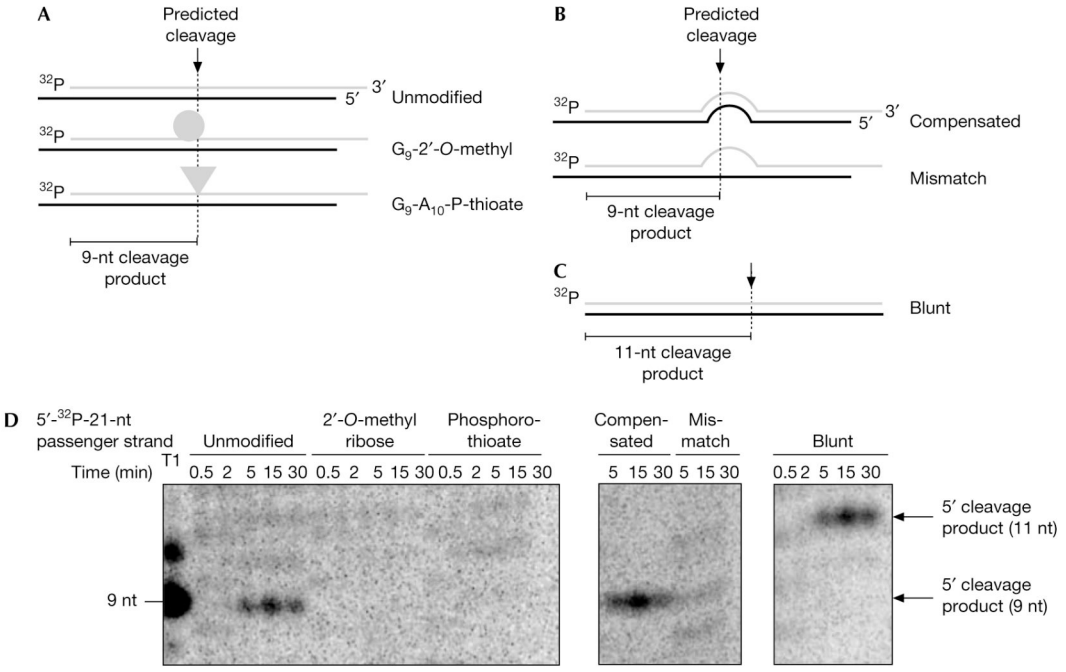

Fig 2 | The passenger strand is cleaved during RNA-induced silencing complex assembly. (**A**) Graphical representation of short interfering RNAs (siRNAs) composed of unmodified guide strands and unmodified or chemically modified passenger strands. In all cases, the passenger strands were 5′ phospho-radiolabelled (indicated by '^{32}P'). The dotted line depicts the position where cleavage is predicted to take place on the passenger strand, that is, between guanosine-9 (G_9) and adenosine-10 (A_{10}). The expected 9-nt cleavage product is indicated. (**B**) Graphical representation of an siRNA formed by a 5′-phospho-radiolabelled, unmodified passenger strand (for the sequence, see 'mismatch 9–12' in the legend of Fig 1E) and guide strands, the sequence of which either compensates for the 4-nt mutation in the passenger strand or leads to a central 4-nt mismatch. The dotted line depicts the predicted cleavage position. (**C**) Graphical representation of a blunt siRNA formed by an unmodified guide strand and a 5′-phospho-radiolabelled, unmodified passenger strand, in which the sequence has been shifted 2 nt towards the 5′ end. The dotted line depicts the predicted cleavage position, which has also shifted by 2 nt. The expected 11-nt cleavage product is indicated. (**D**) Phosphorimaging analysis of a time-course cleavage reaction resolved in a 15% denaturing gel electrophoresis. The region of the gel corresponding to sizes between 8 and 12 nt has been enhanced for an optimal visualization of the cleavage products. The picture of the whole gel is depicted in supplementary Fig S4 online.

released intact from the original siRNA (supplementary Fig S3 online). To provide conclusive evidence for the cleavage of the passenger strand during RISC assembly, we set out to detect the predicted 9-nt cleavage product. We performed a time-course analysis using HeLa cytoplasmic extracts and 5′-phospho-radiolabelled siRNAs, the passenger strands of which were left unmodified, or were modified either with a 2′-*O*-methyl ribose at G_9 or with a phosphorothioate bond between G_9 and A_{10} (Fig 2A). The unmodified passenger strand yielded the expected 9-nt cleavage product after only 5 min of incubation, reached a maximum at 15 min and decreased thereafter (Fig 2D, left panel). In sharp contrast, the modified passenger strands were not cleaved (Fig 2D, left panel). Similarly, a passenger strand featuring a central 4-nt mismatch (Fig 2B) failed to yield a 9-nt cleavage product (Fig 2D, central panel). However, passenger strand cleavage could be rescued in the latter case by restoring the complementarity on the guide strand (Fig 2D, central panel). It is worth noting that the profiles of the 9-nt cleavage product differ from the concomitant 3′–5′ exonucleolytic degradation of the passenger strand, which leads to the steady accumulation of $<$21 nt species during the course of the reaction (supplementary Fig S4 online). Moreover, this unspecific degradation is present in all cases, irrespective of whether the passenger strand is being cleaved or not.

Interestingly, the cleavage of the passenger strand correlates temporally with the interaction of Ago2 and the siRNA (compare Fig 2D with supplementary Fig S2D online). As soon as Ago2 contacts the passenger strand of the siRNA, the 9-nt cleavage product emerges, supporting our hypothesis that the passenger strand is cleaved in the course of RISC assembly.

It is well established that the cleavage position on a target RNA is located 10 nt from the 5′ end of the guide strand (Elbashir *et al*, 2001b). To test whether this rule also applies to the cleavage of the passenger strand, we extended the 5′ end of the guide strand by 2 nt, resulting in a blunt-ended siRNA (Fig 2C). This duplex cleaved a complementary target RNA with a 2-nt shift (data not shown). The cleavage site on the passenger strand was also shifted by 2 nt, now generating an 11-nt cleavage product (Fig 2D, right panel). This argues that RISC, during assembly, cleaves the passenger strand by a mechanism similar to that by which functional RISC cleaves a complementary target RNA.

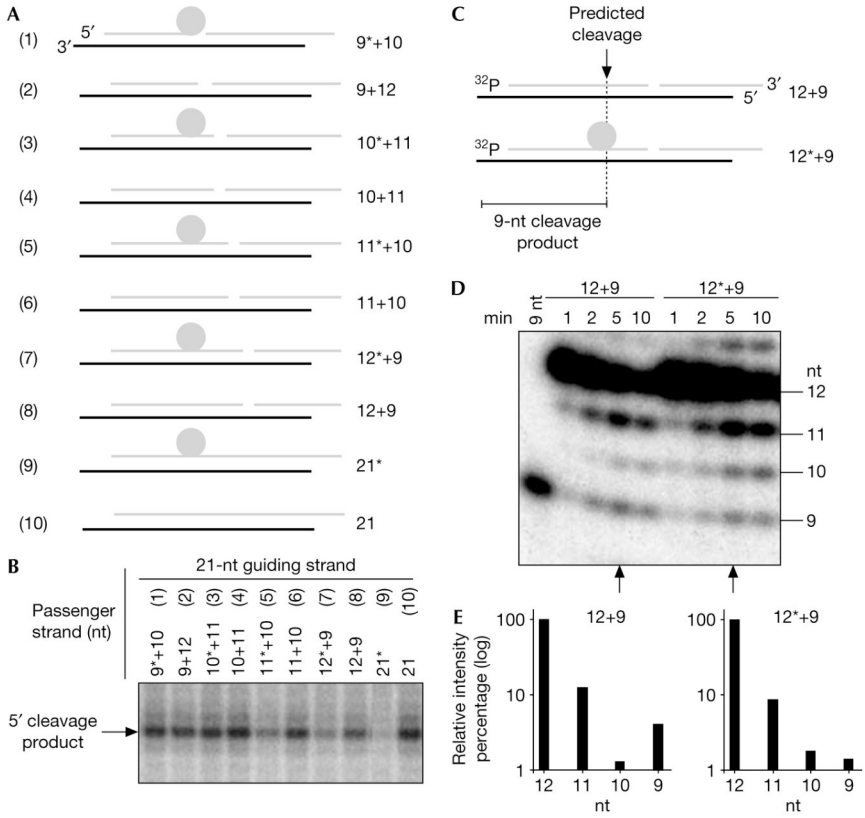

Fig 3 | Functional RNA-induced silencing complex assembles on a short interfering RNA in which an otherwise non-cleavable passenger strand is nicked at the putative cleavage site. (**A**) Graphical representation of short interfering RNAs (siRNAs) formed by one (21 nt) or two passenger strands ($x+y$) of different lengths leading to a nicked passenger strand of 21 nt. Numbers on the right refer to the length of the strands in nucleotides. The asterisk indicates a 2′-*O*-methyl ribose at G_9. (**B**) Phosphorimaging analysis of a cleavage reaction resolved in a 6% denaturing gel electrophoresis showing the efficiency of target RNA cleavage as a function of the position of a nick on the passenger strand and the presence or absence of a 2′-*O*-methyl ribose at the cleavage position. (**C**) Graphical representation of siRNAs formed by two passenger strands (12 nt + 9 nt), in which the 12-nt fragment has been 5′ phospho-radiolabelled (indicated by '^{32}P'), and either left unmodified (duplex 12 + 9) or modified with a 2′-*O*-methyl ribose at position G_9 (duplex 12* + 9). Numbers on the right refer to the length of the strands in nucleotides. The dotted line depicts the position where cleavage is predicted to take place on the passenger strand, that is, between G_9 and A_{10}. The expected 9-nt cleavage product is indicated. (**D**) Phosphorimaging analysis of a time-course cleavage reaction resolved in a 15% denaturing gel electrophoresis. A phosphorylated, 9-nt RNA oligonucleotide was used as a marker. Note the different pattern between the cleavable and non-cleavable passenger strand. Whereas unspecific 3′-to-5′ exonucleolytic degradation of the non-cleavable passenger strand leads to the steady accumulation of <12 nt species during the course of the reaction, the cleavable passenger strand, which is subjected to a similar degradation, shows a clear enrichment of the 9-nt species. Arrows indicate the time point at which the quantification in (**E**) was performed. (**E**) Quantification of the phosphorimaging analysis in (**D**). Bars represent the relative intensity of the bands, the sizes of which are indicated along the *x* axis. The 9-nt cleavage product accumulates only when using the unmodified, cleavable 12-nt fragment of the passenger strand.

Bypassing the passenger strand cleavage event

Why does the cleavage of the passenger strand facilitate the generation of functional RISC? A nick in the passenger strand is expected to result in a drastic change in the thermodynamic profile of the siRNA duplex, which could sustain the removal of the passenger strand. We therefore generated an siRNA by annealing two passenger strands of 9 and 12 nt length to a 21-nt guide strand, a so-called '9 + 12', nicked siRNA (Fig 3A). This siRNA faithfully interacted with Ago2 (data not shown) and guided target RNA cleavage as efficiently as an siRNA containing a conventional 21-nt passenger strand did (Fig 3B, lanes 2,10). This result indicates that the Ago2-mediated cleavage event *per se* appears to be not essential for the generation of functional RISC, as it can be bypassed by a pre-existing nick. It thus argues against a model in which the cleavage event imposes a conformational change that would facilitate the removal of the passenger strand.

We also generated a duplex '9* + 12', in which a 2′-*O*-methyl group was placed at the G_9 position (the cleavage site) of the 9-nt passenger strand (Fig 3A). This duplex efficiently cleaved the target RNA, demonstrating that a 2′-*O*-methyl group at the cleavage site has no effect on the removal of the cleaved passenger strand (Fig 3B, lane 1). More importantly, the complete rescue of target

RNA cleavage by providing a nick on the cleavage site of an otherwise non-cleavable passenger strand highlights the importance of passenger strand cleavage during RISC assembly.

Interestingly, we found that displacing the nick stepwise further downstream along the passenger strand and, additionally, maintaining its non-cleavable character (Fig 3A, 10*+11, 11*+10, 12*+9) led to a reduction in target RNA cleavage, as the distance between the nick and the 2′-*O*-methyl group increased (Fig 3B, lanes 3,5,7). In contrast, duplexes with unmodified passenger strands (Fig 3A, 10+11, 11+10, 12+9) guided efficient cleavage of the target RNA (Fig 3B, lanes 4,6,8), underlining the relevance of passenger strand cleavage at the 'natural' position, that is, the phosphodiester bond between nt 9 and 10 counting from its 5′ end. An intact, 21-nt non-cleavable passenger strand showed the most pronounced impairment of target RNA cleavage compared with a 21-nt cleavable passenger strand (Fig 3B, lanes 9, 10, respectively). We proposed that the inhibition of target RNA cleavage observed for the 12*+9 duplex should correlate with the inability to cleave the 12-nt, modified passenger strand into a 9-nt cleavage product. Indeed, specific accumulation of the 9-nt cleavage product was observed only when using the unmodified 12+9 duplex and not the modified 12*+9 duplex (Fig 3C–E).

These findings raise a couple of interesting questions. As a central 4-nt mismatch on the siRNA also impaired the removal of the passenger strand, an explanation has to be found for how microRNAs (miRNAs) with several internal bulges, even at the putative cleavage site, are loaded into microRISC (miRISC). Furthermore, Ago1, Ago3 and Ago4 have been shown to be associated with mature miRNAs (Liu *et al*, 2004; Meister *et al*, 2004). As in mammals only Ago2 is known to harbour endonucleolytic activity, how do the catalytically inactive Argonaute proteins remove the passenger strand? Clearly, a bypass pathway should exist, which allows the assembly of miRISC in the absence of slicer activity. During miRNA maturation, an auxiliary factor might assist in the loading of miRISC independently of the presence of a catalytically active Ago protein. A different possibility might rely on the reduced thermodynamic stability of miRNA duplexes, as, in contrast to siRNAs, miRNA duplexes feature bulges of non-paired bases at different positions. Interestingly, cleavage assays carried out at 37 °C rescued target RNA cleavage guided by an siRNA containing a central, 4-nt mismatch on the passenger strand (Fig 4A,B). In contrast, siRNAs featuring fully complementary passenger strands and showing 2′-*O*-methyl or phosphorothioate modifications at the cleavage site showed a minor rescue (Fig 4A,B).

Finally, we tested the effect of siRNAs containing modified passenger strands *in vivo*. We co-transfected HeLa cells with a plasmid containing the firefly luciferase gene together with siRNAs harbouring differently modified passenger strands (Fig 4C) and analysed luciferase activities normalized to cells transfected with a mock siRNA. An unmodified siRNA effectively silenced the reporter gene, whereas we observed a major impairment in silencing with a passenger strand containing a 2′-*O*-methyl ribose at position 9 (Fig 4D), certifying that cleavage of the passenger strand also has a role *in vivo*. The same modification at position 10, however, did not affect the knockdown efficiency. The most severe impairment in silencing was caused by a passenger strand containing both a 2′-*O*-methyl ribose at position 9 and a phosphorothioate bond between nt 9 and 10. A passenger strand with a central mismatch at positions 9 and 10 was also very inefficient in silencing after 6 h. However, in contrast to all other modifications that impaired the knockdown, silencing improved slightly after 24 h, probably owing to a putative bypass mechanism.

We also tested silencing of an endogenous gene, human cohesin (Scc1), using both unmodified and modified duplexes (Fig 4E). A passenger strand featuring a 2′-*O*-methyl ribose at position 9 led to a less efficient silencing than an unmodified passenger strand (Fig 4F). However, after enhancing the non-cleavable character by adding a phosphorothioate bond between nt 9 and 10 of the passenger strand, a severe impairment was detected (Fig 4F).

In conclusion, we show that the cleavage of the passenger strand is indeed a prerequisite for effective assembly of functional human RISC. Our results may also provide valuable clues for the findings in *D. melanogaster*, in which RISC assembly has been shown to depend on the presence of Ago2 (Okamura *et al*, 2004; Tomari *et al*, 2004a, b). The results from HeLa cytoplasmic extracts favour a model in which efficient and fast removal of the passenger strand is dependent on the catalytic activity of Ago2. We also propose that removal of the cleaved passenger strand during RISC assembly follows similar rules as the removal of the cognate target RNA after cleavage: RISC, during its assembly, has to be liberated from the passenger strand that would otherwise block the recognition of a target RNA. In turn, functional RISC, as every multiple turnover enzyme (Hutvágner & Zamore, 2002; Haley & Zamore, 2004; Martinez & Tuschl, 2004), has to guarantee product release only after catalysis.

Note: During the submission process, Matranga *et al*, Rand *et al* (Cell, Immediate Early Publication, 3 November 2005) and Miyoshi *et al* (Genes and Development, December 2005) reported a similar function of the passenger strand in *Drosophila*. Kraynack & Baker (RNA, Epub ahead of print, 21 November 2005) report that for some siRNA sequences, passenger strands fully modified with 2′-*O*-methyl residues do not impair silencing.

METHODS

Short interfering RNA duplexes. The sequence of the passenger strand was 5′-CGUACGCGGAAUACUUCGAAA-3′. The sequence of the guide strand was 5′-UCGAAGUAUUCCGC GUACGUG-3′. All duplexes contained symmetric 2-nt overhangs at the 3′ end. Duplexes were annealed to a final concentration of 10 μM in 100 mM KOAc, 2 mM $Mg(OAc)_2$ and 30 mM Hepes (pH 7.4), and dilutions were made thereof. Oligoribonucleotides were obtained from Dharmacon Research Inc. (Lafayette, CO, USA) and PROLIGO Primers and Probes (Paris, France) and were generously provided by Professor Tom Tuschl (The Rockefeller University).

In the case of 4S-U-modified passenger strands in Fig 1C, the base at the positions indicated was exchanged by a 4S-U residue.

The sequences of the passenger strands in Fig 1E were 5′-CGU AGCGCGAAUACUUCGAAA-3′ for 'mismatch 5–8', 5′-CGUACG CGAGUAACUUCGAAA-3′ for 'mismatch 9–12', 5′-CGUACGCG GAAUAUUCAGAAA-3′ for 'mismatch 13–16' and 5′-CGUACGC GGAAUACUUAGCAA-3′ for 'mismatch 17–19'.

The sequence of the passenger strand in Fig 2C was 5′-CGUA CGCGAGUAACUUCGAAA-3′. To restore complementarity, the sequence of the guide strand was changed accordingly.

To generate the blunt siRNA duplex in Fig 2C, the sequence of the guide strand was changed to 5′-UUUCGAAGUAUUCCGCG UACG-3′.

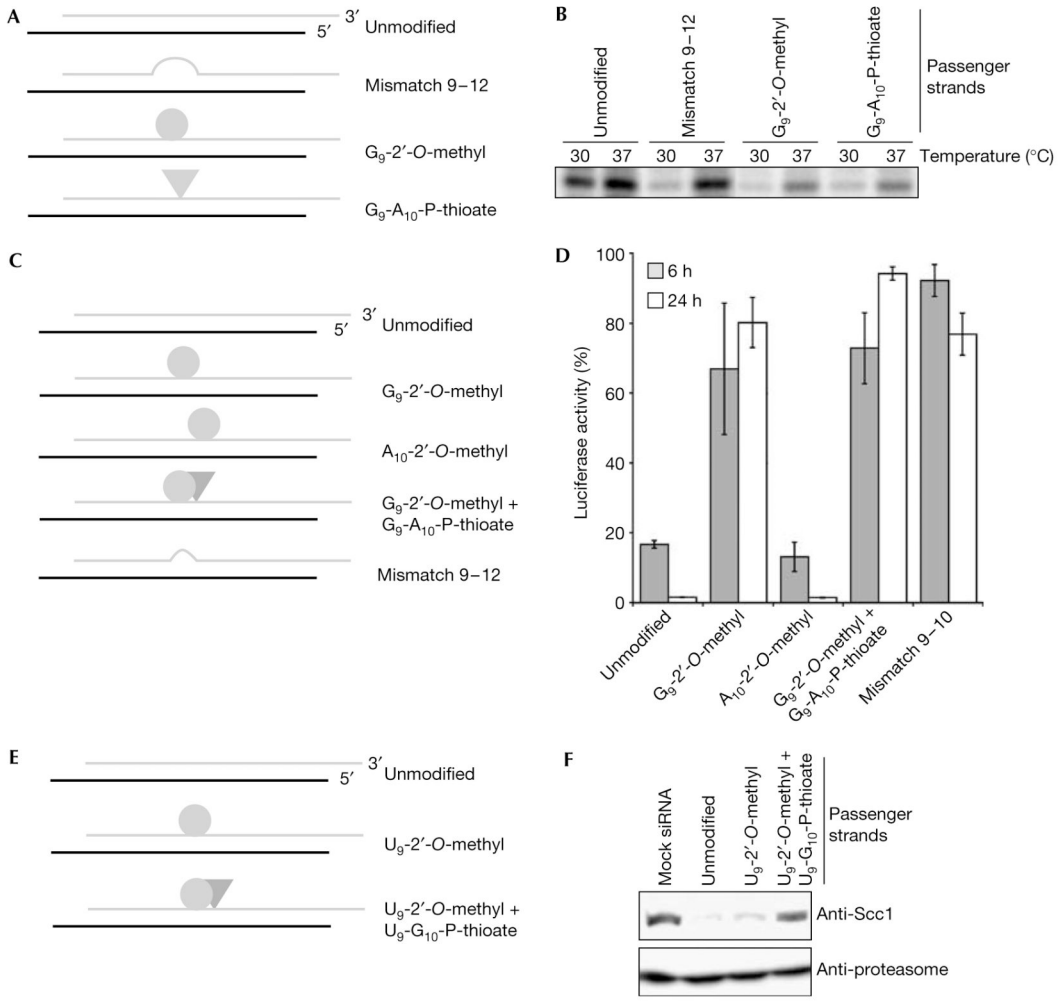

Fig 4 | *In vitro* and *in vivo* analysis of a putative bypass mechanism for RNA-induced silencing complex assembly. (**A**) Graphical representation of short interfering RNA (siRNAs) containing unmodified or chemically modified passenger strands. (**B**) Phosphorimaging analysis of a cleavage reaction resolved in a 6% denaturing gel electrophoresis. (**C**) Same as (**A**). (**D**) Luciferase activities measured after 6 or 24 h after transfecting HeLa cells with siRNAs depicted in (**C**). (**E**) Same as (**A**). (**F**) Western blot analysis of a knockdown experiment in HeLa cells 24 h after transfecting HeLa cells with siRNAs depicted in (**E**).

The sequences of the duplexes used in the knockdown experiment in Fig 4E,F were taken from Hirota *et al* (2004).

The sequence of the passenger strands used in the luciferase assay (Fig 4C,D) was 5′-CUUACGCUGAGUACUUCGAAA-3′. For the duplex 'mismatch 9–10', the sequence was 5′-CUUACGC UACGUACUUCGAAA-3′. The sequence of the guide strand was 5′-UCGAAGUACUCAGCGUAAGUG-3′.

When indicated in the figure legends, 5′ phospho-radiolabelling of the respective strands was performed as described previously (Martinez & Tuschl, 2004).

Cleavage reactions. Cleavage reactions were performed as described previously (Martinez *et al*, 2002), with the exceptions that $MgCl_2$ was used at 5 mM and that the final concentration of siRNAs was adjusted to 10 nM. HeLa cytoplasmic extracts were provided by Professor Reinhard Luhrmann (Department of Cellular Biochemistry, Max Planck Institute for Biophysical Chemistry, Göttingen, Germany) and by Paragon Bioservices Inc. (Baltimore, MD, USA). The substrate RNA is ^{32}P-cap-labelled (Elbashir *et al*, 2001b). Radiolabelled markers were generated by partial RNase T1 digestion of the ^{32}P-cap-labelled RNA substrate.

Passenger strand cleavage experiments were performed as cleavage reactions, the difference being the absence of ^{32}P-cap-labelled substrate RNA.

Cell culture and transfections. Cell culture and transfections were performed as described previously (Hirota *et al*, 2004). HeLa cells were seeded at a density of 4×10^4 cells per 12-well plate, 1 day before transfection. siRNA duplexes were used at a final concentration of 200 nM. At 24 h after transfection, the cells were washed with cold PBS and lysed directly in 1 × SDS–polyacrylamide gel electrophoresis sample buffer. For luciferase assays, HeLa cells were cultured in 24-well plates and transfected with 100 nM siRNAs, 0.2 μg of pGL3 promoter (Pp-luc)

and 0.01 μg of phRL-TK control vector (Rr-luc; Promega, Madison, WI, USA) for internal standardization. We used sextuplicates for each condition. Cells were collected and extracts were assayed 6 and 24 h after transfection.

Western blotting. Samples were sonicated and boiled before being loaded on an 8% SDS–polyacrylamide gel electrophoresis. Gels were blotted onto polyvinylidene difluoride membranes using the semi-dry method. Membranes were blocked in 3% non-fat dry milk in Tris-buffered saline + 0.05% Tween. Antibodies against human cohesin (Scc1) and the proteasome were used at a concentration of 2 μg/ml (Sumara *et al*, 2002). Secondary antibodies were from JacksonImmunoResearch (Sigma Aldrich, West Grove, PA, USA).

Supplementary information is available at *EMBO reports* online (http://www.emboreports.org).

ACKNOWLEDGEMENTS

We thank A. Kuras, G. Obernosterer, D. Pezic and S. Weitzer, members of the laboratory, for encouragement and suggestions during the completion of this work, Professor R. Schroeder and C. Ribeiro for critically reading the manuscript, H. Manninga for the synthesis of 4-thio-uridine-modified siRNAs and for comments on the manuscript and Y. Dorsett for discussions. J.M. is a Junior Group Leader at IMBA. P.J.F.L. is funded by the Boehringer Ingelheim Fonds PhD Scholarship and S.L.A. is funded by the Vienna Biocenter PhD program and partly by Fonds zur Förderung der Wissenschaftlichen Forschung through WK001. IMBA is the Institute of Molecular Biotechnology supported by the Austrian Academy of Sciences.

REFERENCES

Bernstein E, Caudy AA, Hammond SM, Hannon GJ (2001) Role for a bidentate ribonuclease in the initiation step of RNA interference. *Nature* **409:** 363–366

Elbashir SM, Lendeckel W, Tuschl T (2001a) RNA interference is mediated by 21 and 22 nt RNAs. *Genes Dev* **15:** 188–200

Elbashir SM, Martinez J, Patkaniowska A, Lendeckel W, Tuschl T (2001b) Functional anatomy of siRNAs for mediating efficient RNAi in *Drosophila melanogaster* embryo lysate. *EMBO J* **20:** 6877–6888

Filipowicz W (2005) RNAi: the nuts and bolts of the RISC machine. *Cell* **122:** 17–20

Fire A, Xu S, Montgomery MK, Kostas SA, Driver SE, Mello CC (1998) Potent and specific genetic interference by double-stranded RNA in *Caenorhabditis elegans*. *Nature* **391:** 806–811

Haley B, Zamore PD (2004) Kinetic analysis of the RNAi enzyme complex. *Nat Struct Mol Biol* **11:** 599–606

Hammond SM, Bernstein E, Beach D, Hannon GJ (2000) An RNA-directed nuclease mediates post-transcriptional gene silencing in *Drosophila* cells. *Nature* **404:** 293–296

Hirota T, Gerlich D, Koch B, Ellenberg J, Peters JM (2004) Distinct functions of condensin I and II in mitotic chromosome assembly. *J Cell Sci* **117:** 6435–6445

Hutvágner G, Zamore PD (2002) A microRNA in a multiple-turnover RNAi enzyme complex. *Science* **297:** 2056–2060

Khvorova A, Reynolds A, Jayasena SD (2003) Functional siRNAs and miRNAs exhibit strand bias. *Cell* **115:** 209–216

Lee YS, Nakahara K, Pham JW, Kim K, He Z, Sontheimer EJ, Carthew RW (2004) Distinct roles for *Drosophila* Dicer-1 and Dicer-2 in the siRNA/miRNA silencing pathways. *Cell* **117:** 69–81

Liu J, Carmell MA, Rivas FV, Marsden CG, Thomson JM, Song JJ, Hammond SM, Joshua-Tor L, Hannon GJ (2004) Argonaute2 is the catalytic engine of mammalian RNAi. *Science* **305:** 1437–1441

Martinez J, Tuschl T (2004) RISC is a 5′ phosphomonoester-producing RNA endonuclease. *Genes Dev* **18:** 975–980

Martinez J, Patkaniowska A, Urlaub H, Lührmann R, Tuschl T (2002) Single-stranded antisense siRNAs guide target RNA cleavage in RNAi. *Cell* **110:** 563–574

Meister G, Landthaler M, Patkaniowska A, Dorsett Y, Teng G, Tuschl T (2004) Human Argonaute2 mediates RNA cleavage targeted by miRNAs and siRNAs. *Mol Cell* **15:** 185–197

Nykänen A, Haley B, Zamore PD (2001) ATP requirements and small interfering RNA structure in the RNA interference pathway. *Cell* **107:** 309–321

Okamura K, Ishizuka A, Siomi H, Siomi MC (2004) Distinct roles for Argonaute proteins in small RNA-directed RNA cleavage pathways. *Genes Dev* **18:** 1655–1666

Pham JW, Sontheimer EJ (2005) Molecular requirements for RNA-induced silencing complex assembly in the *Drosophila* RNA interference pathway. *J Biol Chem* **280:** 39278–39283

Pham JW, Pellino JL, Lee YS, Carthew RW, Sontheimer EJ (2004) A Dicer-2-dependent 80s complex cleaves targeted mRNAs during RNAi in *Drosophila*. *Cell* **117:** 83–94

Schwarz DS, Hutvagner G, Du T, Xu Z, Aronin N, Zamore PD (2003) Asymmetry in the assembly of the RNAi enzyme complex. *Cell* **115:** 199–208

Schwarz DS, Tomari Y, Zamore PD (2004) The RNA-induced silencing complex is a Mg^{2+}-dependent endonuclease. *Curr Biol* **14:** 787–791

Song JJ, Smith SK, Hannon GJ, Joshua-Tor L (2004) Crystal structure of Argonaute and its implications for RISC slicer activity. *Science* **305:** 1434–1437

Sumara I, Vorlaufer E, Stukenberg PT, Kelm O, Redemann N, Nigg EA, Peters JM (2002) The dissociation of cohesin from chromosomes in prophase is regulated by Polo-like kinase. *Mol Cell* **9:** 515–525

Tomari Y, Du T, Haley B, Schwarz DS, Bennett R, Cook HA, Koppetsch BS, Theurkauf WE, Zamore PD (2004a) RISC assembly defects in the *Drosophila* RNAi mutant armitage. *Cell* **116:** 831–841

Tomari Y, Matranga C, Haley B, Martinez N, Zamore PD (2004b) A protein sensor for siRNA asymmetry. *Science* **306:** 1377–1380

Zamore PD, Tuschl T, Sharp PA, Bartel DP (2000) RNAi: double-stranded RNA directs the ATP-dependent cleavage of mRNA at 21 to 23 nucleotide intervals. *Cell* **101:** 25–33

Supplemental Figures

Leuschner et al. Fig. S1

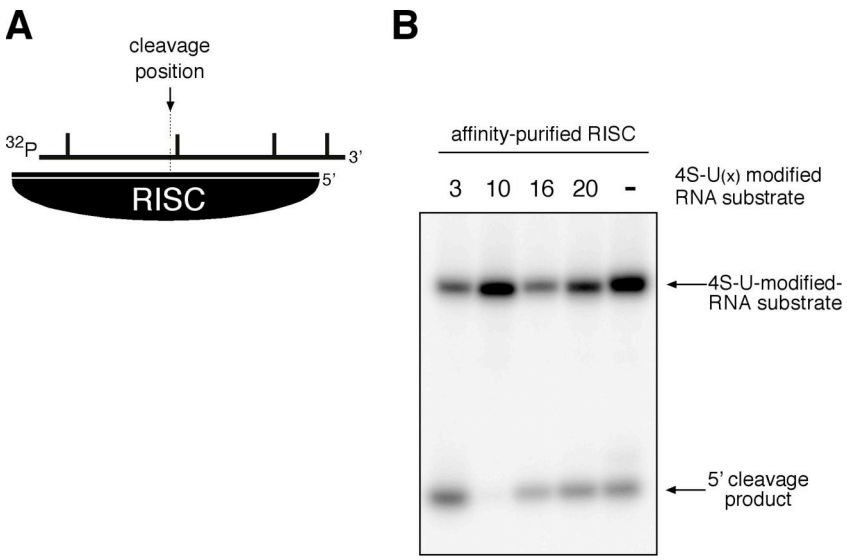

Figure S1. Affinity purified RISC is not able to cleave a short RNA substrate displaying a 4S-U modification adjacent to the cleavage site (4S-U10).
(A) Graphic representation of 4S-U-modified short RNA substrates. 4S-U-modifications are depicted as bars. Affinity-purified RISC (purified as previously described (Martinez et al., 2002)) is depicted in black below the guide strand. RNA substrates were 5′ phospho-radiolabeled.
(B) Phosphorimaging analysis of a cleavage reaction resolved in a 15% denaturing gel electrophoresis. Arrows point to the 4S-U-modified RNA substrates and the labeled 5′ cleavage product.

Leuschner et al. Fig. S2

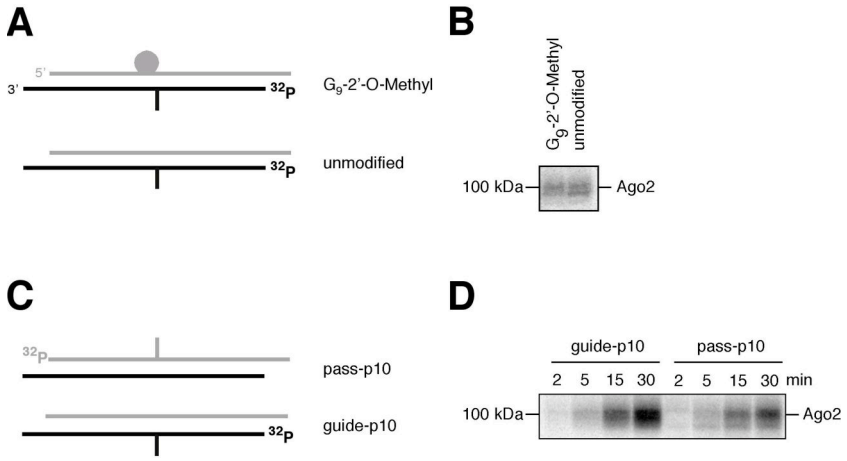

Figure S2. Initial assembly of RISC is not disturbed by modifications on the passenger strand that impair target RNA cleavage and occurs on a double-stranded siRNA.
(A) Graphic representation of duplex siRNAs containing chemically modified or unmodified passenger strands (2´-O-methyl groups are depicted as circles), and a 5′ phospho-radiolabeled guide strand modified at position 10 with 4S-U (4S-U10; depicted as a bar) to allow the cross-linking of proteins in close proximity to the center of the siRNA.
(B) Phosphorimaging of a cross-linking reaction using siRNAs depicted in (A) resolved on a 7.5% SDS-polyacrylamide gel.
(C) Graphic representation of siRNAs composed of a 5′ phospho-radiolabeled passenger strand modified with 4S-U10 and an unmodified guide strand, or an unmodified passenger strand annealed to a 5′ phospho-radiolabeled guide strand modified with 4S-U10.
(D) Time course analysis on the gradual recruitment of Ago2 to the siRNA, as monitored by cross-linking to both the guide and the passenger strands, resolved on a 7.5% SDS-polyacrylamide gel.

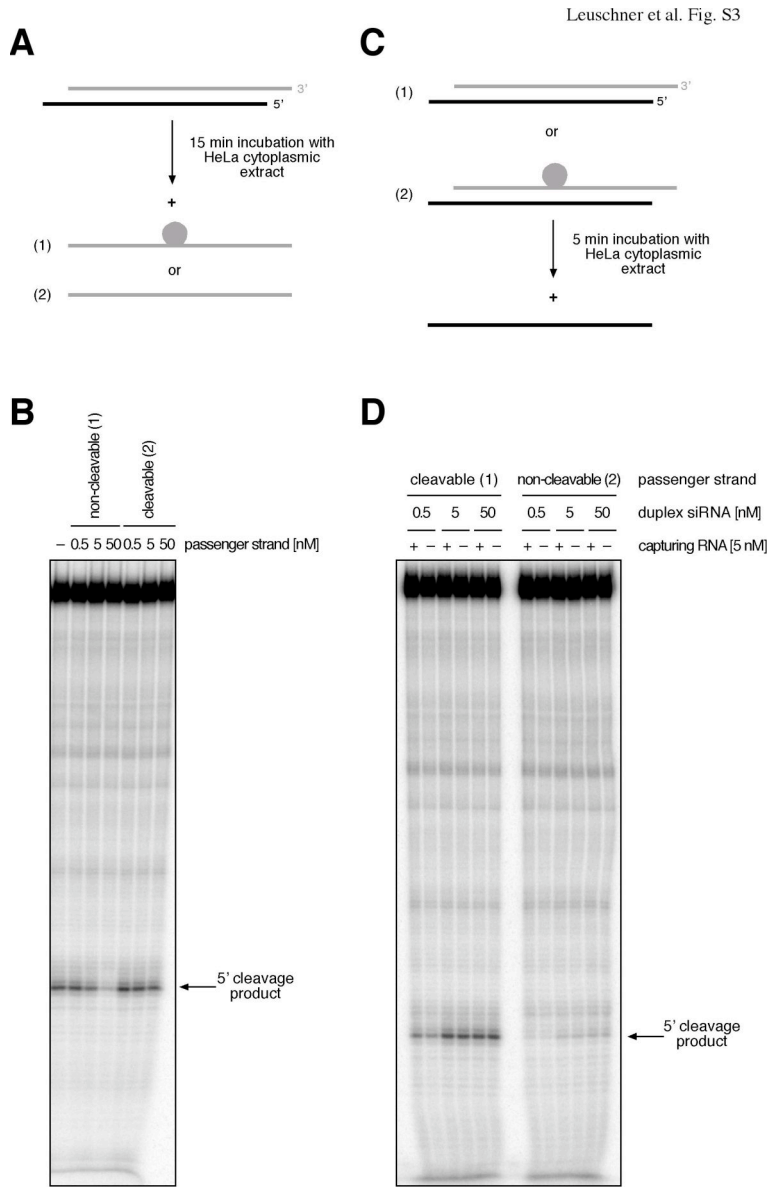

Figure S3. Non-cleavable passenger strands are not released from the siRNA.
(A) Graphic representation of the experiment. HeLa cytoplasmic extract was incubated together with 5 nM unmodified siRNA. After 15 min, when RISC assembly has already occurred, different amounts of both non-cleavable or cleavable passenger strands were added. At 30 min, the complementary target-RNA (10 nM) was introduced and the cleavage reaction was continued for 2 h. **(B)** Phosphorimaging analysis of the cleavage reaction described in (A) resolved in a 6% denaturing gel electrophoresis showing the effect of the addition of a single-stranded, non-cleavable or cleavable passenger strands on target-RNA cleavage. Since addition of 5 nM single stranded, non-cleavable passenger strand caused no significant reduction in target-RNA cleavage, re-binding of a potentially released non-cleavable passenger strand from the siRNA duplex (also 5 nM) could not account for the drastic inhibition of target-RNA cleavage. Only when added in large excess (50 nM), enough non-cleavable passenger strand molecules managed to escape unspecific degradation in the extract and acted as 'suicide targets'. An unmodified passenger strand did not impair cleavage, not even at 50 nM, most probably because it was immediately cleaved by functional RISC and then released. **(C)** Graphic representation of the experiment. HeLa cytoplasmic extract was incubated together with different concentrations of siRNAs containing either cleavable or non-cleavable passenger strands. The capturing RNA (complementary to the passenger strand) was added after 5 minutes of initiating the reaction, to prevent premature degradation. **(D)** Phosphorimaging analysis of the cleavage reaction described in (C) resolved in a 6% denaturing gel electrophoresis showing the effect of adding a capturing RNA, complementary to the passenger strand, to a target-RNA cleavage reaction. The addition of the capturing strand to cleavage reactions programmed with siRNAs featuring a cleavable passenger strand did not affect target-RNA cleavage. The reduction in target-RNA cleavage observed when using 0.5 nM siRNA is due to sub-saturated levels of RISC. Importantly, addition of the capturing strand to siRNAs featuring a non-cleavable passenger strand never rescued target-RNA cleavage, not even when the capturing strand was in a 10-fold excess over the siRNA. Taken these data together, we conclude that a non-cleavable passenger strand is never released from the original duplex, probably because its cleavage does not take place, resulting in inhibition of target-RNA cleavage through impairment of RISC assembly.

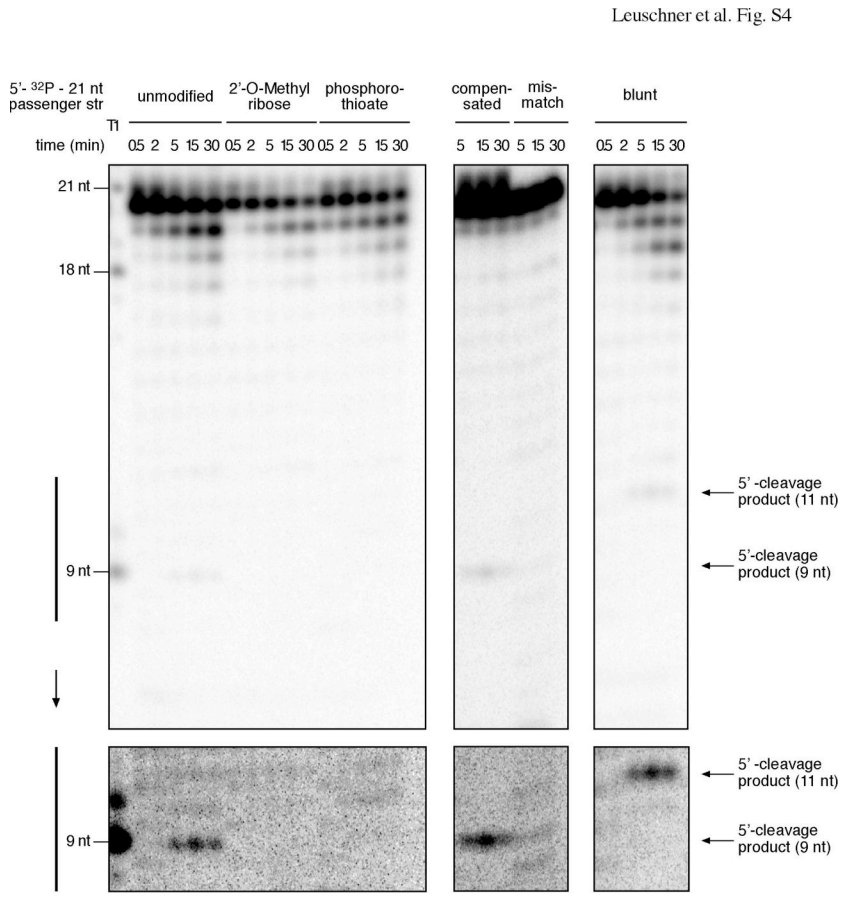

Figure S4. The passenger strand is cleaved during RISC assembly.
Picture of the whole gel depicted in Fig. 2D showing the concomitant 3′–5′ exonucleolytic degradation of the passenger strand. This degradation leads to the steady accumulation of <21 nt species during the course of the reaction irrespective of the passenger being cleaved during RISC assembly. The region of the gel corresponding to sizes between 8 and 12 nt has been enhanced for an optimal visualization of the cleavage products.

4.2. Post-transcriptional regulation of microRNA expression

REPORT

Post-transcriptional regulation of microRNA expression

GREGOR OBERNOSTERER,[1,3] PHILIPP J.F. LEUSCHNER,[1,3] MATTIAS ALENIUS,[2,3] and JAVIER MARTINEZ[1]

[1]Institute of Molecular Biotechnology of the Austrian Academy of Sciences (IMBA), A-1030 Vienna, Austria
[2]Institute of Molecular Pathology (IMP), A-1030 Vienna, Austria

ABSTRACT

microRNAs (miRNAs) are endogenous, noncoding ~22-nucleotide RNA molecules that have recently emerged as fundamental, post-transcriptional regulators of cognate target gene expression. Many mammalian miRNAs are expressed in a tissue-specific manner, a phenomenon that has so far been attributed to transcriptional regulation. We here show by Northern blots and in situ hybridization experiments that the expression of mammalian miRNAs can be regulated at the post-transcriptional level. In particular, miR-138 is spatially restricted to distinct cell types, while its precursor, pre-miR-138-2, is ubiquitously expressed throughout all tissues analyzed. Furthermore, pre-miR-138-2 is exported from the nucleus to the cytoplasm, suggesting that cleavage of this pre-miRNA by Dicer is restricted to certain tissues and cell types. Thus, differential processing of pre-miRNAs might be an alternative mechanism to control miRNA function.

Keywords: microRNAs; post-transcriptional regulation; Dicer; tissue-specific expression

INTRODUCTION

miRNAs are a family of small (~22 nucleotides [nt]), endogenous, noncoding RNAs that, by binding complementary sequences in the 3′ untranslated region (3′ UTR) of messenger RNAs (mRNAs), either mediate translational repression or direct mRNA cleavage (Pillai 2005). miRNAs are transcribed as mono- or polycistronic, long, primary precursor transcripts (pri-miRNAs) that are cleaved into ~70-nt precursor hairpins, known as pre-miRNAs, by the nuclear RNase III-like enzyme Drosha (Lee et al. 2003). Subsequently, pre-miRNA hairpins are exported to the cytoplasm by Exportin-5 (Yi et al. 2003; Bohnsack et al. 2004; Lund et al. 2004), where they are processed by a second RNase III-like enzyme, termed Dicer, into ~22-nt duplexes (Bernstein et al. 2001; Hutvágner et al. 2001; Ketting et al. 2001; Knight & Bass 2001), followed by the asymmetric assembly of one of the two strands into a functional miRNP or miRISC (Khvorova et al. 2003; Schwarz et al. 2003).

More than 800 miRNAs have so far been experimentally discovered in mammals (Lagos-Quintana et al. 2001, 2002; Bentwich et al. 2005) and some of them are highly conserved between invertebrates and vertebrates (Bartel 2004). However, through the development of increasingly sophisticated algorithms based on machine learning techniques, the number of predicted miRNAs currently amounts to a few thousand (Lim et al. 2003; Bentwich et al. 2005; Berezikov et al. 2005). Many mammalian miRNAs are tissue- and/or developmental stage-specifically expressed. Several microarray profiling studies have shown that the expression pattern of a large number of miRNAs can be attributed to regulatory sequences present in their promoters (Babak et al. 2004; Barad et al. 2004; Calin et al. 2004; Liu et al. 2004; Miska et al. 2004; Sempere et al. 2004). Furthermore, host genes harboring miRNA sequences in their intronic sites impose their pattern of expression to the respective miRNAs (Bartel 2004; Rodriguez et al. 2004).

The current view suggests that miRNA expression is mainly controlled at the transcriptional level. For example, the transcription factors MyoD, Mef2, and SRF determine the heart-specific expression of miR-1 (Zhao et al. 2005). A recent study by O'Donnell and colleagues (O'Donnell et al. 2005) shows that the proto-oncogene c-Myc activates the expression of the *miR-17-92* cluster. However, like other RNAs, miRNA expression could potentially be controlled at the post-transcriptional level (Pillai 2005). It has been shown in *Caenorhabditis elegans* that *miR-38* is regulated in a temporal manner by differential maturation of pre-miR-38 during development (Ambros et al. 2003). We here

[3]These authors contributed equally to this work.

Reprint requests to: Javier Martinez, Institute of Molecular Biotechnology of the Austrian Academy of Sciences, Dr.-Bohr-Gasse 3-5, A-1030 Vienna, Austria; e-mail: javier.martinez@imba.oeaw.ac.at; fax: +43 (1) 79044-110.

Article published online ahead of print. Article and publication date are at http://www.rnajournal.org/cgi/doi/10.1261/rna.2322506.

provide conclusive evidence that also mammalian miRNA expression can be regulated at the level of miRNA processing.

RESULTS AND DISCUSSION

As a first step in validating targets of a set of brain-specific miRNAs, we isolated total RNA from brain and other mouse tissues, as well as from HeLa cells, and performed Northern blots with miRNA-specific probes. As expected for *miR-138*, the mature ~23-nt miRNA was detectable only in brain tissue (Fig. 1A). In particular, we found that *miR-138* was expressed in the cerebrum, the cerebellum, and the midbrain of adult mice as well as in the murine neuroblastoma cell line N2A (Fig. 1B). Strikingly, its putative ~69-nt precursor was present in all tissues and cells analyzed (Fig. 1A, left panel; 1B), suggesting that the ubiquitously expressed precursor is processed into the mature miRNA in a tissue-specific manner.

Two putative precursors were recently predicted for miR-138, termed "pre-miR-138-1" and "pre-miR-138-2," which are encoded on different chromosomal loci and are 62 nt and 69 nt in size, respectively (Lagos-Quintana et al. 2002; Griffiths-Jones 2004; Weber 2005). Multiple sequence alignments (Schwartz et al. 2000) of the two chromosomal regions showed high conservation of the mature miRNA among different vertebrate species, whereas only the locus of miR-138-2 showed an overall conservation pattern in the flanking sequences (Supplemental Material).

To check that (1) the ~69-nt band is indeed a precursor miRNA and, if so, (2) which of the two precursors is ubiquitously expressed, we performed Northern blots with total RNA isolated from HeLa cells and probed against the mature sequence as well as sequences specific for the loop regions of the two different precursors. Interestingly, the probe against the mature miR-138 showed a single band at 69 nt, which was also revealed by a probe against the loop region of pre-miR-138-2 (Fig. 1C). Mismatches in the probes against the sequences of the mature miR-138 and of pre-miR-138-2 abolished detection of the 69-nt band (Supplemental Material), indicating that the ubiquitously expressed ~69-nt band shown in Figure 1, A and B, is indeed a precursor of miR-138, and that the mature miR-138 derives from pre-miR-138-2. In agreement with this, we were not able to detect a 62-nt band that would correspond to pre-miR-138-1 (Fig. 1C) either with a mature probe or with a probe against the loop region of pre-miR-138-1.

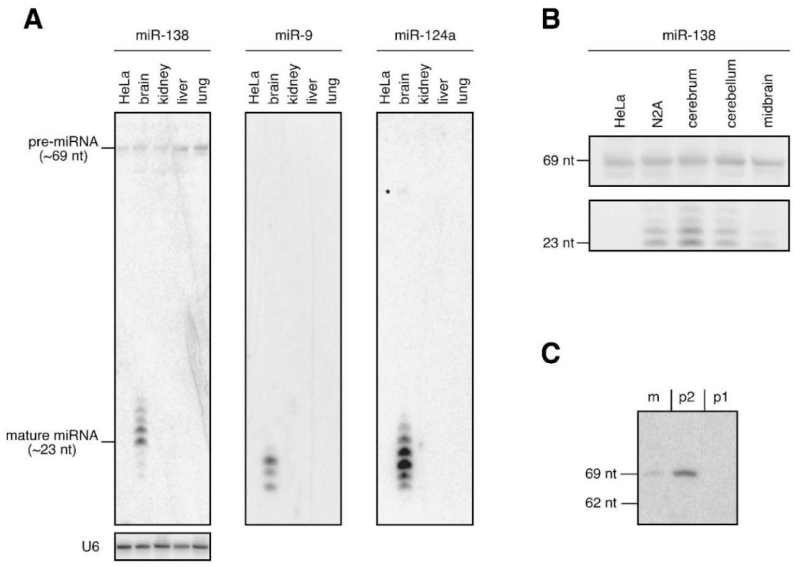

FIGURE 1. (*A*) Northern blot analysis of different brain-specific miRNAs. Thirty micrograms of total RNA from HeLa cells and from different mouse tissues were blotted and probed with a 5′-radiolabeled, LNA-modified oligodeoxynucleotide complementary to the indicated miRNAs. Equal loading of total RNA on the gel was verified by hybridizing with a probe complementary to the U6 snRNA. Note that only the precursor of miR-138 displays a ubiquitous pattern. The asterisk highlights the faint band of pre-miR-124a seen in the lane of murine brain at ~57 nt. (*B*) Northern blot analysis of total RNA isolated from HeLa cells, from the murine neuroblastoma cell line N2A, and from different neuronal tissues of murine brain showing the tissue-specific processing of the ubiquitous 69-nt pre-miRNA. The band at 69 nt corresponds to the precursor, which is present in all cells and tissues that were analyzed. The 23- to 24-nt bands represent the mature miR-138, which is specifically expressed in the cerebrum as well as in the cerebellum, midbrain, and N2A cells, albeit to a lower extent. (*C*) Northern blot analysis of pre-miR-138-2 and pre-miR-138-1. One hundred micrograms of total RNA from murine brain were blotted and probed with 5′-radiolabeled, LNA-modified oligonucleotide probes complementary to the mature sequence of miR-138 (m), to the terminal loop of pre-miR-138-2 (p2), and to the terminal loop of pre-miR-138-1 (p1).

To further investigate the overall distribution of miR-138 and its precursor, we performed in situ hybridizations with 3′ DIG-labeled LNA oligonucleotide probes on cryo-sections of E17 mouse embryos (Fig. 2A) and adult brain (Fig. 2B). We observed a strong staining in the central nervous system (CNS) for mature miR-138 (Fig. 2A, left panel). In particular, miR-138 was primarily localized to most neurons in the hippocampus and to specific regions of the neocortex, but also to the cerebellum (Fig. 2A, left panel; 2B, upper panel). This clearly demonstrates that expression of miR-138 is not uniform throughout the brain but restricted to distinct neuronal populations. Surprisingly, *miR-138* was also expressed in fetal liver (Fig. 2A, left panel; 2C) but not in adult liver (Fig. 2C), indicating that the expression of miR-138 is also developmentally regulated. To confirm the ubiquitous expression observed for pre-miR-138-2 in Northern blots performed with total

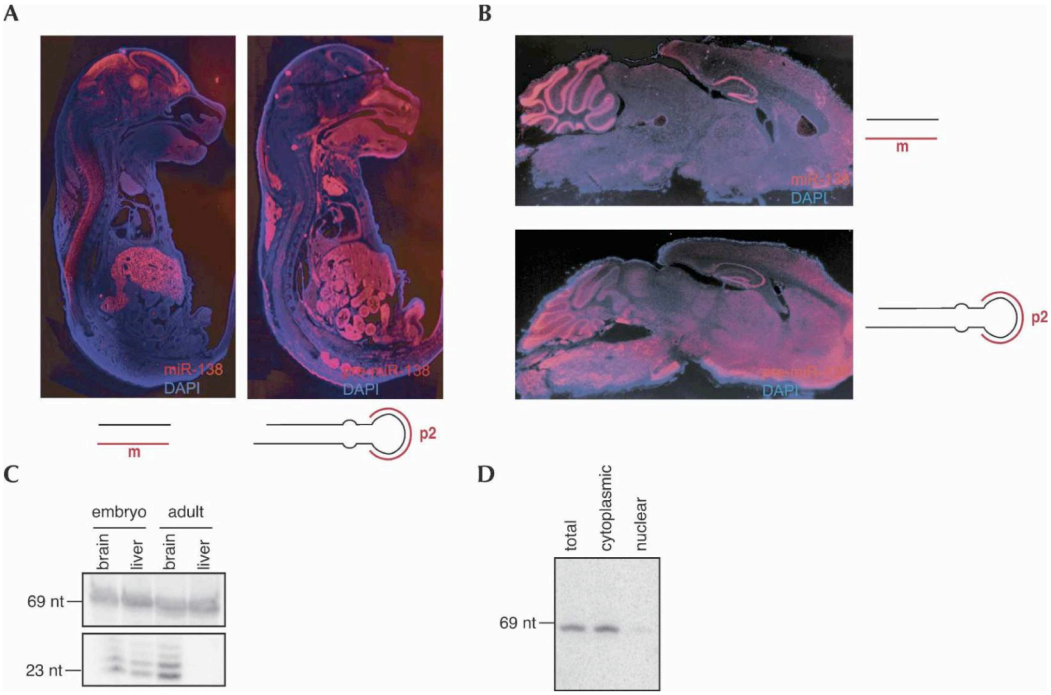

FIGURE 2. (*A*) In situ hybridization experiment on cryo-sections of E17 mouse embryos using LNA-modified probes that recognize mature miR-138 (*left* panel) or pre-miR-138-2 (*right* panel). The probe against mature miR-138 shows a strong expression in neuronal tissues (brain, CNS) and also in fetal liver, while the probe hybridizing to pre-miR-138-2 gives a strong signal in almost all tissues of the embryo. The seemingly low level of pre-miR-138-2 in brain can be explained by a low cellular density of the brain region as well as to a short exposure time used to prevent overexposure of tissues with higher cellular density. Magnifications of the fetal brain region can be seen in the Supplemental Material, where exposure time has been optimized to visualize expression of both mature miR-138 and pre-miR-138-2. (*B*) In situ hybridization experiments on cryo-sections of adult mouse brain using LNA-modified oligonucleotide probes that recognize mature miR-138 (*upper* panel) or pre-miR-138-2 (*lower* panel). miR-138 is primarily located to specific regions of the neocortex, most neurons in the hippocampus, and granule and purkinje cells of the cerebellum, while pre-miR-138-2 is essentially uniformly distributed. Magnifications of the cerebellum can be seen in the Supplemental Material. (*C*) Northern blot analysis of miR-138 expression in fetal and adult brain and liver. One hundred micrograms of total RNA prepared from the indicated tissues were blotted and probed for miR-138. In the mouse embryo, miR-138 is expressed in both brain and liver, which is in agreement with the findings in the in situ hybridization experiments. In the adult, miR-138 is restricted to brain. (*D*) Northern blot of total HeLa RNA and cytoplasmic and nuclear RNA fractions from HeLa cells probed against pre-miR-138-2. The band at 69 nt corresponds to pre-miR-138-2 that is mainly found in the cytoplasmic fraction, indicating nuclear export of the precursor.

RNA from adult tissues, we prepared a probe recognizing the loop region of the pre-miR-138-2 hairpin. Like Northern blots, in situ hybridizations showed a broad expression of pre-miR-138-2 in most organs of the embryo (Fig. 2A, right panel) as well as in adult brain (Fig. 2B, lower panel). To summarize, these data (Northern blots and in situ hybridizations) suggest that pre-miR-138-2 processing is both temporally and spatially regulated.

How is this differential processing achieved? A tempting hypothesis is that the export of pre-miR-138-2 is impaired in all tissues except brain, thus preventing cleavage by Dicer in the cytoplasm. To evaluate this possibility, we isolated cytoplasmic and nuclear RNA from HeLa cells, where pre-miR-138-2 is not processed, and examined its subcellular distribution. Northern blot analysis showed that the precursor is effectively exported to the cytoplasm (Fig. 2D), indicating that cleavage by Dicer could be the regulated step.

We envision that tissue-specific expression could be achieved either by an activator present in tissues that express *miR-138* or, alternatively, by an inhibitor acting on tissues that lack expression of *miR-138*. We were able to show that recombinant Dicer enzyme is able to convert pre-miR-138-2 into mature miR-138, a result that rules out the activator model (Fig. 3A). Thus, we favor the presence of an inhibitory factor, which binds pre-miR-138-2 and prevents its conversion into a mature miR-138 by Dicer in all tissues not expressing *miR-138*. This hypothesis is fostered by in vitro experiments, where the addition of increasing amounts of HeLa cytoplasmic extracts readily abolished processing of pre-miR-138-2 by recombinant Dicer (Fig. 3B). Importantly, processing of pre-miR-19a, a miRNA that is normally expressed in HeLa cells (Lagos-Quintana et al. 2001), was not abolished by titrating increasing amounts of HeLa cytoplasmic extracts (Fig.

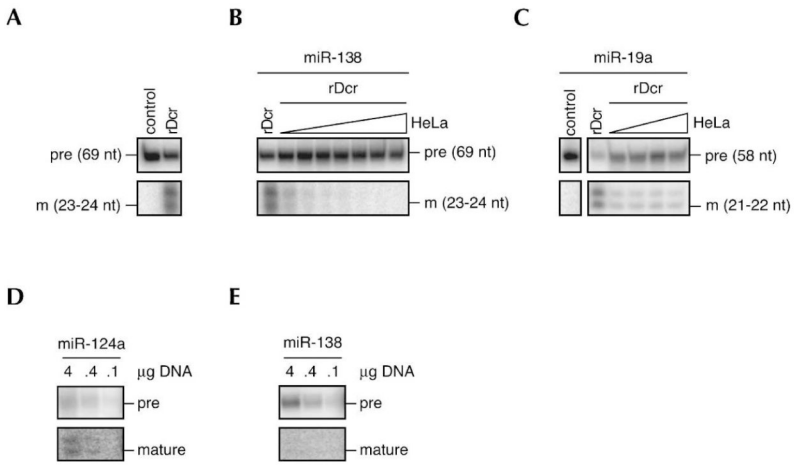

FIGURE 3. (*A*) Processing reaction of pre-miR-138-2 into mature miR-138 by recombinant Dicer (rDcr) resolved on a 15% denaturing PAGE. (*B*) As in *A*. The addition of increasing amounts of HeLa cytoplasmic extract effectively abolishes the processing of pre-miR-138-2. The band corresponding to the respective pre-miRNA is indicated by "pre," whereas the band representing the mature miRNA is designated by "m." (*C*) Processing of pre-miR-19a into mature miR-19a is not abolished by addition of increasing amounts of HeLa cytoplasmic extract. The efficiency of processing is reduced by the addition of HeLa cytoplasmic extracts; however, the level of processing does not decrease with higher amounts of HeLa cytoplasmic extracts. (*D*) HeLa cells were transfected with the indicated amounts of a plasmid encoding the sequence of pre-miR-124a. The conversion of pre-miR-124a into mature miR-124a was monitored by Northern blotting. (*E*) HeLa cells were transfected with the indicated amounts of a plasmid encoding the sequence of pre-miR-138-2. In contrast to pre-miR-124a, HeLa cells failed to process pre-miR-138-2 into mature miR-138. Note that pre-miR-138-2 is more abundant than pre-miR-124a.

3C). We further analyzed pre-miRNA processing in living cells. For this purpose, we transfected HeLa cells transiently with plasmids encoding either pre-miR-124a or pre-miR-138-2 under the control of the H1 promoter. Northern blots showed that pre-miR-124a was converted into the mature miR-124a, whereas pre-miR-138-2 was not processed (Fig. 3D,E). This suggests that HeLa cells, and possibly all other tissues and cells that do not express *miR-138*, may contain a factor that specifically recognizes pre-miR-138-2 and inhibits its processing by Dicer. Thus, tissues and cells that do express *miR-138* may lack this factor or may render it inactive, allowing Dicer cleavage to occur (Fig. 4).

In this report we demonstrate that differential processing of precursor miRNAs into mature miRNAs leads to tissue- and developmental-specific miRNA expression in mammals. The presence of an unprocessed miRNA precursor in most tissues of the organism is intriguing. It could be envisioned that the unprocessed precursor might play a different role in the cell, irrespective of the function of the mature miRNA. This novel mechanism could be a more general feature for the regulation of miRNA expression. Obviously, we are left with the question of why cells employ such a complex and energy wasteful method of restricting the function of one particular miRNA to certain cellular populations. Clearly, such regulation allows higher expression stringency, but also an opportunity for quick regulation. The precursor form of the functional miRNA is already expressed, and the cells can quickly produce the mature miRNA by modifying the regulator. This could be very important for fast responses like coupling neuronal processes in time, like LTP gene expression.

MATERIALS AND METHODS

Isolation of total RNA from cells, mouse tissues, and Northern blotting

Isolation of total RNA from cultured cells or tissues and subsequent Northern blotting was performed as previously described (Lagos-Quintana et al. 2001). Twenty micrograms of total RNA were separated in a 15% polyacrylamide gel (20 × 25 cm) containing 8 M urea (SEQUAGEL, National Diagnostics), transferred to a Hybond-N+ membrane (Amersham Biosciences), fixed by ultraviolet cross-linking (2× auto cross-link on a Stratalink 2400 [Stratagene]), and subsequently baked for 1 h at 80°C. Membranes were probed with 10 pmol of 5′ ^{32}P-labeled (T4 polynucleotide kinase [New England Biolabs]) DNA/LNA (locked nucleic acid) modified oligonucleotides (Proligo), complementary to the mature and precursor miRNAs. We used DNA/LNA probes, where every third position was substituted by a LNA nucleotide, in order to obtain an improved miRNA detection (Valoczi et al. 2004). LNA nucleotides are indicated by "*X." The sequences for the probes were as follows: miR-138, 5′-C*GGC*CTG*ATT*CAC*AAC*ACC*AGC*T-3′. To differentiate between miRNA precursors and mature miRNAs, the following probes against the loop regions of the two different hairpins were designed and labeled: pre-miR-138-1, C*GTT*CTC*TGA*TTG*GCA*A-3′; pre-miR-138-2, 5′-G*GTA*AGA*GGA*TGC*GCT*GCT*CGT-3′. As a control for specificity of the probes, we used mismatch probes against pre-miR-138-2 and miR-138: mismatch-loop, 5′-TAAGAGGATGCGCTGCTAAAAAACCTGATTCACAACACCA-3′, and mismatch-mature, 5′-CGGCCTGATTAAAAAAACCAGCT-3′.

Prehybridization of membranes was carried out in a buffer containing 5× SSC, 20 mM Na_2HPO_4 (pH 7.2), 7% SDS, 1× Denhardt's solution, and 0.1 mg/mL sonicated salmon sperm DNA (Stratagene). Hybridizations were carried out in the same solution at 80°C. 5′-^{32}P-labeled probes were heated for 1 min at 95°C before addition to the hybridization solution. After hybridization, the membranes were washed twice in 5× SSC, 5% SDS and once in 1× SSC, 1% SDS at 70°C for 1–2 min each. Northern blots were then analyzed by PhosphorImaging (Storm 860, Molecular Dynamics).

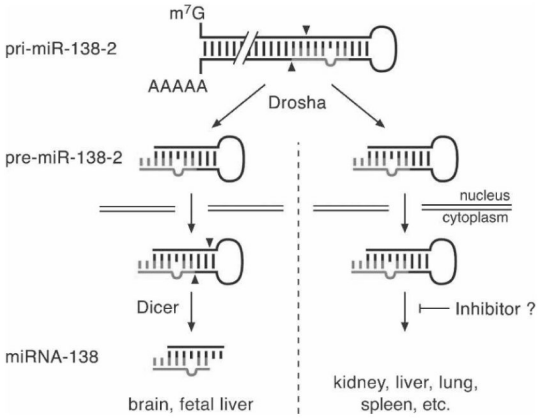

FIGURE 4. Model depicting how differential processing of an otherwise ubiquitously expressed pre-miRNA mediates tissue- and/or developmental stage-specific expression of the mature miRNA. In both tissues, expressing or not expressing the mature miR-138, its gene is transcribed into pri-miR-138-2, which is cleaved in the nucleus by Drosha into pre-miR-138-2 and then exported to the cytoplasm. Here, the presence or the absence of an inhibitory factor determines whether pre-miR-138-2 becomes processed or not, thus leading to differential expression of mature miR-138.

Cell culture

HeLa human cervix-carcinoma cells as well as N2A murine neuroblastoma cells were grown in Dulbecco's modified Eagle's medium (DMEM) (Invitrogen) supplemented with 10% fetal calf serum (FCS) (Invitrogen), 100 u/mL penicillin (Sigma-Aldrich), 100 μg/mL penicillin/streptomycin (Sigma-Aldrich), and 20 mM HEPES (pH 7.3) at 37°C in an atmosphere containing 5% CO_2 in 15-cm dishes up to 90%–95% confluency.

HeLa cells were transfected with the indicated amounts of pSUPER.neo+GFP plasmid (Oligoengine), where the sequences of pre-miR-124a or pre-miR-138-2 were previously inserted between the BglII and the HindIII restriction sites. For pre-miR-124a, we used 124a-fwd, 5′-GATCCCCGTGTTCACAGCGGACCTTGATTTAAATGTCCATACAATTAAGGCACGCGGTGAATGCCATTTTTA-3′, and 124a-rev, 5′-AGCTTAAAAATGGCATTCACCGCGTGCCTTAATTGTATGGACATTTAAATCAAGGTCCGCTGTGAACACGGG-3′. For pre-miR-138-2, we used 138-2-fwd, 5′-GATCCCCAGCTGGTGTTGTGAATCAGGCCGACGAGCAGCGCATCCTCTTACCCGGCTATTTCACGACACCAGGGTTTTTA-3′, and 138-2-rev, 5′-AGCTTAAAAACCCTGGTGTCGTGAAATAGCCGGGTAAGAGGATGCGCTGCTCGTCGGCCTGATTCACAACACCAGCTGGG-3′. Transfections were perfomed in 6-well plates (Nunc) using the Lipofectamine 2000 reagent (Invitrogen) with concentrations according to the product manual. Total RNA was isolated 6 h after the start of transfection as described above.

Preparation of cellular extracts

HeLa or N2A cells were briefly washed with 1× PBS and harvested in 1 mL of a buffer containing 100 mM KCl, 5 mM $MgCl_2$, 10% glycerol, 30 mM HEPES (pH 7.4), 0.1 mM AEBSF, and 0.5 mM DTT by scraping with a rubber policeman. Cells were effectively lysed by sonication. The remaining cell debris was removed by centrifugation.

Nuclear and cytoplasmic extracts were prepared as previously described (Lehnertz et al. 2003). Briefly, to prepare cytoplasmic extracts, cells were harvested by trypsinization, washed, and pelleted by centrifugation. The pellet was resuspended in 1× PBS and pelleted again by spinning. PBS was removed, and the cell pellet was resuspended in cold buffer A (10 mM HEPES at pH 7.9, 10 mM KCl, 0.1 mM EDTA, 0.1 mM EGTA, 1 mM DTT, 0.5 mM PMSF) by gentle pipetting. After swelling, a 10% solution of Nonidet NP–40 (Fluka) was added and the tube was vigorously vortexed. The homogenate was centrifuged, and the supernatant containing the cytoplasm and the cytoplasmic RNA was transferred to a fresh tube and subsequently used for RNA extraction and Northern blot analysis. Nuclei were prepared by centrifugation of the cells through a cushion of nuclear isolation buffer (20% [v/v] Ficoll-Paque Pharmacia, 80 mM Tris/HCl at pH 7.4, 8 mM $MgCl_2$, 8 mM $CaCl_2$, 1.6% [v/v] NP–40, 1.3% [v/v] Triton X-100, and 0.001% [v/v] DMSO). Nuclear pellets were washed once in ice-cold PBS, snap-frozen in liquid nitrogen, and subsequently used for the preparation of nuclear RNA. To obtain nuclear extracts, nuclei were resuspended in immunoprecipitation (IP) buffer (45 mM HEPES/NaOH at pH 7.5, 0.45 M NaCl, 0.9 mM EDTA, 0.9% [v/v] NP–40, 8.7% [v/v] glycerol, 1 mM NaF, 10 mM β-glycerophosphate, 1 tablet/50 mL protease inhibitor cocktail [Roche, no. 1836145]) and sonicated. After centrifugation, the supernatant was snap-frozen in liquid nitrogen and subsequently used for RNA extraction and Northern blot analysis.

In vitro processing assays

For in vitro processing assays, DNA templates encoding the sequences of various miRNAs were transcribed by T7 polymerase (MEGAshortscript T7, Ambion) in the presence of ^{32}P-α-UTP (Amersham), thus generating radiolabeled, synthetic precursor miRNAs. The DNA templates were annealed to a T7 runoff DNA oligonucleotide (AATTTAATACGACTCACTATAGG) that spans the T7 promoter site. The sequences used were as follows: pre-miR-19a, 5′-TCAGTTTTGCATAGATTTGCACAACTACATTCTTCTTGTAGTGCAACTATGCAAAACCTATAGTGAGTCGTATTAA-3′; pre-miR-138-2, 5′-AACCCTGGTGTCGTGAAATAGCCGGGTAAGAGGATGCGCTGCTCGTCGGCCTGATTCACAACACCAGCCTATAGTGAGTCGTATTAA-3′. These synthetic precursors were folded into their hairpin-shaped structure by heating for 1 min at 95°C and cooling slowly to room temperature. Processing with recombinant Dicer was performed as previously described (Zhang et al. 2002). Precursors were used at a concentration of 10 nM and were pretreated for 10 min at 30°C with increasing amounts of HeLa cytoplasmic extract (2, 4, 6, 8, 16, 24, and 32 μg protein for pre-miR-138-2; 2, 6, 16, and 32 μg protein for pre-miR-19a). After 2 min incubation at 37°C, the reaction products were separated on a 15% denaturing PAGE and visualized by autoradiography.

In situ hybridizations

All mice were maintained at the animal facility at the IMP, under pathogen-free conditions. C57BL/6 mice were mated to generate embryos for analyses and the morning of the vaginal plug was considered as E0.5. Embryos, livers, and brains were post-fixed

in 4% paraformaldehyde, cryoprotected (30% sucrose in PBS), embedded in Tissue-Tek OCT compound, and cryosectioned. Ten-micron cryosections were pretreated, hybridized with LNA digoxygenin-labeled probes (Exiqon), and washed according to Schaeren-Wiemers and Gerfin-Moser (1993), with some modifications. Probe sequences were as follows: miR-122a, 5′-ACAAAC ACCATTGTCACACTCCA-3′; miR-138, 5′-CGGCCTGATTCA CAACACCAGCT-3′; and pre-miR-138-2, 5′-GGTAAGAGGATG CGCTGCTCGT-3′. Briefly, sections were fixed in 4% paraformaldehyde for 10 min, acetylated, and treated with 5 μg/mL proteinase K (Roche) in PBS for 5 min, washed, and prehybridized for 4 h at room temperature. Hybridization with 22-nt LNA probes ($T_m \sim 80°C$) was performed at 55°C overnight. Slides were then washed at 60°C and incubated with alkaline phophatase-conjugated goat anti-DIG Fab fragments (1:2000 [Roche]) at 4°C overnight. Fluorescent detection was performed using a Fast Red reaction (Dako Cytomation) for 1 h at room temperature. Sections were analyzed with a with a Zeiss Axioplan-2 microscope and photographed with a digital camera (Coolsnap HQ, Photometrics). A subset of images was adjusted for levels, brightness, contrast, hue, and saturation with Adobe Acrobat 7.0 imaging software to optimally visualize the expression patterns.

SUPPLEMENTAL MATERIAL

Supplemental Material can be found at http://www.imba.oeaw.ac.at/index.php?id=142.

ACKNOWLEDGMENTS

We thank Stefan Ameres, Stefan Weitzer, and the members of the laboratory for encouragement and suggestions during the completion of this work, and Prof. Renée Schroeder for critically reading the manuscript. J.M. is a Junior Group Leader at IMBA. P.J.F.L. is funded by the Boehringer Ingelheim Fonds Ph.D. Scholarship. M.A. was supported by an EMBO long-term fellowship and a Marie Curie fellowship.

Received December 12, 2005; accepted April 24, 2006.

REFERENCES

Ambros, V., Lee, R.C., Lavanway, A., Williams, P.T., and Jewell, D. 2003. MicroRNAs and other tiny endogenous RNAs in *C. elegans*. *Curr. Biol.* **13:** 807–818.

Babak, T., Zhang, W., Morris, Q., Blencowe, B.J., and Hughes, T.R. 2004. Probing microRNAs with microarrays: Tissue specificity and functional inference. *RNA* **10:** 1813–1819.

Barad, O., Meiri, E., Avniel, A., Aharonov, R., Barzilai, A., Bentwich, I., Einav, U., Gilad, S., Hurban, P., Karov, Y., et al. 2004. MicroRNA expression detected by oligonucleotide microarrays: System establishment and expression profiling in human tissues. *Genome Res.* **14:** 2486–2494.

Bartel, D.P. 2004. MicroRNAs: Genomics, biogenesis, mechanism, and function. *Cell* **116:** 281–297.

Bentwich, I., Avniel, A., Karov, Y., Aharonov, R., Gilad, S., Barad, O., Barzilai, A., Einat, P., Einav, U., Meiri, E., et al. 2005. Identification of hundreds of conserved and nonconserved human microRNAs. *Nat. Genet.* **37:** 766–770.

Berezikov, E., Guryev, V., van de Belt, J., Wienholds, E., Plasterk, R.H., and Cuppen, E. 2005. Phylogenetic shadowing and computational identification of human microRNA genes. *Cell* **120:** 21–24.

Bernstein, E., Caudy, A.A., Hammond, S.M., and Hannon, G.J. 2001. Role for a bidentate ribonuclease in the initiation step of RNA interference. *Nature* **409:** 363–366.

Bohnsack, M.T., Czaplinski, K., and Gorlich, D. 2004. Exportin 5 is a RanGTP-dependent dsRNA-binding protein that mediates nuclear export of pre-miRNAs. *RNA* **10:** 185–191.

Calin, G.A., Liu, C.G., Sevignani, C., Ferracin, M., Felli, N., Dumitru, C.D., Shimizu, M., Cimmino, A., Zupo, S., Dono, M., et al. 2004. MicroRNA profiling reveals distinct signatures in B cell chronic lymphocytic leukemias. *Proc. Natl. Acad. Sci.* **101:** 11755–11760.

Griffiths-Jones, S. 2004. The microRNA registry. *Nucleic Acids Res.* **32:** D109–D111.

Hutvágner, G., McLachlan, J., Bálint, É., Tuschl, T., and Zamore, P.D. 2001. A cellular function for the RNA interference enzyme Dicer in small temporal RNA maturation. *Science* **93:** 834–838.

Ketting, R.F., Fischer, S.E., Bernstein, E., Sijen, T., Hannon, G.J., and Plasterk, R.H. 2001. Dicer functions in RNA interference and in synthesis of small RNA involved in developmental timing in *C. elegans*. *Genes & Dev.* **15:** 2654–2659.

Khvorova, A., Reynolds, A., and Jayasena, S.D. 2003. Functional siRNAs and miRNAs exhibit strand bias. *Cell* **115:** 209–216.

Knight, S.W. and Bass, B.L. 2001. A role for the RNase III enzyme DCR-1 in RNA interference and germ line development in *C. elegans*. *Science* **2:** 2.

Lagos-Quintana, M., Rauhut, R., Lendeckel, W., and Tuschl, T. 2001. Identification of novel genes coding for small expressed RNAs. *Science* **294:** 853–858.

Lagos-Quintana, M., Rauhut, R., Yalcin, A., Meyer, J., Lendeckel, W., and Tuschl, T. 2002. Identification of tissue-specific microRNAs from mouse. *Curr. Biol.* **12:** 735–739.

Lee, Y., Ahn, C., Han, J., Choi, H., Kim, J., Yim, J., Lee, J., Provost, P., Radmark, O., Kim, S., et al. 2003. The nuclear RNase III Drosha initiates microRNA processing. *Nature* **425:** 415–419.

Lehnertz, B., Ueda, Y., Derijck, A.A., Braunschweig, U., Perez-Burgos, L., Kubicek, S., Chen, T., Li, E., Jenuwein, T., and Peters, A.H. 2003. Suv39h-mediated histone H3 lysine 9 methylation directs DNA methylation to major satellite repeats at pericentric heterochromatin. *Curr. Biol.* **13:** 1192–1200.

Lim, L.P., Glasner, M.E., Yekta, S., Burge, C.B., and Bartel, D.P. 2003. Vertebrate microRNA genes. *Science* **299:** 1540.

Liu, C.G., Calin, G.A., Meloon, B., Gamliel, N., Sevignani, C., Ferracin, M., Dumitru, C.D., Shimizu, M., Zupo, S., Dono, M., et al. 2004. An oligonucleotide microchip for genome-wide microRNA profiling in human and mouse tissues. *Proc. Natl. Acad. Sci.* **101:** 9740–9744.

Lund, E., Guttinger, S., Calado, A., Dahlberg, J.E., and Kutay, U. 2004. Nuclear export of microRNA precursors. *Science* **303:** 95–98.

Miska, E.A., Alvarez-Saavedra, E., Townsend, M., Yoshii, A., Sestan, N., Rakic, P., Constantine-Paton, M., and Horvitz, H.R. 2004. Microarray analysis of microRNA expression in the developing mammalian brain. *Genome Biol.* **5:** R68.

O'Donnell, K.A., Wentzel, E.A., Zeller, K.I., Dang, C.V., and Mendell, J.T. 2005. c-Myc-regulated microRNAs modulate E2F1 expression. *Nature* **435:** 839–843.

Pillai, R.S. 2005. MicroRNA function: Multiple mechanisms for a tiny RNA? *RNA* **11:** 1753–1761.

Rodriguez, A., Griffiths-Jones, S., Ashurst, J.L., and Bradley, A. 2004. Identification of mammalian microRNA host genes and transcription units. *Genome Res.* **14:** 1902–1910.

Schaeren-Wiemers, N. and Gerfin-Moser, A. 1993. A single protocol to detect transcripts of various types and expression levels in neural tissue and cultured cells: In situ hybridization using digoxigenin-labelled cRNA probes. *Histochemistry* **100:** 431–440.

Schwartz, S., Zhang, Z., Frazer, K.A., Smit, A., Riemer, C., Bouck, J., Gibbs, R., Hardison, R., and Miller, W. 2000. PipMaker–A web server for aligning two genomic DNA sequences. *Genome Res.* **10:** 577–586.

Schwarz, D.S., Hutvagner, G., Du, T., Xu, Z., Aronin, N., and Zamore, P.D. 2003. Asymmetry in the assembly of the RNAi enzyme complex. *Cell* **115:** 199–208.

Sempere, L.F., Freemantle, S., Pitha-Rowe, I., Moss, E., Dmitrovsky, E., and Ambros, V. 2004. Expression profiling of mammalian microRNAs uncovers a subset of brain-expressed microRNAs with possible roles in murine and human neuronal differentiation. *Genome Biol.* **5:** R13.

Valoczi, A., Hornyik, C., Varga, N., Burgyan, J., Kauppinen, S., and Havelda, Z. 2004. Sensitive and specific detection of microRNAs by northern blot analysis using LNA-modified oligonucleotide probes. *Nucleic Acids Res.* **32:** e175.

Weber, M.J. 2005. New human and mouse microRNA genes found by homology search. *FEBS J.* **272:** 59–73.

Yi, R., Qin, Y., Macara, I.G., and Cullen, B.R. 2003. Exportin-5 mediates the nuclear export of pre-microRNAs and short hairpin RNAs. *Genes & Dev.* **17:** 3011–3016.

Zhang, H., Kolb, F.A., Brondani, V., Billy, E., and Filipowicz, W. 2002. Human Dicer preferentially cleaves dsRNAs at their termini without a requirement for ATP. *EMBO J.* **21:** 5875–5885.

Zhao, Y., Samal, E., and Srivastava, D. 2005. Serum response factor regulates a muscle-specific microRNA that targets Hand2 during cardiogenesis. *Nature* **436:** 214–220.

Supplemental Figures

Obernosterer *et al.*, Figure S1

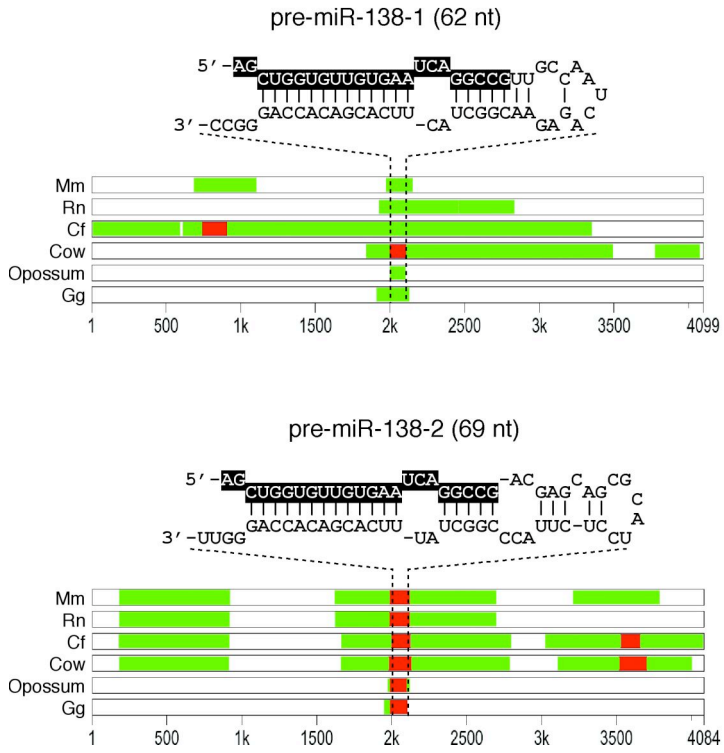

Figure S1.
Multiple sequence alignments of the flanking regions of chromosomal loci encoding miR-138. Regions in red represent >90%, and regions in green 50–90% sequence homology. Note, that the pre-miR-138-2 surrounding sequences are highly conserved, while this is not the case for miR-138-1. (Abbreviations: Mm = Mus musculus; Rn = Rattus norvegicus; Cf = Canis familiaris).

Obernosterer *et al.*, Figure S2

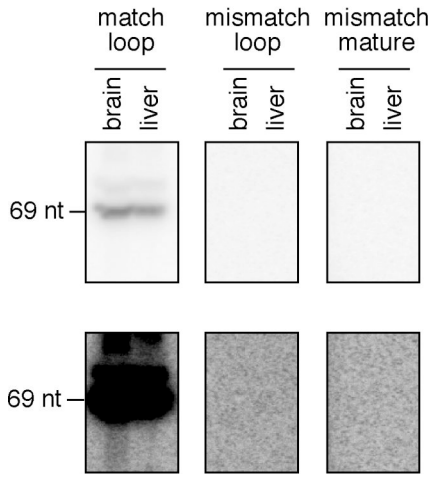

Figure S2.
Northern blot analysis of total RNA from adult mouse brain and liver. A probe containing a central, contiguous 6-nt mismatch spanning the boundary between the mature miRNA and the loop region (mismatch loop) does not recognize the 69-nt band that is observed when probing for the loop or pre-miR-138-2 (match loop). A probe against the mature miR-138-2 that contains mismatched nucleotides (mismatch mature) also unable to detect the 69-nt band. The lower panel shows an enhanced picture.

Obernosterer *et al.*, Figure S3

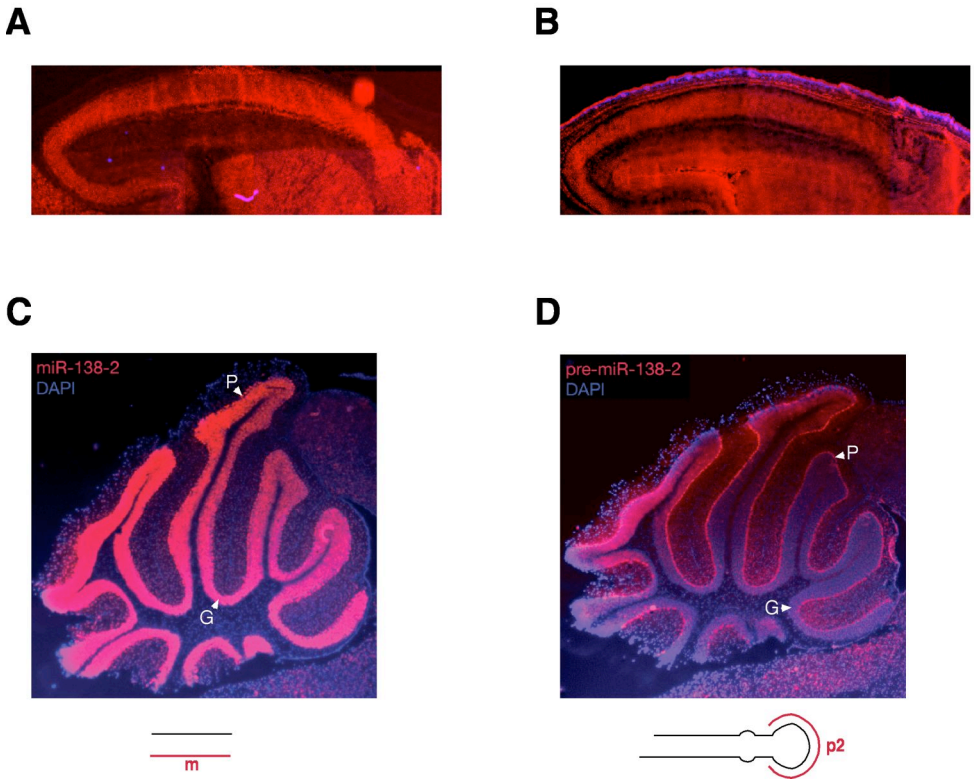

Figure S3.
(A) High magnification images of in situ hybridization experiments on cryo-sections of fetal mouse brain, showing the expression of mature miR-138 in neocortex.
(B) As (A) with the exception that the section was probed for pre-miR-138-2.
(C) High magnification images of in situ hybridization experiments on cryo-sections of adult mouse cerebellum, showing the expression of mature miR-138 in the granule cells (G) and in the Purkinje cell layer (P) of the cerebellum.
(D) The levels of pre-miR-138-2 are lower in the above mentioned cell layers, indicating an efficient conversion of pre-miR-138-2 into the mature miR-138, and a consequent depletion of the precursor.

Obernosterer *et al.*, Figure S4

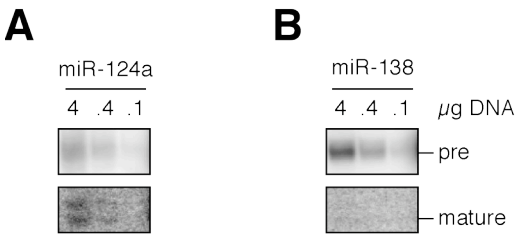

Figure S4. Northern blot analysis of pre-miRNA processing in HeLa cells.
(A) HeLa cells were transfected with the indicated amounts of a plasmid encoding the sequence of pre-miR-124a. The conversion of pre-miR-124a into mature miR-124a was monitored by Northern blotting.
(B) HeLa cells were transfected with the indicated amounts of a plasmid encoding the sequence of pre-miR-138-2. In contrast to pre-miR-124a, HeLa cells failed to process pre-miR-138-2 into mature miR-138. Note that pre-miR-138-2 is more abundant than pre-miR-124a.

4.3. Analyzing the mechanism for differential, context-dependent microRNA processing

4.3.1. An inhibitory factor blocks processing of pre-miR-138-2

Since the *in vitro* processing experiments clearly indicate the existence of a specific negative regulator for Dicer-mediated cleavage of pre-miR-138-2, the most intriguing and immediate questions were, what constitutes this inhibitory factor, and does it act *in trans* or *in cis?* We addressed this problem by splitting the *in vitro* cleavage assay with recombinant Dicer and cellular extracts into two parts: first, the 5′ radiolabeled substrate was pre-incubated in protein extracts that are thought to either contain or lack the inhibitor. Second, following proteinase K digestion, phenol-chloroform extraction of the RNA, ethanol precipitation and refolding in RNA structure buffer, cleavage by recombinant Dicer was evaluated. If the inhibitory factor acted *in trans*, e.g. by modifying the precursor, a difference in processing efficiency should be visible even after removing it; if not, this would indicate that the inhibitory factor acted *in cis,* meaning that it needs to bind the precursor in order to block processing by Dicer. Since fluorescence *in situ* hybridization experiments showed that miR-138 is matured in fetal liver but is absent in adult liver, I chose to generate cellular extracts from these two tissues.

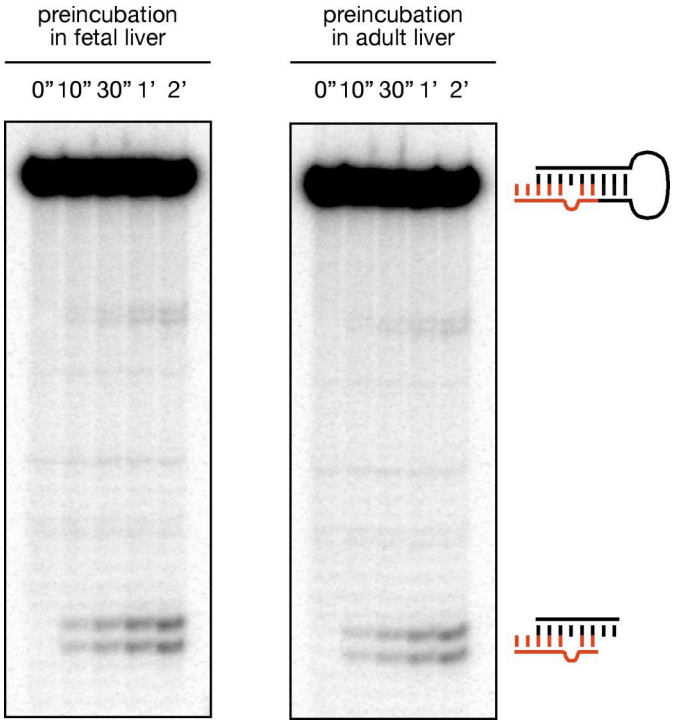

Figure 4. *In vitro* processing assay of pre-miR-138-2 by recombinant Dicer.
5′-end radiolabeled pre-miR-138-2 was pre-incubated in fetal (middle panel) or adult mouse liver extracts (right panel). Dicer-mediated cleavage was assessed after removing the protein fraction by proteinase K digest, phenol/chloroform extraction, ethanol precipitation and reannealing in assay-buffer. The left panel displays a control cleavage assay performed in the presence of high concentrations of bulk RNA (tRNA).

Figure 4 demonstrates that there are no visible differences in the processing of substrates that were differentially pre-treated prior to Dicer cleavage. This indicates that an enzymatic modification of pre-miR-138-2 during the pre-incubation is rather unlikely to be the cause of inhibition. First, processing of pre-miR-138-2 by recombinant Dicer is abolished very quickly after the addition of an inhibiting cellular extract. Second and more important, a longer pre-incubation in the extract did not affect the subsequent enzymatic processing of the substrate that was carried out after removing the protein present in the extract by proteinase K digestion. Furthermore, one can also rather disregard an RNA-molecule as the inhibiting factor that could anneal to parts of the pre-miR-138-2 hairpin thereby altering the overall geometry and thus impeding processing. Such an RNA inhibitor should have been imported into the processing reaction during the phenol-chloroform extraction and should have annealed to pre-miR-138-2 during refolding in the assay buffer. The most plausible candidate for the inhibitor therefore is a protein that, by interacting specifically with pre-miR-138-2, abolishes cleavage by Dicer. In tissues that do mature pre-miR-138-2 this protein may not be expressed or may be modified—by alternative splicing or post-translationally—to render it unable to bind pre-miR-138-2.

4.3.2. How does the inhibitor recognize pre-miR-138-2?

A recurring question concerning post-transcriptional regulation of pre-miR-138-2 processing is, what attributes of the pre-miRNA are recognized by the regulating factor? The secondary structure of pre-miR-138-2 features two unpaired nucleotides at the 5′-end, two internal loops and a single nucleotide bulge close to the terminal loop (Figure 5A). Dicer cleavage occurs adjacent to the second internal loop yielding the ~23-24 nt miR-138. To check whether these internal loops play a role in the recognition of pre-miR-138-2 by the inhibitor, I generated mutant pre-miR-138-2-hairpins, where the sequence of the miRNA* strands were altered in order to close the first, the second and also both loops. Figure 5A displays the structure of the different pre-miRNA hairpins.

Hairpin precursors were 5′-end labeled with ^{32}P-γ-ATP and compared in *in vitro* processing assays using recombinant Dicer alone or in the presence of the inhibiting HeLa S100 cytoplasmic extract (Figure 5B). In contrast to loop 2, closing of loop 1 alone (pre-miR-138-2-L1) was enough to largely abolish the inhibition of Dicer cleavage on pre-miR-138-2, suggesting that the inhibitor recognizes loop 1. Another interesting observation is that closing of either loop has an impact on the size of Dicer's cleavage

products. The genuine pre-miR-138-2 yields 23-nt and 24-nt miRNA species at a 1:1 ratio. Closing loop 1 (pre-miR-138-2-L1) shifts the cleavage site and generates a single miR-138 species of 23 nt, whereas closing loop 2 (pre-miR-138-2-L2) favors the 24-nt species. If both loops are closed (pre-miR-138-2-L1L2), the most abundant species is the 23-nt miR-138.

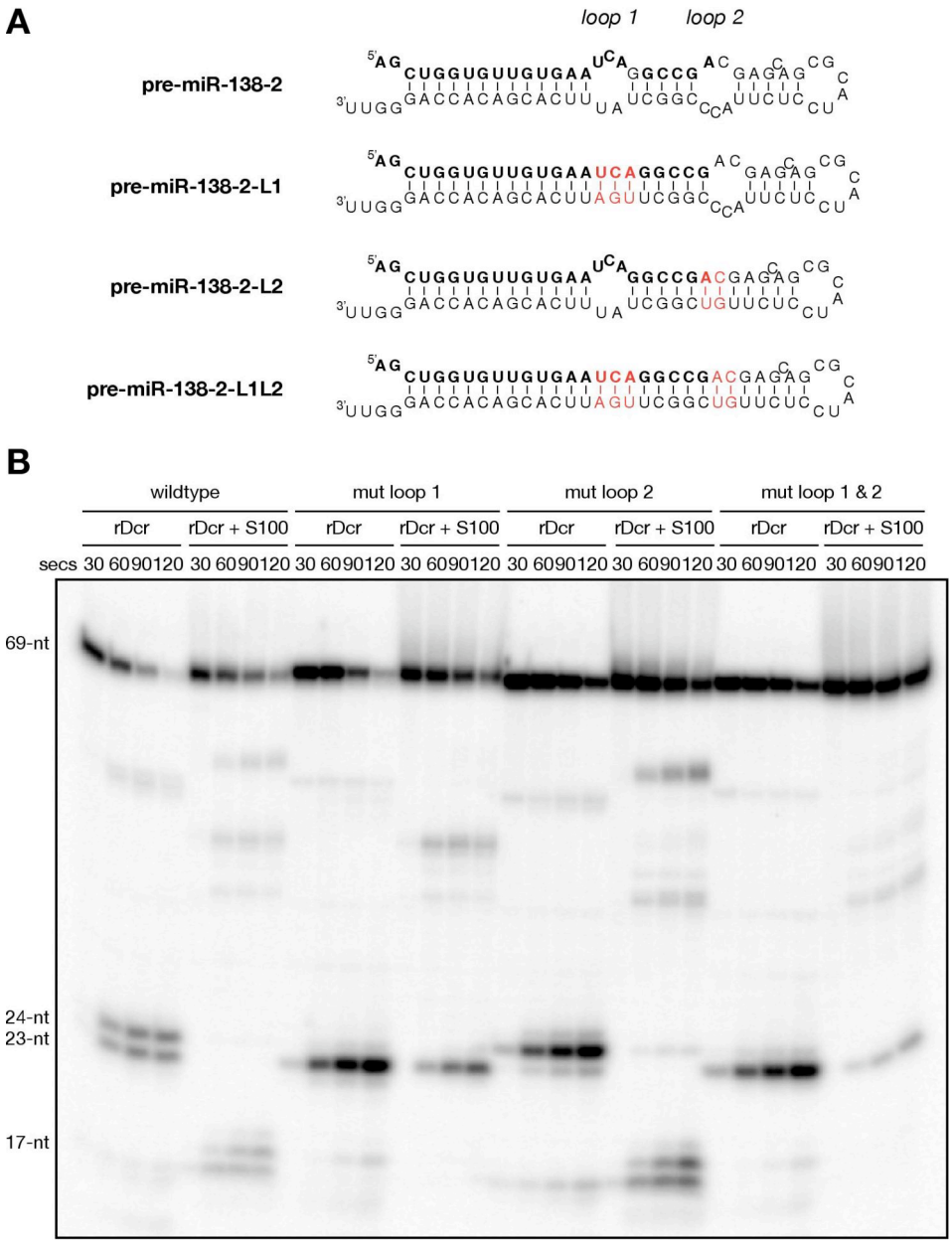

Figure 5. Analysis of the secondary structure of pre-miR-138-2 and its involvement in differential processing

(A) Secondary structure predictions of the four different pre-miR-138-2 hairpins used to assess the structure requirements of inhibitor binding. The upper hairpin displays the genuine sequence of pre-miR-138-2. The mature miR-138 sequence is indicated in bold. The loops were closed by adjusting the sequence of the miR-138* arm. **(B)** *In vitro* Dicer-processing reaction of the pre-miR-138-2 structural variants displayed in (A). The pre-miR-138-2 hairpins were 5′ end labeled using γ-^{32}P-ATP and processed using (a) recombinant Dicer enzyme alone and (b) recombinant Dicer enzyme plus HeLa cytoplasmic extract (S100). The processing of the hairpin by Dicer alone indicates correct folding and recognition as a genuine pre-miRNA. The addition of HeLa cytoplasmic extract to the processing reaction indicates, whether the hairpin is still recognized by the inhibitor. Closing of the loop 1 greatly abolishes inhibition of processing.

4.3.3. Purification of the inhibitory factor

4.3.3.1. Classical chromatography

Since we performed the *in vitro* processing assays using HeLa cytoplasmic extracts and since such extracts are readily available in large quantities, an obvious endeavor was to attempt the purification of the inhibitor employing classical chromatography. After a period of scouting various resins for the ability to retain and elute the inhibitory activity upon changes in the salt concentration, I was able to concatenate seven purification steps leading to a specific enrichment (Figure 6). The aim was to reduce the number of proteins co-eluting with the inhibitory activity to a reasonable figure, where the candidate proteins could then be evaluated. The validation of candidate proteins consisted of (a) an RNAi-mediated knock-down of the factor in HeLa cells and subsequent testing of the cellular extract in an *in vitro* processing reaction for a lack of inhibition and (b) recombinant expression of the factor in bacteria and testing the protein in *in vitro* processing assay for inhibition of pre-miR-138-2 processing.

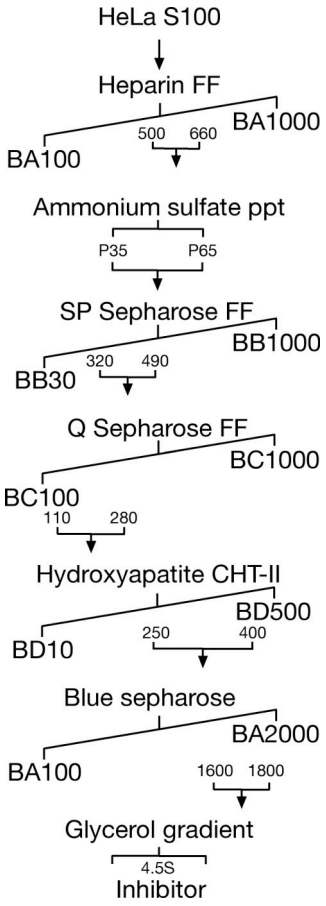

Figure 6. Chromatographic purification strategy for the inhibitor of pre-miR-138-2 processing.
HeLa S100 cytoplasmic extract was applied to the designated resins using buffers indicated below the scales ("BA" = buffer A, etc.). The numbers given below the scales indicate the molarity of KCl, or KP_i in the case of BD, in [mM] in the eluted fractions, where the inhibiting activity was detected. These fractions were pooled and dialyzed to the buffer conditions used in the following column.

The ability to inhibit Dicer-mediated processing of a 5′-radiolabeled pre-miR-138-2 substrate was used to assay the fractions for the presence or absence of the inhibitor. We confirmed the specificity of the inhibitor for pre-miR-138-2 by also assaying the fractions for cleavage of pre-miR-19a, a miRNA abundant in HeLa cells. Figure 7 displays autoradiographies of denaturing polyacrylamide gels loaded with such processing reactions after the sixth purification step (Blue Sepharose, see Figure 6). pre-miR-19a was processed in all fractions, including the input, with roughly the same efficiency indicating the specificity of the inhibitor towards binding pre-miR-138-2, where processing was inhibited strongly in a restricted set of consecutive fractions.

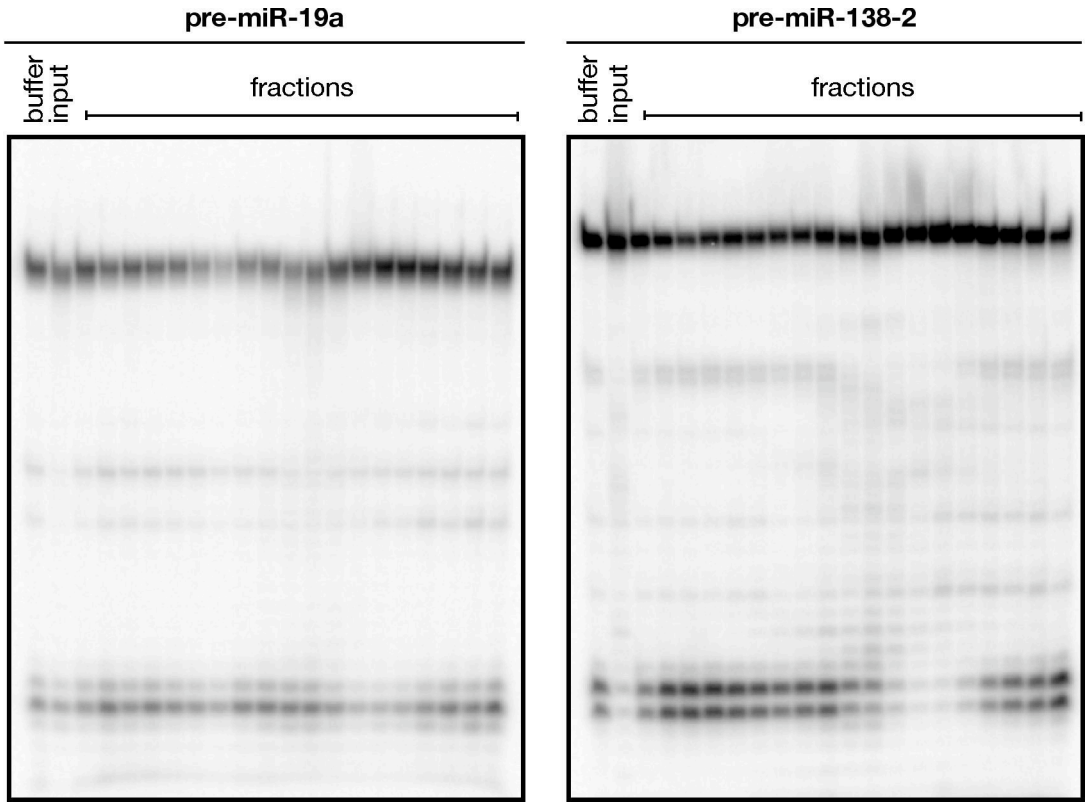

Figure 7. *In vitro* Dicer-processing reaction of pre-miR-19a (left) and pre-miR-138-2 (right) using the fractions collected from the 6th purification step (Blue Sepharose)
Each fraction collected from the elution of the Blue Sepharose column was assayed for the presence of the inhibitory factor by *in vitro* processing using recombinant Dicer enzyme. While processing of pre-miR-138-2 was inhibited in several fractions, this phenomenon was not observed for the processing of pre-mir-19a.

After the final purification step, the fractions were precipitated using TCA and loaded onto an SDS-polyacrylamide gel. The protein content was visualized by silver staining followed by mass-spectrometry to identify the proteins. The *in vitro* processing assay and the silver staining of the SDS-PAGE are shown in Figure 8. The last purification step in the purification chain was a 5–20% glycerol gradient (Figure 6),

where protein complexes sediment according to their molecular weight. The sedimentation coefficient of the inhibitory activity was determined to be 4.5 S, corresponding to a size of ~50–70 Da (The standard bovine serum albumine [BSA] with a molecular weight of 66 kDa sediments at 4.6 S). However, we could not macroscopically identify protein bands running at the determined size range on the silver gel, which also co-fractionate with the inhibitory activity. We therefore compared liquid samples taken (a) from a fraction with peak activity (fraction 5, "LiqPlus") and (b) from a fraction with no activity (fraction 12, "LiqMinus"). The mass spectra can be seen in appendix A (pages 54–58).

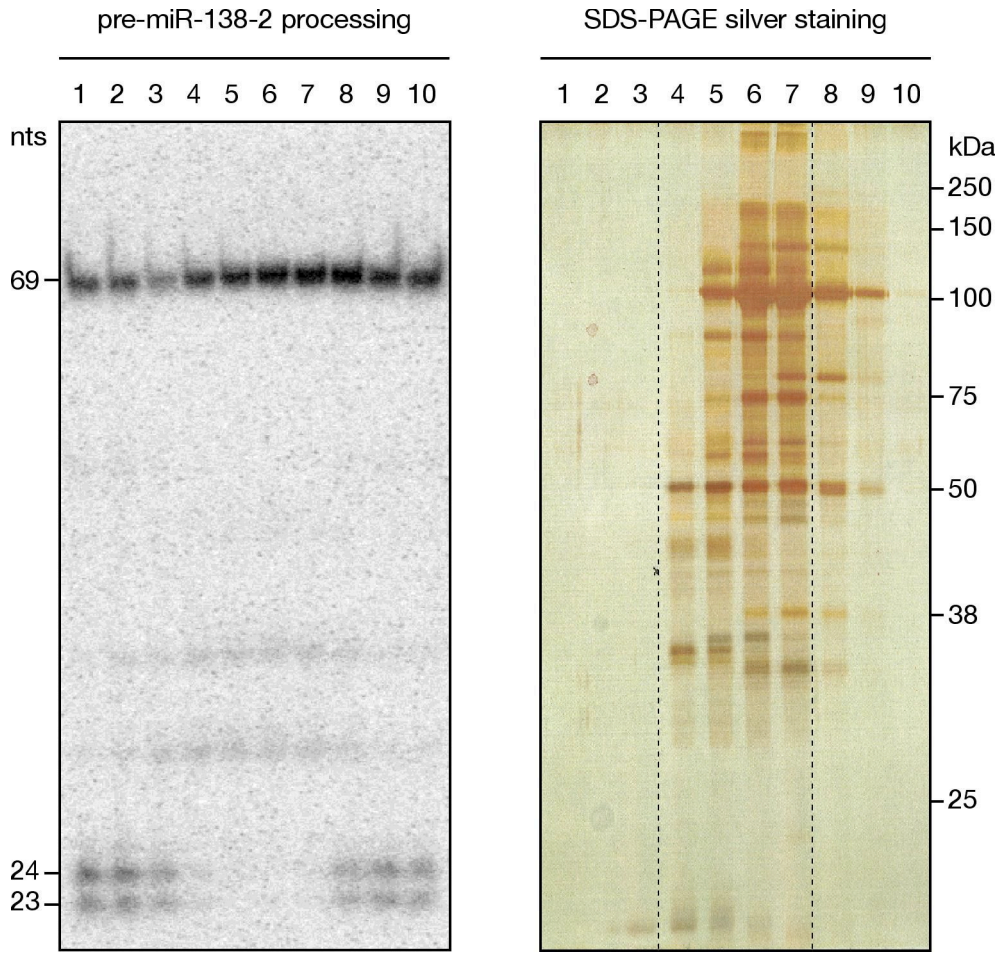

Figure 8. *In vitro* Dicer-processing reaction of pre-miR-138-2 (left) and silver staining of a SDS-PAGE (right) of fractions 1–10 from the last purification step (glycerol gradient)
The fractions 1 to 10 collected from the 5–20% glycerol gradient were assayed using the in vitro processing assay. Strong inhibition was observed in fractions 4–7. These fractions are indicated in the silver staining by dotted lines. Candidate bands that only show up between these boundaries were cut out and sent for identification by mass-spectrometry.

4.3.3.2. Affinity purification using the StreptoTag

Despite a considerable enrichment of the inhibitor during the seven purification steps, silver gel analysis and mass-spectrometry still yielded a large number of candidate proteins co-eluting with the inhibitory activity. This complicated the selection and testing of candidate genes. Therefore, I chose to apply a different purification strategy relying solely on affinity chromatography, called StreptoTag (Windbichler and Schroeder, 2006). Here, the streptomycin RNA aptamer is fused to an RNA sequence, whose binding partners are to be determined. This hybrid RNA is subsequently immobilized on a streptomycin affinity matrix. The protein mixture is applied to the resin, washed extensively and finally eluted by the addition of excess streptomycin allowing the recovery of RNA–protein complexes. To reduce the complexity of the extract, I pre-purified the inhibitory activity. During the scouting period for the classical chromatography, I noticed that both Heparin-coupled Sepharose and Blue-Sepharose displayed a very strong affinity to bind and retain the inhibitor. It elutes at >500 mM KCl from Heparin Sepharose and at >1.6 M KCl from Blue-Sepharose (Figure 6). This allowed me to concatenate these two resins without the need for dialysis in between to pre-purify the inhibitor from HeLa cytoplasmic S100 extract for StreptoTag chromatography.

The RNA fusion-oligonucleotide featured the pre-miR-138-2 structure at the 5′-end, the streptomycin aptamer (StreptoTag) at the 3′-end and a 6 nt spacer in between (Figure 9). *In vitro* processing assays of this RNA oligonucleotide showed a weak affinity of Dicer to cleave the embedded pre-miR-138-2 hairpin. However, the addition of HeLa S100 abolished this cleavage indicating that the inhibitor effectively binds this fusion RNA construct (data not shown). The eluate of the StreptoTag purification was analyzed by mass-spectrometry. The spectra can be seen in appendix B (page 51).

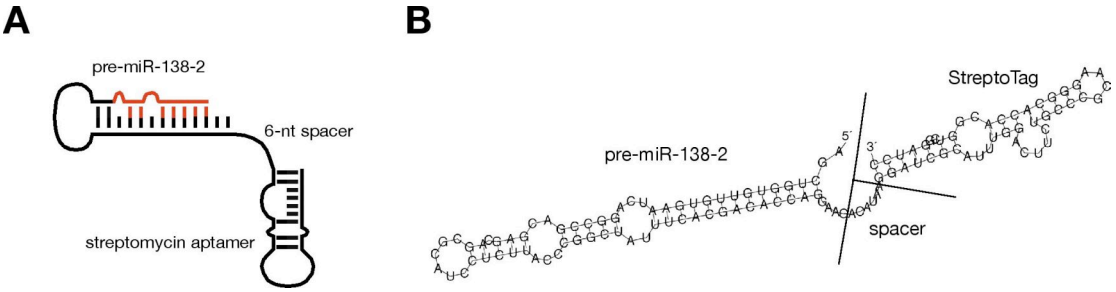

Figure 9. Fusion RNA oligonucleotide used in StreptoTag affinity purification
(A) Design of the RNA fusion oligonucleotide consisting of the pre-miR-138-2 at the 5′ end and the streptomycin aptamer at the 3′ end. The mature miR-138 is indicated in red. (B) Secondary structure prediction of the RNA fusion oligonucleotide using RNAfold.

4.3.3.3. Size exclusion chromatography

Gel filtration was not used during the purification chain described in 4.3.3.1 because of excessive dilution of the inhibitory activity, which could no longer be observed in the *in vitro* processing assay. For the StreptoTag method, the pre-purification of the inhibitory activity using Heparin Sepharose and Blue Sepharose generated a sample, which was highly enriched for the inhibitor. We therefore chose this approach to pre-purify the activity for subsequent size exclusion chromatography and succeeded in determining the size of the inhibitor at around 15 kDa. Interestingly, this figure is different from the molecular weight determined in the glycerol gradient. While the inhibitory activity sedimented at 4.5 S (~50–70 kDa) in the glycerol gradient, the size exclusion chromatography suggests a smaller size, ~15–20 kDa (Figure 10). This probably explains, why we never observed a protein band in the silver gels co-eluting with the inhibitory activity in the processing gels (Figure 8), since we were looking at bands with a molecular weight greater than ~25 kDa.

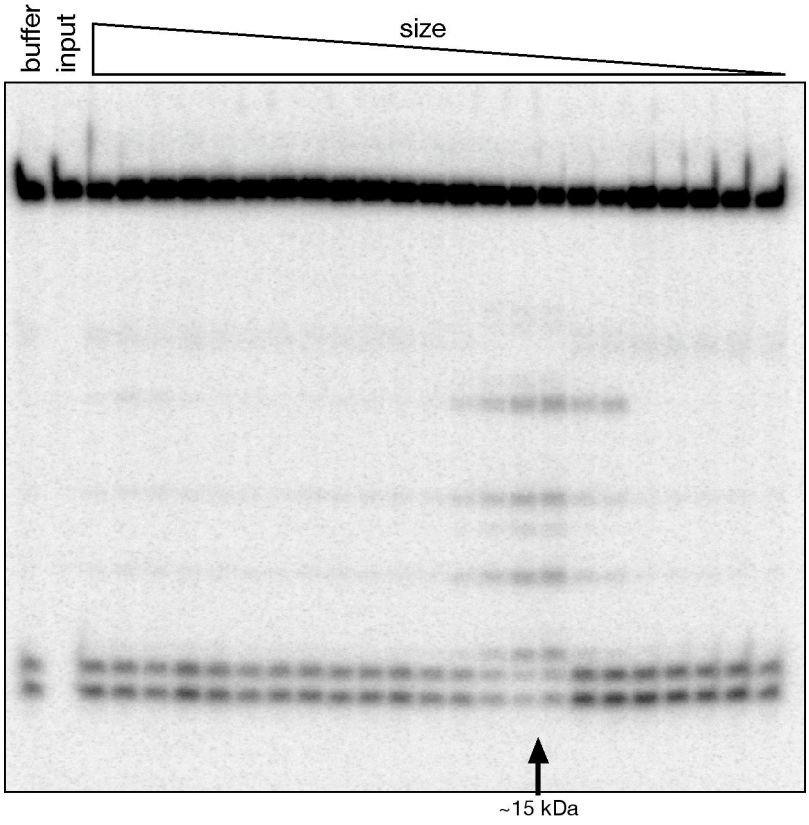

Figure 10. Fractions from the size exclusion chromatography assayed for the presence of the inhibitory activity by *in vitro* Dicer-processing of pre-miR-138-2
The fractions collected from the size exclusion chromatography were assayed using the *in vitro* processing assay. Inhibition of processing was observed in fractions corresponding to a size of ~15–20 kDa.

Probability Lege...
over 95%
80% to 94%
50% to 79%
20% to 49%
0% to 19%

Bio View:
Identified Proteins (115)

#	Visible?	Protein Starred?	Identified Proteins (115)	Accession Number	Molecular Weight	LigMinus	LigPlus
1	☐	☆	NOL1/NOP2/Sun domain family 2 protein //:CRAI17900046298521 3_9606 /def=refINP_060225.4l NOL1/NOP2/Sun domain family 2 protein [Homo sapiens] /...	rfINP_060225.4	86 kDa	177	296
2	☐	☆	Sjogren syndrome antigen B (autoantigen La) //:CRAI19700006492600 6_9606 /def=CRAIhCP1793365 /gene_name=Sjogren syndrome antigen B (autoanti...	cralhCP1793365 (+1)	47 kDa	81	230
3	☐	☆	tRNA pseudouridine synthase A (EC 4.2.1.70) (Pseudouridylate synthase I) (Uracil hydrolyase) //:CRAI33500113108814 2_9606 ...	sptlQ9Y606	44 kDa	62	96
4	☐	☆	hypothetical protein FLJ20485 //:CRAI19700006948224_9606 /def=CRAIhCP1765749.1 /gene_name=hypothetical protein FLJ20485 /panther_id=PTHR133...	cralhCP1765749.1 (+1)	75 kDa		59
5	☐	☆	OTTHUMP00000062376 //:CRAI17900081556894 8_9606 /def=OTTHUMP00000062376 /gene_name=GD:XXbac-BPG249D20.4-001 /panther_id=PTHR19211:SF...	trmlQ5STZ7	96 kDa	15	45
6	☐	☆	Ras GTPase-activating protein 3 (GAP1(IP4BP)) (Ins P4-binding protein) //:CRAI14900010174478 5_9606 /def=Ras GTPase-activating protein 3 (GAP1(IP4...	sptlQ14644 (+1)	96 kDa		45
7	☐	☆	hypothetical protein FLJ10415 //:CRAI19700006494077 4_9606 /def=CRAIhCP1764838.1 /gene_name=hypothetical protein FLJ10415 /panther_id=PTHR160...	cralhCP1764838.1 (+3)	81 kDa	28	44
8	☐	☆	3' exoribonuclease //:CRAI22200005047965 8_9606 /def=gblAAQ21219.1l 3' exoribonuclease [Homo sapiens] /gene_name=NULL /panther_id=PTHR10483:...	gblAAQ21219.1 (+1)	40 kDa	8	35
9	☐	☆	catenin (cadherin-associated protein), alpha 1, 102kDa //:CRAI20800003024256 9_9606 /def=CRAIhCP1704204.2 /gene_name=catenin (cadherin-associated...	cralhCP1704204.2 (+2)	100 kDa		33
10	☐	☆	chromosome 21 open reading frame 6 //:CRAI19700006495583 6_9606 /def=CRAIhCP1761185 /gene_name=chromosome 21 open reading frame 6 /panther...	cralhCP1761185 (+2)	27 kDa	29	31
11	☐	☆	keratin 1 (epidermolytic hyperkeratosis) //:CRAI19700006941296 7_9606 /def=CRAIhCP1609934.2 /gene_name=keratin 1 (epidermolytic hyperkeratosis) /pa...	cralhCP1609934.2 (+3)	66 kDa	5	21
12	☐	☆	survival motor neuron domain containing 1 //:CRAI19700006945018 7_9606 /def=CRAIhCP1766446.1 /gene_name=survival motor neuron domain containi...	cralhCP1766446.1 (+3)	27 kDa		20
13	☐	☆	guanine nucleotide binding protein (G protein), alpha inhibiting activity polypeptide 3 //:CRAI20900007379548 5_9606 /def=CRAIhCP1882096 /gene_name...	cralhCP1882096 (+2)	41 kDa	4	19
14	☐	☆	PDGFA associated protein 1 //:CRAI19700006940660 8_9606 /def=CRAIhCP1873344 /gene_name=PDGFA associated protein 1 /panther_id=PTHR11584:SF...	cralhCP1873344 (+2)	21 kDa	28	18
15	☐	☆	interleukin enhancer binding factor 3, 90kDa //:CRAI19700006944869 5_9606 /def=CRAIhCP1895431 /gene_name=interleukin enhancer binding factor 3, 90...	cralhCP1895431 (+18)	95 kDa		18
16	☐	☆	RNA, U3 small nucleolar interacting protein 2 //:CRAI19700006493577 5_9606 /def=CRAIhCP51951.2 /gene_name=RNA, U3 small nucleolar interacting prot...	cralhCP51951.2 (+1)	52 kDa		17
17	☐	☆	KIAA0261 //:CRAI19700006936792 6_9606 /def=CRAIhCP1854792 /gene_name=KIAA0261 /panther_id=PTHR11915 /family=SPECTRIN-RELATED /subfamily...	cralhCP1854792 (+5)	127 kDa		15
18	☐	☆	DEAH (Asp-Glu-Ala-His) box polypeptide 16 //:CRAI19700006936707 2_9606 /def=CRAIhCP1712858.1 /gene_name=DEAH (Asp-Glu-Ala-His) box polypepti...	cralhCP1712858.1 (+6)	119 kDa		14
19	☐	☆	interleukin enhancer binding factor 2, 45kDa //:CRAI19700006937293 1_9606 /def=CRAIhCP1859797 /gene_name=interleukin enhancer binding factor 2, 45...	cralhCP1859797 (+2)	43 kDa		13
20	☐	☆	eukaryotic translation initiation factor 2, subunit 2 beta, 38kDa //:CRAI19700006937141 8_9606 /def=CRAIhCP1858284 /gene_name=eukaryotic translation i...	cralhCP1858284 (+5)	38 kDa		12
21	☐	☆	hypothetical protein DKFZp434K1421 //:CRAI19700006936888 3_9606 /def=CRAIhCP1607369.3 /gene_name=hypothetical protein DKFZp434K1421 /panthe...	cralhCP1607369.3 (+4)	66 kDa		11
22	☐	☆	casein kinase 1, alpha 1 //:CRAI19700006944756 3_9606 /def=CRAIhCP1777673.1 /gene_name=casein kinase 1, alpha 1 /panther_id=PTHR11909:SF3 /family...	cralhCP1777673.1 (+6)	39 kDa	39	11
23	☐	☆	KIAA0648 protein //:CRAI19700006938537 2_9606 /def=CRAIhCP1862238 /gene_name=KIAA0648 protein /panther_id=PTHR12663:SF6 /family=BIMD-RELA...	cralhCP1862238 (+3)	151 kDa	3	10
24	☐	☆	RCC1-like //:CRAI30000023629306_9606 /def=CRAIhCP1854944.1 /gene_name=RCC1-like /panther_id=PTHR11254:SF64 /family=UBIQUITIN-PROTEIN LIG...	cralhCP1854944.1 (+3)	56 kDa	8	9
25	☐	☆	NRAA Best Hit: Hypothetical protein ZK512.4 [Caenorhabditis elegans] //:CRAI19700006945076 2_9606 /def=CRAIhCP1718102.1 /gene_name=NULL /panth...	cralhCP1718102.1 (+3)	10 kDa		9
26	☐	☆	Signal recognition particle 14kDa (homologous Alu RNA binding protein) //:CRAI78000199117618_9606 /def=gblAAH35495.1l Signal recognition particle ...	gblAAH35495.1	15 kDa		9
27	☐	☆	SMC1 structural maintenance of chromosomes 1-like 1 (yeast) //:CRAI30000023170754_9606 /def=CRAIhCP37548.2 /gene_name=SMC1 structural mainten...	cralhCP37548.2 (+6)	143 kDa		9
28	☐	☆	UPF3 regulator of nonsense transcripts homolog B (yeast) //:CRAI19700006942614 5_9606 /def=CRAIhCP1882881 /gene_name=UPF3 regulator of nonsen...	cralhCP1882881 (+5)	58 kDa	10	8
29	☐	☆	hypothetical protein //:CRAI30000035919867_9606 /def=CRAIhCP1915519 /gene_name=NULL /panther_id=PTHR12785 /family=SPLICEOSOME ASSOCIAT...	cralhCP1915519 (+7)	73 kDa		8
30	☐	☆	hypothetical protein HSPC152 //:CRAI19700006946622 4_9606 /def=CRAIhCP1766290.1 /gene_name=hypothetical protein HSPC152 /panther_id=PTHR1277...	cralhCP1766290.1 (+2)	14 kDa	23	8
31	☐	☆	tumor necrosis factor, alpha-induced protein 8 //:CRAI19700006495438 9_9606 /def=CRAIhCP1763610 /gene_name=tumor necrosis factor, alpha-induced ...	cralhCP1763610 (+3)	23 kDa		8
32	☐	☆	CGI-77 protein //:CRAI19700006935375 2_9606 /def=CRAIhCP1850618 /gene_name=CGI-77 protein /panther_id=PTHR12419:SF5 /family=FAMILY NOT NAM...	cralhCP1850618 (+3)	37 kDa		7
33	☐	☆	transcription factor A, mitochondrial //:CRAI19700006938796 8_9606 /def=CRAIhCP1864834 /gene_name=transcription factor A, mitochondrial /panther_id=...	cralhCP1864834 (+3)	29 kDa	4	7
34	☐	☆	hyaluronoglucosaminidase 3 //:CRAI30000036266099_9606 /def=CRAIhCP1909839.1 /gene_name=hyaluronoglucosaminidase 3 /panther_id=PTHR12354:S...	cralhCP1909839.1 (+6)	66 kDa	8	7
35	☐	☆	polymerase (DNA-directed), delta 3, accessory subunit //:CRAI19700006946542 4_9606 /def=CRAIhCP1902160 /gene_name=polymerase (DNA-directed), de...	cralhCP1902160 (+3)	51 kDa		6
36	☐	☆	thymine-DNA glycosylase //:CRAI19700006942414 1_9606 /def=CRAIhCP1880877 /gene_name=thymine-DNA glycosylase /panther_id=PTHR12159 /family=...	cralhCP1880877 (+4)	46 kDa		6
37	☐	☆	guanine nucleotide binding protein (G protein), alpha inhibiting activity polypeptide 2 //:CRAI20800002773268 9_9606 /def=CRAIhCP1803039 /gene_name...	cralhCP1803039 (+4)	40 kDa		6

Probability Lege...
over 95%
80% to 94%
50% to 79%
20% to 49%
0% to 19%

Bio View:
Identified Proteins (115)

#	Visible?	Protein Starred?		Accession Number	Molecular Weight	LiqMinus	LiqPlus
38	☐	☆	activated RNA polymerase II transcription cofactor 4 //:CRAI197000069426914_9606 /def=CRAIhCP1698824 /gene_name=activated RNA polymerase II tran...	cralhCP1698824 (+6)	14 kDa	6	5
39	☐	☆	heat shock 70kDa protein 5 (glucose-regulated protein, 78kDa) //:CRAI300001258838 98_9606 /def=CRAIhCP44562.4 /gene_name=heat shock 70kDa protei...	cralhCP44562.4 (+3)	72 kDa		5
40	☐	☆	Williams Beuren syndrome chromosome region 22 //:CRAI197000064928971_9606 /def=CRAIhCP1778295.1 /gene_name=Williams Beuren syndrome chro...	cralhCP1778295.1 (+1)	32 kDa	9	5
41	☐	☆	nuclear respiratory factor 1 //:CRAI197000069468410_9606 /def=CRAIhCP1767894.1 /gene_name=nuclear respiratory factor 1 /panther_id=PTHR20338 /fam...	cralhCP1767894.1 (+6)	52 kDa		5
42	☐	☆	DEAH (Asp-Glu-Ala-His) box polypeptide 34 isoform 1 //:CRAI225000078058498_9606 /def=refINP_055496.2l DEAH (Asp-Glu-Ala-His) box polypeptide 34 i...	rfINP_055496.2	128 kDa	45	5
43	☐	☆	Cullin 4A //:CRAI179000662028718_9606 /def=Cullin 4A /gene_name=CUL4A /panther_id=PTHR11932:SF1 /family=CULLIN /subfamily=CULLIN /mol_fn=Mi...	trmIQ6UP08	88 kDa		5
44	☐	☆	N-myristoyltransferase 1 //:CRAI197000064931456_9606 /def=CRAIhCP43580.2 /gene_name=N-myristoyltransferase 1 /panther_id=PTHR11377:SF6 /family...	cralhCP43580.2 (+4)	57 kDa	21	4
45	☐	☆	cleavage and polyadenylation specific factor 5, 25 kDa //:CRAI197000069411538_9606 /def=CRAIhCP1878274 /gene_name=cleavage and polyadenylation ...	cralhCP1878274 (+4)	26 kDa	7	4
46	☐	☆	RAS p21 protein activator 2 //:CRAI197000064918272_9606 /def=CRAIhCP1777314 /gene_name=RAS p21 protein activator 2 /panther_id=PTHR10194:SF10...	cralhCP1777314 (+4)	97 kDa		4
47	☐	☆	suppressor of potassium transport defect 3 //:CRAI197000069465294_9606 /def=CRAIhCP1752361 /gene_name=suppressor of potassium transport defec...	cralhCP1752361 (+5)	79 kDa		4
48	☐	☆	eukaryotic translation initiation factor 2, subunit 1 alpha, 35kDa //:CRAI197000069390065_9606 /def=CRAIhCP1866931 /gene_name=eukaryotic translation...	cralhCP1866931 (+6)	36 kDa		4
49	☐	☆	sorting nexin associated golgi protein 1 //:CRAI300000023720303_9606 /def=CRAIhCP1814099.2 /gene_name=sorting nexin associated golgi protein 1 /pan...	cralhCP1814099.2 (+2)	59 kDa		4
50	☐	☆	guanine nucleotide binding protein (G protein), alpha inhibiting activity polypeptide 1 //:CRAI197000069406747_9606 /def=CRAIhCP1873483 /gene_name...	cralhCP1873483 (+5)	40 kDa		4
51	☐	☆	catenin (cadherin-associated protein), alpha-like 1 //:CRAI197000069405628_9606 /def=CRAIhCP44242.1 /gene_name=catenin (cadherin-associated protei...	cralhCP44242.1 (+2)	82 kDa		4
52	☐	☆	PYM protein //:CRAI197000069413580_9606 /def=CRAIhCP1622240.3 /gene_name=PYM protein /panther_id=PTHR13227:SF5 /family=FAMILY NOT NAMED ...	cralhCP1622240.3 (+3)	22 kDa		4
53	☐	☆	MAD, mothers against decapentaplegic homolog 9 (Drosophila) //:CRAI197000069429511_9606 /def=CRAIhCP1761420 /gene_name=MAD, mothers agains...	cralhCP1761420 (+15)	43 kDa		4
54	☐	☆	PHD finger protein 6 //:CRAI197000069427847_9606 /def=CRAIhCP1701499.2 /gene_name=PHD finger protein 6 /panther_id=PTHR12420 /family=FAMILY N...	cralhCP1701499.2 (+2)	41 kDa		4
55	☐	☆	PC4 and SFRS1 interacting protein 1 //:CRAI300000535847 45_9606 /def=CRAIhCP1889353.2 /gene_name=PC4 and SFRS1 interacting protein 1 /panther_i...	cralhCP1889353.2 (+9)	38 kDa		4
56	☐	☆	heat shock 70kDa protein 8 //:CRAI206000044899919_9606 /def=CRAIhCP1852232 /gene_name=heat shock 70kDa protein 8 /panther_id=PTHR19375:SF77 ...	cralhCP1852232 (+2)	71 kDa	30	3
57	☐	☆	hnRNP U protein //:CRAI620000570185 94_9606 /def=emblCAA46472.1l hnRNP U protein [Homo sapiens] /gene_name=NULL /panther_id=PTHR12381:SF3 ...	emblCAA46472.1 (+10)	89 kDa	6	3
58	☐	☆	hypothetical protein BC013949 //:CRAI197000069449646_9606 /def=CRAIhCP1896382 /gene_name=hypothetical protein BC013949 /panther_id=PTHR1191...	cralhCP1896382 (+2)	26 kDa		3
59	☐	☆	splicing factor, arginine/serine-rich 2 //:CRAI197000064921682_9606 /def=CRAIhCP1766720.1 /gene_name=splicing factor, arginine/serine-rich 2 /panther_...	cralhCP1766720.1 (+4)	25 kDa	2	3
60	☐	☆	chaperonin containing TCP1, subunit 4 (delta) //:CRAI197000064958032_9606 /def=CRAIhCP201120.1 /gene_name=chaperonin containing TCP1, subunit ...	cralhCP201120.1 (+2)	58 kDa	12	2
61	☐	☆	S100 calcium-binding protein A13 //:CRAI335001130461025_9606 /def=S100 calcium-binding protein A13 /gene_name=S100A13 /panther_id=PTHR11639:...	sptIQ99584	11 kDa	4	2
62	☐	☆	leucyl-tRNA synthetase //:CRAI197000069447707_9606 /def=CRAIhCP1704125.2 /gene_name=leucyl-tRNA synthetase /panther_id=PTHR11946:SF10 /famil...	cralhCP1704125.2 (+7)	80 kDa		2
63	☐	☆	low density lipoprotein receptor-related protein associated protein 1 //:CRAI197000069388554_9606 /def=CRAIhCP1865420 /gene_name=low density lipo...	cralhCP1865420 (+2)	41 kDa		2
64	☐	☆	polymerase (DNA directed), delta 1, catalytic subunit 125kDa //:CRAI197000069407752_9606 /def=CRAIhCP40379.3 /gene_name=polymerase (DNA directe...	cralhCP40379.3 (+3)	124 kDa	3	2
65	☐	☆	keratin 8 //:CRAI300000359037 95_9606 /def=CRAIhCP1879660 /gene_name=keratin 8 /panther_id=PTHR18893:SF5 /family=KERATIN TYPE II/HSP 70-RELA...	cralhCP1879660 (+10)	54 kDa	48	
66	☐	☆	DEAH (Asp-Glu-Ala-His) box polypeptide 15 //:CRAI300000364762 28_9606 /def=CRAIhCP1915733 /gene_name=DEAH (Asp-Glu-Ala-His) box polypeptide ...	cralhCP1915733 (+3)	89 kDa	25	
67	☐	☆	chaperonin containing TCP1, subunit 8 (theta) //:CRAI197000064955819_9606 /def=CRAIhCP1750414.1 /gene_name=chaperonin containing TCP1, subuni...	cralhCP1750414.1 (+3)	59 kDa	22	
68	☐	☆	SWAP-70 protein //:CRAI197000069374652_9606 /def=CRAIhCP1861518 /gene_name=SWAP-70 protein /panther_id=PTHR14383 /family=SWAP-70 RECOM...	cralhCP1861518 (+4)	69 kDa	27	
69	☐	☆	t-complex 1 //:CRAI197000069408610_9606 /def=CRAIhCP1875346 /gene_name=t-complex 1 /panther_id=PTHR11353:SF2 /family=T-COMPLEX PROTEIN 1...	cralhCP1875346 (+3)	60 kDa	21	
70	☐	☆	annexin A6 //:CRAI197000069447503_9606 /def=CRAIhCP1894239 /gene_name=annexin A6 /panther_id=PTHR10502:SF33 /family=ANNEXIN /subfamily=A...	cralhCP1894239 (+8)	75 kDa	18	
71	☐	☆	Hypothetical protein LOC56931 //:CRAI67000094270750_9606 /def=Hypothetical protein LOC56931 /gene_name=LOC56931 /panther_id=PTHR11082:SF37 ...	trmIQ96G46 (+1)	72 kDa	16	
72	☐	☆	nei like 2 (E. coli) //:CRAI197000064923844_9606 /def=CRAIhCP1791203 /gene_name=nei like 2 (E. coli) /panther_id=PTHR16085 /family=FAMILY NOT NAM...	cralhCP1791203 (+5)	37 kDa	21	
73	☐	☆	chaperonin containing TCP1, subunit 6A (zeta 1) //:CRAI197000069370035_9606 /def=CRAIhCP1856901 /gene_name=chaperonin containing TCP1, subun...	cralhCP1856901 (+4)	39 kDa	12	
74	☐	☆	elongation factor for selenoprotein translation //:CRAI197000064918633_9606 /def=CRAIhCP49878.2 /gene_name=elongation factor for selenoprotein tra...	cralhCP49878.2 (+2)	65 kDa	10	

Probability Lege...
over 95%
80% to 94%
50% to 79%
20% to 49%
0% to 19%

#	Visible?	Protein Starred?	Bio View: Identified Proteins (115)	Accession Number	Molecular Weight	LigMinus	LigPlus
75	☐	☆	tripartite motif-containing 56 //:CRAI19700006946789 9_9606 /def=CRAIhCP1604617.2 /gene_name=tripartite motif-containing 56 /panther_id=PTHR13712 /...	crailhCP1604617.2 (+2)	81 kDa	10	
76	☐	☆	misshapen/NIK-related kinase //:CRAI19700006943373 9_9606 /def=CRAIhCP1890475 /gene_name=misshapen/NIK-related kinase /panther_id=PTHR11584:...	crailhCP1890475 (+8)	146 kDa	11	
77	☐	☆	ribonuclease P 40kDa subunit //:CRAI19700006492354 4_9606 /def=CRAIhCP1766787.1 /gene_name=ribonuclease P 40kDa subunit /panther_id=PTHR1539...	crailhCP1766787.1 (+3)	39 kDa	10	
78	☐	☆	Centaurin gamma 3 //:CRAI19400004441223 0_9606 /def=Centaurin gamma 3 /gene_name=CENTG3 /panther_id=PTHR14248:SF5 /family=CENTAURIN-REL...	sptlQ96P47 (+1)	95 kDa	10	
79	☐	☆	RNA (guanine-7-) methyltransferase //:CRAI19700006943552 6_9606 /def=CRAIhCP1773916.1 /gene_name=RNA (guanine-7-) methyltransferase /panther_i...	crailhCP1773916.1 (+6)	55 kDa	13	
80	☐	☆	mortality factor 4 like 2 //:CRAI19700006940593 9_9606 /def=CRAIhCP1761455 /gene_name=mortality factor 4 like 2 /panther_id=PTHR10880:SF8 /family=M...	crailhCP1761455 (+4)	32 kDa	7	
81	☐	☆	similar to RIKEN cDNA 2610307I21 //:CRAI19700006493199 6_9606 /def=CRAIhCP1799355 /gene_name=similar to RIKEN cDNA 2610307I21 /panther_id=PTH...	crailhCP1799355 (+3)	52 kDa	11	
82	☐	☆	SET and MYND domain containing 3 //:CRAI20700000962903 1_9606 /def=CRAIhCP1763203.2 /gene_name=SET and MYND domain containing 3 /panther_i...	crailhCP1763203.2 (+3)	49 kDa	10	
83	☐	☆	polyglutamine binding protein 1 //:CRAI19700006946448 1_9606 /def=CRAIhCP37606.2 /gene_name=polyglutamine binding protein 1 /panther_id=PTHR15...	crailhCP37606.2 (+1)	30 kDa	6	
84	☐	☆	DEAH (Asp-Glu-Ala-His) box polypeptide 36 //:CRAI19700006491794 1_9606 /def=CRAIhCP43427.2 /gene_name=DEAH (Asp-Glu-Ala-His) box polypeptide ...	crailhCP43427.2 (+4)	115 kDa	5	
85	☐	☆	phospholipase C, beta 3 (phosphatidylinositol-specific) //:CRAI20900007393950 9_9606 /def=CRAIhCP38927.1 /gene_name=phospholipase C, beta 3 (pho...	crailhCP38927.1 (+2)	139 kDa	4	
86	☐	☆	hypothetical protein MGC3329 //:CRAI20600000459368 14_9606 /def=CRAIhCP1890699 /gene_name=hypothetical protein MGC3329 /panther_id=PTHR13393...	crailhCP1890699 (+2)	64 kDa	7	
87	☐	☆	heat shock 70kDa protein 1A //:CRAI20700000700021 1_9606 /def=CRAIhCP1784169.1 /gene_name=heat shock 70kDa protein 1A /panther_id=PTHR19375:...	crailhCP1784169.1 (+5)	70 kDa	6	
88	☐	☆	chaperonin containing TCP1, subunit 3 (gamma) //:CRAI19700006937261 1_9606 /def=CRAIhCP1764391.1 /gene_name=chaperonin containing TCP1, sub...	crailhCP1764391.1 (+7)	56 kDa	6	
89	☐	☆	hypothetical protein MGC2574 //:CRAI19700006946887 9_9606 /def=CRAIhCP50163.2 /gene_name=hypothetical protein MGC2574 /panther_id=PTHR13557...	crailhCP50163.2 (+1)	40 kDa	11	
90	☐	☆	tripartite motif-containing 28 //:CRAI30000035270879 _9606 /def=CRAIhCP201747.1 /gene_name=tripartite motif-containing 28 /panther_id=PTHR13863:SF...	crailhCP201747.1 (+2)	89 kDa	5	
91	☐	☆	PKE protein kinase //:CRAI20800002785668 9_9606 /def=CRAIhCP1896564 /gene_name=PKE protein kinase /panther_id=PTHR11584:SF141 /family=PROTE...	crailhCP1896564 (+1)	55 kDa	4	
92	☐	☆	cleavage and polyadenylation specific factor 6, 68kDa //:CRAI19700006941328 3_9606 /def=CRAIhCP1763501.1 /gene_name=cleavage and polyadenylation...	crailhCP1763501.1 (+6)	59 kDa	3	
93	☐	☆	formin-like 1 //:CRAI19700006493143 6_9606 /def=CRAIhCP1798795 /gene_name=formin-like 1 /panther_id=PTHR20597 /family=FORMIN-RELATED /subfa...	crailhCP1798795 (+4)	127 kDa	4	
94	☐	☆	S100 calcium binding protein A16 //:CRAI19700006937288 9_9606 /def=CRAIhCP1724824.1 /gene_name=S100 calcium binding protein A16 /panther_id=PT...	crailhCP1724824.1 (+3)	12 kDa	3	
95	☐	☆	chaperonin containing TCP1, subunit 2 (beta) //:CRAI19700006941330 0_9606 /def=CRAIhCP1763503.1 /gene_name=chaperonin containing TCP1, subunit...	crailhCP1763503.1 (+5)	53 kDa	3	
96	☐	☆	chaperonin containing TCP1, subunit 5 (epsilon) //:CRAI19700006941200 7_9606 /def=CRAIhCP47417.3 /gene_name=chaperonin containing TCP1, subuni...	crailhCP47417.3 (+3)	60 kDa	4	
97	☐	☆	DEAD (Asp-Glu-Ala-Asp) box polypeptide 3, X-linked //:CRAI19700006946406 6_9606 /def=CRAIhCP1731279.1 /gene_name=DEAD (Asp-Glu-Ala-Asp) box ...	crailhCP1731279.1 (+11)	73 kDa	4	
98	☐	☆	chromosome condensation 1 //:CRAI19700006495371 5_9606 /def=CRAIhCP1761309 /gene_name=chromosome condensation 1 /panther_id=PTHR11254:...	crailhCP1761309 (+10)	53 kDa	5	
99	☐	☆	lysyl-tRNA synthetase //:CRAI19700006942741 3_9606 /def=CRAIhCP1752595 /gene_name=lysyl-tRNA synthetase /panther_id=PTHR10218:SF13 /family=G...	crailhCP1752595 (+6)	68 kDa	3	
100	☐	☆	chromosome 9 open reading frame 12 //:CRAI19700006493776 6_9606 /def=CRAIhCP45053.2 /gene_name=chromosome 9 open reading frame 12 /panther...	crailhCP45053.2 (+2)	56 kDa	4	
101	☐	☆	thyroid autoantigen 70kDa (Ku antigen) //:CRAI19700006493081 8_9606 /def=CRAIhCP1798177 /gene_name=thyroid autoantigen 70kDa (Ku antigen) /pant...	crailhCP1798177 (+4)	70 kDa	5	
102	☐	☆	T-cell activation protein //:CRAI20700000617475 2_9606 /def=CRAIhCP1699243.2 /gene_name=T-cell activation protein /panther_id=PTHR13140:SF89 /fami...	crailhCP1699243.2 (+2)	15 kDa	5	
103	☐	☆	WW domain binding protein 11 //:CRAI19700006943356 3_9606 /def=CRAIhCP1890299 /gene_name=WW domain binding protein 11 /panther_id=PTHR1336...	crailhCP1890299 (+3)	70 kDa	2	
104	☐	☆	eukaryotic translation elongation factor 1 alpha 2 //:CRAI19700006937018 7_9606 /def=CRAIhCP1857053 /gene_name=eukaryotic translation elongation fa...	crailhCP1857053 (+21)	50 kDa	2	
105	☐	☆	disabled homolog 2, mitogen-responsive phosphoprotein (Drosophila) //:CRAI30000070910899 _9606 /def=CRAIhCP1741508.3 /gene_name=disabled ho...	crailhCP1741508.3 (+11)	82 kDa	4	
106	☐	☆	katanin p60 (ATPase-containing) subunit A 1 //:CRAI19700006940896 4_9606 /def=CRAIhCP1875700 /gene_name=katanin p60 (ATPase-containing) subun...	crailhCP1875700 (+3)	56 kDa	2	
107	☐	☆	SET domain and mariner transposase fusion gene //:CRAI19700006493515 3_9606 /def=CRAIhCP1765463 /gene_name=SET domain and mariner transpos...	crailhCP1765463 (+5)	52 kDa	3	
108	☐	☆	basic transcription factor 3 //:CRAI19700006493983 8_9606 /def=CRAIhCP1766083 /gene_name=basic transcription factor 3 /panther_id=PTHR10351 /famil...	crailhCP1766083 (+2)	18 kDa	4	
109	☐	☆	hypothetical protein MGC2714 //:CRAI19700006936471 0_9606 /def=CRAIhCP1851576 /gene_name=hypothetical protein MGC2714 /panther_id=PTHR12281...	crailhCP1851576 (+3)	28 kDa	2	
110	☐	☆	NRAA Best Hit: AF100657_3 Hypothetical protein F52C12.2 [Caenorhabditis elegans] //:CRAI19700006944651 6_9606 /def=CRAIhCP52005.2 /gene_name=...	crailhCP52005.2 (+1)	34 kDa	3	
111	☐	☆	NRAA Best Hit: Hypothetical protein C56C10.8 [Caenorhabditis elegans] //:CRAI19700006495262 1_9606 /def=CRAIhCP1809980 /gene_name=NULL /panth...	crailhCP1809980 (+3)	17 kDa	2	

#	Visible?	Protein Starred?	Bio View: Identified Proteins (115)	Accession Number	Molecular Weight	LiqMinus	LiqPlus
112	☐	☆	ribonuclease P 14kDa subunit //:CRAI1000682315080_9606 /def=refINP_008973.1l ribonuclease P 14kDa subunit [Homo sapiens] /gene_name=NULL /pant...	rfINP_008973.1 (+1)	14 kDa	4	
113	☐	☆	RNA-binding region (RNP1, RRM) containing 2 //:CRAI1970000693712 72_9606 /def=CRAIhCP1858138 /gene_name=RNA-binding region (RNP1, RRM) con...	cralhCP1858138 (+11)	50 kDa	3	
114	☐	☆	sorting nexin 8 //:CRAI1970000649204 66_9606 /def=CRAIhCP1761792.1 /gene_name=sorting nexin 8 /panther_id=PTHR17425:SF1 /family=SORTING NEXI...	cralhCP1761792.1 (+2)	53 kDa	3	
115	☐	☆	methionine-tRNA ligase (EC 6.1.1.10) - human //:CRAI7800016951499 3_9606 /def=pirlJC5224 methionine-tRNA ligase (EC 6.1.1.10) - human /gene_name=...	pirlJC5224 (+2)	101 kDa	2	

Probability Lege...
over 95%
80% to 94%
50% to 79%
20% to 49%
0% to 19%

Probability Legen..
over 95%
80% to 94%
50% to 79%
20% to 49%
0% to 19%

Bio View:
Identified Proteins (28)

#	Visible?	Protein Starred?	Identified Proteins (28)	Accession Number	Molecular Weight	E1	E2
1	✓	☆	Lupus La protein (Sjogren syndrome type B antigen) (SS-B) (La ribonucleoprotein) (La autoantigen) //:CRAI335001131095756_9606 /def=Lupus La protein (...	sptlP05455 (...	47 kDa	19	11
2	✓	☆	Signal recognition particle 14kDa (homologous Alu RNA binding protein) //:CRAI780001991176l8_9606 /def=gblAAH35495.1l Signal recognition particle 14k...	gblAAH3549...	15 kDa	9	8
3	✓	☆	MGC11257 protein (Hypothetical protein FP15621) //:CRAI147000073462506_9606 /def=MGC11257 protein (Hypothetical protein FP15621) /gene_name=FP15...	trmlQ9BRJ6	22 kDa	8	6
4	✓	☆	40S ribosomal protein S7 //:CRAI179000658458669_9606 /def=40S ribosomal protein S7 /gene_name=RPS7 /panther_id=PTHR11278:SF1 /family=40S RIBOSO...	sptlP62081 (...	22 kDa	8	6
5	✓	☆	Signal recognition particle 9 kDa protein (SRP9) //:CRAI335001131100964_9606 /def=Signal recognition particle 9 kDa protein (SRP9) /gene_name=SRP9 /pa...	sptlP49458 (...	10 kDa	5	5
6	✓	☆	histone 1, H2bi //:CRAI197000064923490_9606 /def=CRAIhCP1610914.1 /gene_name=histone 1, H2bi /panther_id=PTHR11425:SF4 /family=HISTONE H2B /sub...	cralhCP1610...	14 kDa	6	4
7	✓	☆	40S ribosomal protein S25 //:CRAI179000670379704_9606 /def=40S ribosomal protein S25 /gene_name=RPS25 /panther_id=PTHR12850 /family=40S RIBOSO...	sptlP62851 (...	14 kDa	4	4
8	✓	☆	Eukaryotic translation initiation factor 1A, X-chromosomal (eIF-1A X isoform) (eIF-4C) //:CRAI335001130998929_9606 /def=Eukaryotic translation initiation fa...	sptlP47813 (...	16 kDa	5	4
9	✓	☆	squamous cell carcinoma antigen recognised by T cells 3 //:CRAI197000069424292_9606 /def=CRAIhCP33409.2 /gene_name=squamous cell carcinoma antig...	cralhCP3340...	110 kDa	7	
10	✓	☆	chromosome 1 open reading frame 33 //:CRAI197000069368177_9606 /def=CRAIhCP1765604 /gene_name=chromosome 1 open reading frame 33 /panther_id=...	cralhCP1765...	28 kDa	2	2
11	✓	☆	N-acetyltransferase-like protein //:CRAI197000069374054_9606 /def=CRAIhCP1860920 /gene_name=N-acetyltransferase-like protein /panther_id=PTHR10925:...	cralhCP1860...	116 kDa	5	
12	✓	☆	NRAA Best Hit: cationic trypsinogen //:CRAI208000027269689_9606 /def=CRAIhCP39590.4 /gene_name=NULL /panther_id=PTHR19355:SF179 /family=SERIN...	cralhCP3959...	30 kDa	2	2
13	✓	☆	DnaJ homolog subfamily C member 9 (DnaJ protein SB73) //:CRAI179000695650823_9606 /def=DnaJ homolog subfamily C member 9 (DnaJ protein SB73) /...	sptlQ8WXX5 ...	30 kDa	3	
14	✓	☆	desmoplakin //:CRAI197000064923624_9606 /def=CRAIhCP35698.2 /gene_name=desmoplakin /panther_id=PTHR13739:SF7 /family=DESMOPLAKIN-RELATED...	cralhCP3569...	332 kDa		4
15	✓	☆	Activated RNA polymerase II transcriptional coactivator p15 (Positive cofactor 4) (PC4) (p14) //:CRAI335001131076272_9606 /def=Activated RNA polymerase I...	sptlP53999 (...	14 kDa	2	
16	✓	☆	NOL1/NOP2/Sun domain family 2 protein //:CRAI179000462985213_9606 /def=refINP_060225.4l NOL1/NOP2/Sun domain family 2 protein [Homo sapiens] /gen...	rflNP_06022...	86 kDa	3	
17	✓	☆	Histone H1x //:CRAI335001131015964_9606 /def=Histone H1x /gene_name=H1FX /panther_id=PTHR15325:SF1 /family=H1 HISTONE FAMILY MEMBER FACTO...	sptlQ92522 (...	22 kDa	3	
18	✓	☆	T-complex protein 1, gamma subunit (TCP-1-gamma) (CCT-gamma) //:CRAI335001131103101_9606 /def=T-complex protein 1, gamma subunit (TCP-1-gam...	sptlP49368 (...	60 kDa	3	
19	✓	☆	small nuclear ribonucleoprotein polypeptide B'' //:CRAI197000069386538_9606 /def=CRAIhCP1773978 /gene_name=small nuclear ribonucleoprotein polypep...	cralhCP1773...	25 kDa		2
20	✓	☆	keratin 6A //:CRAI209000073934485_9606 /def=CRAIhCP1879668 /gene_name=keratin 6A /panther_id=PTHR18893:SF5 /family=KERATIN TYPE II/HSP 70-RELA...	cralhCP1879...	60 kDa		2
21	✓	☆	junction plakoglobin //:CRAI197000064954782_9606 /def=CRAIhCP1725599.1 /gene_name=junction plakoglobin /panther_id=PTHR11553:SF6 /family=BETA-...	cralhCP1725...	82 kDa		2
22	✓	☆	T-complex protein 1, theta subunit (TCP-1-theta) (CCT-theta) //:CRAI335001131103139_9606 /def=T-complex protein 1, theta subunit (TCP-1-theta) (CCT-th...	sptlP50990 (...	59 kDa	3	
23	✓	☆	T-complex protein 1, beta subunit (TCP-1-beta) (CCT-beta) //:CRAI335001131103096_9606 /def=T-complex protein 1, beta subunit (TCP-1-beta) (CCT-beta) /...	sptlP78371 (...	57 kDa	2	
24	✓	☆	Hypothetical protein MGC4308 //:CRAI147000073462977_9606 /def=Hypothetical protein MGC4308 /gene_name=MGC4308 /panther_id=PTHR10967:SF39 /fam...	trmlQ9BQ75 ...	32 kDa	2	
25	✓	☆	DEAD (Asp-Glu-Ala-Asp) box polypeptide 55 //:CRAI179000462918875_9606 /def=refINP_065987.1l DEAD (Asp-Glu-Ala-Asp) box polypeptide 55 [Homo sapien...	rflNP_06598...	69 kDa	2	
26	✓	☆	Nucleolar GTP-binding protein 2 (Autoantigen NGP-1) //:CRAI335001131015795_9606 /def=Nucleolar GTP-binding protein 2 (Autoantigen NGP-1) /gene_nam...	sptlQ13823 (...	84 kDa	3	
27	✓	☆	histone 1, H2bj //:CRAI300000355054O_9606 /def=CRAIhCP1626301 /gene_name=histone 1, H2bj /panther_id=PTHR11425:SF4 /family=HISTONE H2B /subfa...	cralhCP1626...	14 kDa	2	
28	✓	☆	pleiotropic regulator 1 (PRL1homolog, Arabidopsis) //:CRAI197000069431232_9606 /def=CRAIhCP1777346.1 /gene_name=pleiotropic regulator 1 (PRL1homo...	cralhCP1777...	56 kDa	2	

5. Discussion

5.1. Passenger strand cleavage for efficient RNAi

The studies on passenger strand cleavage in human cells and *D. melanogaster* showed that siRNAs are loaded into RISC while still being in the duplex configuration (Leuschner et al., 2006; Matranga et al., 2005; Miyoshi et al., 2005; Rand et al., 2005). Earlier models implied an elusive RNA helicase to remove the passenger strand prior to RISC assembly (Pham et al., 2004). Still, the hypothesis of an RNA helicase removing the cleavage products during RISC loading as well as during RISC recycling under multiple turnover conditions is valid. Since recombinant Ago2 can only be programmed by single-stranded siRNAs (Rivas et al., 2005), this immediately suggests that the role of a putative RISC loading complex (RLC) is to enable the loading of a duplex siRNA into Ago2 (Pham et al., 2004). In the human context, the phenomenon of passenger strand cleavage remains obscure. In contrast to *D. melanogaster,* no RLC or holo-RISC has been described most probably owing to the fact that the RNAi pathway does not exist. However, challenging the cells with "Dicer-like" pre-processed siRNAs provokes strong silencing. In this case, passenger strand cleavage takes place and is an important prerequisite. Since passenger strand cleavage enforces siRNA asymmetry by destroying one strand thus removing it from the scene, this could be valuable for the future design of synthetic siRNAs. Rendering the guide strand "uncleavable" but still functional by a phosphorothioate between the nt 9 and 10 should prevent RISC from stochastic loading onto the passenger strand thus removing off-target effects without altering the efficiency and specificity of the guide strand.

Concerning the bypass mechanism, where an intact passenger strand has to be removed, two important questions need to be addressed: (a) how does Ago2-RISC remove the miRNA* strand where central mismatches impede passenger strand cleavage; (b) how do human Ago1, Ago3 and Ago4—that associate with siRNAs and miRNAs but lack slicer activity (Liu et al., 2004; Meister et al., 2004)—remove the passenger strand? Matranga and colleagues addressed these problems beautifully in *D. melanogaster* and HeLa cells (Matranga et al., 2005). In accordance with our results, the bypass pathway acts slower in unwinding the duplex, when compared to the cleavage-assisted pathway. An important consequence of passenger strand cleavage within an siRNA is the dramatic change in the thermodynamic profile of the duplex, making it easier to unwind. It

appears that especially the bases of the seed have to be unpaired to dismantle RISC from the target. Matranga and colleagues compared the genuine miR-1/miR-1* duplex featuring a 2-nt bulge at the seed, a "miR-1-siRNA" with perfect baseparing over the whole duplex and a "miR-1-GU-siRNA", where a bulge was introduced at position 2 of miR-1 (Figure 11). In addition, the passenger strands either featured phosphates or phosphorothioates between bases 9 and 10 thus rendering it cleavable or uncleavable, respectively. In stark contrast to both miR-1-siRNA types, the miR-1/miR-1* miRNA duplex with an uncleavable passenger strand did not show significant drop in silencing efficiency. The biggest decrease in target RNA cleavage was observed for the miR-1-siRNA. For the miR-1-GU-siRNA, this effect was lower but still significant.

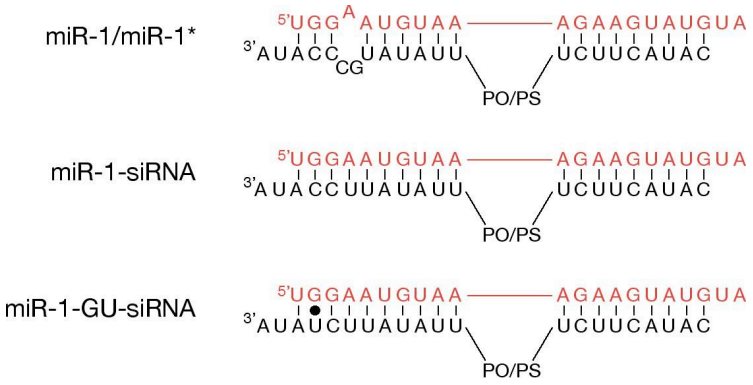

Figure 11. Analyzing the bypass pathway
Matranga et al. compared passenger strand removal on the genuine miR-1 duplex to a miR-1-siRNA with perfect complementarity and to a miR-1-GU-siRNA with a GU-basepair at position 2 of miR-1. The scissile phosphodiester-bond either contained a phosphate (PO) or a phosphorothioate (PS). *taken from* (Matranga et al., 2005)

The main conclusion from these results is that a bulge in the seed region abrogates the necessity for passenger strand cleavage. In this case the bypass pathway is able to unwind the duplex fast and easily. A GU-pair in the seed also assists unwinding, albeit at a much reduced speed if the passenger strand cannot be cleaved. These findings are very important in the context of the slicer-dead Argonaute proteins Ago1, Ago3 and Ago4. Here, even if the passenger strand could be cleaved, cleavage would not happen and the passenger strand has to be removed intact. Comparing known miRNA/miRNA* duplexes (Griffiths-Jones, 2004) it becomes evident that many feature at least one unpaired base within the seed, which will greatly assist unwinding during RISC loading. This is in line with current publications underlining the importance of target RNA binding via the bases of the seed. It appears that the seed, which was originally described for miRNAs, also plays an important role for siRNAs in finding and binding a target (Ameres et al., 2007): the bases of the 5′ create a thermodynamic threshold that has to be overcome to allow a stable association of RISC to the target RNA—an mRNA or even the passenger strand.

5.2. Differential, context-dependent processing of pre-miR-138-2 confers tissue specificity

5.2.1. Modes of post-transcriptional regulation of microRNA expression

Shortly after the publication of our results, more evidence on post-transcriptional regulation of miRNA expression surfaced. While the phenomenon we observed was restricted to a single pre-miRNA hairpin, Thomson and colleagues reported extensive post-transcriptional regulation of miRNA expression at the level of Drosha processing (Thomson et al., 2006). They found that both in early mouse development and primary tumors, the level of the nuclear RNase III Drosha, which initiates the miRNA processing cascade, is down-regulated while miRNA genes are being transcribed. This leads to an accumulation of primary transcripts with no mature miRNAs present. These findings are in line with the current view that the expression of the large majority of miRNAs is induced during mid-to-late embryonic development, culminating in adult and terminally differentiated tissues (Kloosterman and Plasterk, 2006). Thus, miRNAs are hypothesized to mainly function by "freezing" the terminally differentiated status of cells (Bartel and Chen, 2004). In primary tumors, many miRNAs can be found to be down-regulated, which could indicate a loss of cellular differentiation (Lu et al., 2005; Takamizawa et al., 2004). While this down-regulation could be attributed to transcriptional modulation on the miRNAs promoter level, it is tempting to speculate that a down-regulation of Drosha could globally lead to the same effect. Further evidence for extensive post-transcriptional regulation of miRNA expression was put forward by van Rooij and colleagues, who analyzed miRNA expression signatures associated with cardiac hypertrophy (van Rooij et al., 2006). In several cases, they observed differential accumulation of mature miRNAs versus their pre-miRNA hairpins. However, they did not analyze these observations further to assess, whether these variable ratios could be explained by regulation of Drosha or Dicer or whether they are due to other phenomena.

Kawahara and colleagues reported RNA A→I editing of a pri-miRNA to be responsible for differential processing of the resulting pre-miRNA (Kawahara et al., 2007). Such editing by Adenosine Deaminases Acting on RNA (ADARs) has already been described earlier (Yang et al., 2006), but the fate of edited pri-miRNAs was largely

unknown. Kawahara and colleagues showed that the conversion of two specific adenosine residues to inosine on the pri-miR-151 interfered with the interaction between the pre-miR-151 and the Dicer-TRBP complex. However, this A→I editing of pri-miR-151 in neuronal tissues is not absolute. Approximately 60–70% of the pre-miR-151 transcripts remain unedited in neuronal cells and are processed faithfully to the mature miR-151. This is a major difference to the phenomenon we described, where we observe a complete block in the processing of pre-miR-138-2 to mature miR-138. It appears that editing of pri-miR-151 is used to adjust the levels of miR-151 in neuronal tissues.

Guil and Caceres provided the latest contribution to post-transcriptional regulation. In contrast to all previous examples, where miRNA expression is negatively regulated, Guil and Caceres described an auxiliary factor that acts positively on miRNA processing (Guil and Caceres, 2007). hnRNP A1 was found to bind specifically to the pri-miR-18 hairpin within the primary transcript of the *miR-17–92* cluster, and assist in its cleavage by Drosha. If cells are depleted of hnRNP A1, the amounts of pre-miR-18 and mature miR-18 are significantly lower. hnRNP A1 is known to be expressed in a tissue specific manner (Hanamura et al., 1998), indicating a potential involvement in regulating tissue specific miRNA expression. Furthermore, the dependency of an auxiliary factor to efficiently process a miRNA hairpin from a polycistronic miRNA-cluster elegantly uncouples its expression from the other co-transcribed miRNAs and allows function independent from the polycistron.

These studies have been published within one year and, in my opinion, constitute just the starting point in the field of post-transcriptional regulation of miRNA expression. The early view, where the miRNA biogenesis cascade was thought to be a default pathway, that is executed as soon as a miRNA gene is transcribed, has been overhauled thoroughly. Still, it remains undisputed that regulation on the promoter level has the biggest contribution to tissue- and developmental stage-specific expression of miRNAs. However, after the stage is set, cells employ additional tricks during miRNA maturation to finetune and modulate the expression of specific miRNAs. This allows complex regulation at various positions.

5.2.2. Purpose of post-transcriptional regulation of microRNA expression

The question remains, what could be the biological relevance of post-transcriptional regulation? In most cases, the purpose appears to be evident. Regulation

by pri-miRNA editing seems to fine-tune the level of the mature, functional miRNA. Neuronal cells obviously require a lower amount of miR-151 than other tissues. Another reason could be the uncoupling of one miRNA from other co-transcribed RNAs. Such RNAs can be different miRNAs residing in the same polycistron, but also an mRNA, where the particular miRNA is residing in an intron. As a consequence, the miRNA will be expressed, whenever the host-gene is transcribed, although the requirement for the host gene and the miRNA could be different. Regulation similar to hnRNP A1 and miR-18 could in this case ensure that the miRNA is only matured when needed. We hypothesized that this could be the explanation for the differential expression of miR-138. We envisioned that the locus *miR-138-2* could be encoded in an intron of a constitutively expressed gene. By post-transcriptional regulation, expression of the mature functional miR-138 is restricted to neuronal cells. However, analysis of the genomic context showed that *miR-138-2* resides in an independent transcription unit. Thus, the purpose of post-transcriptional regulation of pre-miR-138-2 still remains obscure.

5.2.3. Insights from the secondary structure of pre-miR-138-2

Comparing the secondary structure of pre-miR-138-2 to other pre-miRNAs does not reveal any striking differences. Nevertheless, we envision that the inhibitor recognizes pre-miR-138-2 due to its sequence and the resulting secondary structure. Structural variants clearly showed that the internal loop 1, which is next to the open end of the hairpin precursor, plays a crucial role, since the closing of this loop abrogated inhibition of processing in HeLa cytoplasmic extract. However, it appears that this loop alone is not the only determinant, since removing the loop 2 next to the closed end of the hairpin also relieved inhibition, albeit only slightly. Obviously, the inhibitor recognizes the overall structure of pre-miR-138-2 and not isolated elements. Another interesting observation is the 17-nt cleavage product that accumulates whenever processing is inhibited (Figure 5 bottom of the gel). Counting from the 5′-end, nucleotide 17 is the cytidine base within the loop 1. While this could be easily dismissed as an artifactual activity of an unspecific nuclease in the *in vitro* cleavage assay, one should consider the fact that miR-138 was originally annotated as a 17-nt miRNA with a very low abundance (Tom Tuschl, personal communication). Could it be that loop 1 is not only important for the recognition by the inhibitor but also plays a role in the turnover of non-processed pre-miR-138? Since the *miR-138-2* gene appears to be transcriptionally

active in a constitutive fashion and since faithful processing of pre-miR-138-2 by Dicer is inhibited, cells actually need an exit pathway to get rid of the otherwise accumulating pre-miR-138-2. We never detected a 17-nt band in our Northern blots, probably due to the very short half-life of such an RNA oligonucleotide in the cell. We hypothesize that the inhibitor could fulfil a bipartite function: (a) to inhibit Dicer from processing pre-miR-138-2 and (b) to mediate the degradation of unprocessed pre-miR-138-2. Still, this hypothesis needs experimental validation. A crucial question is, why the 17-nt band is absent, when the loop-1-mutant pre-miR-138 is processed in the presence of HeLa cytoplasmic extract? What is the requirement for cleavage to occur after nucleotide 17: the binding of the inhibitor or the single stranded configuration of the nucleotides 16–18 in the loop? Both conditions are abrogated in the loop-1-mutant pre-miR-138-2. Analyzing the 17-nt cleavage product could shed some light. Does it display a 3′-hydroxy or a 3′-phosphate terminus?

An unrelated observation from the processing studies of the structural mutants was the fidelity of Dicer cleavage. Northern blot analysis with a reasonable resolution at the size of ~21 nt shows that miRNAs do not exist as a single species but in various lengths within a margin of ±2 nt. As consistently shown in both Northern blots and processing gels, miR-138 exists as 23-nt and 24-nt miRNA species at ratio of around 1:1. If loop 1 is closed, the cleavage is shifted towards 23 nt, if loop 2 is closed the cleavage is shifted towards 24 nt. Our interpretation of this phenomenon is that an internal loop acts like a spring, conferring flexibility to the precursor hairpin. Depending on the state of this molecular spring—compressed or relaxed—Dicer cleaves after nucleotide 23 or 24, respectively. Closing the loops removes the spring function and makes the structure rigid, leading to Dicer cutting the precursor at a single site. For miRNAs encoded in the 5′-arm of the precursor hairpin, adding or removing a base at the 3′-end does not matter in terms of miRNA function. For miRNAs in the 3′-arm, however, Dicer sets the actual 5′-end that is important for the location of the seed. Adding or removing one base here would shift the sequence of the seed and will eventually lead to different requirements to bind a target RNA. We envision the existence of sub-classes of target RNAs that are either bound by one or the other miRNA species. If the fidelity of Dicer cleavage on a given pre-miRNA could be modulated by the binding of additional interacting factors, such sub-classes of miRNA-target RNAs could be individually regulated, a hypothetical novel way of post-transcriptional regulation of miRNA function.

5.2.4. Purification attempts

We have employed several techniques to purify the inhibitory activity from HeLa cytoplasmic extracts in order to allow identification of the protein factors involved. So far, no candidate could be positively validated from either purification strategy. For the future, we will attempt to combine the different strategies. First, I will perform glycerol gradient and gel filtration chromatography from the same pre-purified sample to determine the molecular size more accurately using the method of Siegel and Monty (Siegel and Monty, 1966). For the StreptoTag technique, I plan to add the gel filtration step to the pre-purification of the inhibitory activity after Heparin and Blue Sepharose. While the classical chromatographic purification chain leads to a specific enrichment, still a large number of proteins co elute with the inhibitory activity. Here, gel filtration could also potentially help to remove background.

Finally, I also want to add western blotting to the validation of candidate proteins identified from liquid samples. If anti-sera are available, I plan to probe the fractions showing inhibitory activity plus the neighboring ones, in order to see co-purification of the activity and the presence of the protein band on the western blot.

6. Materials and Methods

ELSEVIER

Methods 43 (2007) 105–109

METHODS

www.elsevier.com/locate/ymeth

In vitro analysis of microRNA processing using recombinant Dicer and cytoplasmic extracts of HeLa cells

Philipp J.F. Leuschner *, Javier Martinez

IMBA—Institute of Molecular Biotechnology of the Austrian Academy of Sciences, 1030 Vienna, Dr. Bohr-Gasse 3, Austria

Accepted 13 April 2007

Abstract

MicroRNAs (miRNAs) constitute a novel class of short, non-coding RNAs that play crucial roles as silencers of gene expression during biological processes such as development, growth control, cell death, and differentiation. To ensure correct function, the expression of miRNAs must be tightly regulated, a process that is believed to take place at the promoter level. Regulation of the miRNA processing cascade has only recently been shown to play an important role as well and we envision the discovery of additional factors affecting or modulating miRNA processing and ultimately miRNA expression. The biochemical analysis of such factors requires a robust assay to monitor miRNA processing. Here, we discuss protocols and techniques that were used to investigate how the expression of brain-specific miRNA miR-138 is controlled at the level of precursor-miRNA (pre-miRNA) processing.

Keywords: miRNAs; Pre-miRNA; Dicer; RNase III; Stem-loop; Hairpin; Cleavage

1. Introduction

MicroRNAs (miRNAs) are ~22 nucleotide (nt) short, non-coding RNA molecules that function as post-transcriptional regulators of gene expression [1,2]. Target gene silencing is accomplished by binding of miRNAs to cognate sequences in the 3′-untranslated regions (3′-UTRs) of messenger RNAs (mRNAs). Depending on the extent of complementarity, miRNAs either direct target mRNA cleavage (full complementarity) [3] or mediate translational repression (partial complementarity) [4].

The biogenesis of miRNAs has been described in great detail [5]. The majority of miRNA genes are transcribed by RNA polymerase II as mono- or polycistronic primary transcripts (pri-miRNAs) that are capped and polyadenylated [6,7]. A recent study, however, demonstrated that miRNA genes interspersed along Alu repeats are transcribed by RNA polymerase III [8]. The hallmark of pri-miRNAs are stem-loop structures containing the sequences of mature miRNAs embedded in the arm of a stem. These hairpin-like structures are recognized by the Microprocessor complex, consisting of the double-stranded RNA-binding domain protein (dsRBD) Pasha/DGCR8 and the nuclear RNase III-like enzyme Drosha, which endonucleolytically cleaves the pri-miRNA, releasing a ~65 nt precursor miRNA (pre-miRNA) hairpin [9–12]. Subsequently, pre-miRNAs are exported to the cytoplasm by Exportin-5 [13–15], where they are processed by a second complex consisting of the dsRBD Loquacious/TRBP and the RNase III-like enzyme Dicer into ~22-nt duplexes [16–19], followed by the asymmetric assembly of one of the two strands into a functional miRNA-associated RNA induced silencing complex (miRISC) [20,21].

Many miRNAs display tissue- and/or developmental stage-specific expression patterns, which in most cases is due to transcriptional regulation at the promoter level. Recently, evidence surfaced that miRNA expression is also regulated post-transcriptionally at different levels of the miRNA production cascade. Our laboratory demonstrated that the gene encoding miRNA-138 (miR-138) is

* Corresponding author. Fax: +43 1 79044 110.
E-mail address: philipp.leuschner@imba.oeaw.ac.at (P.J.F. Leuschner).

1046-2023/$ - see front matter © 2007 Elsevier Inc. All rights reserved.
doi:10.1016/j.ymeth.2007.04.005

ubiquitously expressed, but processing of its transcript stalls in the cytoplasm at the precursor level. Only cells of the hippocampus, the neo-cortex, the cerebellum and the fetal liver process this precursor into the active 23–24 nt species [22]. Differential accumulation of pre-miRNA versus mature miRNA was also observed in a study focusing on stress-responsive miRNAs in the heart [23]. Finally, processing of pri-miRNA transcripts by Drosha was also found to be extensively regulated [24].

We here describe assays and techniques aimed to identify and study cellular factors influencing the processing of a pre-miRNA by Dicer.

2. Description of methods

2.1. Preparation of the substrate

2.1.1. Transcription by T7 RNA polymerase

A typical pre-miRNA hairpin that is recognized and cleaved by the RNase III-like enzyme Dicer is approximately 65 nt in length and features a 5′ phosphate together with a 2 nt 3′ overhang. Since ordering multiple synthetic ~65 nt RNA oligos can become very expensive, we generated substrates for processing assays by *in vitro* transcription using the MEGAshortscript™ T7 kit (Ambion). To create the DNA template, we fused the antisense sequence of various pre-miRNAs to the T7-promoter (5′-*antisense-pre-miRNA-sequence*—TATAGTGAGTCGTATTAAATT-3′), which is illustrated in Fig. 1. Pre-miRNA sequences were derived from miRBase [25]. Note that the "stem-loop sequence" that is available and that can be downloaded in FASTA format also contains parts of the primary transcript that are removed by the cleavage of Drosha and which have to be disregarded for the design of the pre-miRNA hairpin. The single stranded DNA-template was annealed to a T7-runoff primer (5′-AATTTAATACGACTCACTATAGG-3′) and adjusted to a final concentration of 10 μM template in TES buffer (10 mM Tris–HCl, pH 8, 1 mM EDTA, 0.1 M NaCl). The mixture was heated for 1 min to 95 °C and slowly cooled to room temperature. The reaction was performed as outlined in the manufacturer's instructions using 30 pmoles of the template and incubating for 4 h at 37 °C. The reaction was stopped by adding 1 volume of 2× STOP buffer (8 M urea, 0.05% bromophenol blue).

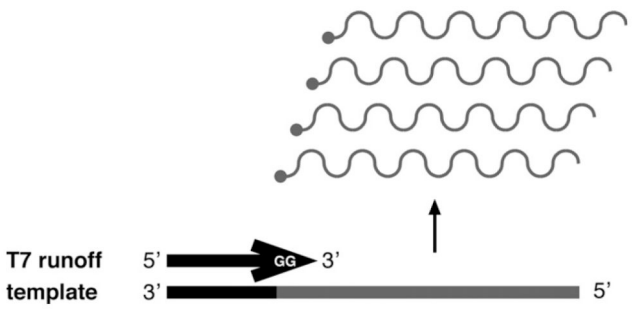

Fig. 1. T7 RNA polymerase runoff template. This figure illustrates the design of DNA templates that can be used for T7 RNA polymerase-mediated *in vitro* transcription. The antisense sequence of the pre-miRNA (gray) is fused to the sequence of the T7 promoter (black). This strand is annealed to a T7 runoff primer (black arrow) that renders the promoter region double-stranded, which allows binding of T7 RNA polymerase and initiation of multiple rounds of transcription.

2.1.2. PAGE-purification

The RNA transcripts were purified using a 17 cm × 23 cm × 1 mm, 8% denaturing polyacrylamide gel (Sequagel, National Diagnostics). The gel was run in 0.5× TBE buffer (45 mM Tris–borate, 1 mM EDTA) at 30 W until the bromophenol blue marker reached the bottom. Radioactive precursors were detected by autoradiography on X-ray films (Kodak Biomax XAR Film). Cold precursor transcripts were visualized by UV epi-illumination using a handheld lamp (Herolab) with a wavelength of 254 nm. Bands corresponding to full-length transcripts were excised from the gel using scalpels with a curved blade and placed into a siliconized eppendorf tube (Thomas Scientific). Elution was carried out overnight in 300 μl of 0.3 M NaCl by shaking at 1000 rpm and 4 °C. The eluate was then precipitated using 3 volumes of 100% ethanol (Merck). Precipitation occurred at –20 °C for 60 min. The pellet was collected at 13,000 rpm on a refrigerated table-top microtube centrifuge and resuspended in an appropriate volume of water to a final concentration of approximately 10 pmoles/μl. The amount of the transcript was determined photometrically using a SmartSpec™ Plus (Bio-Rad).

2.1.3. Labeling of the transcript

Two different methods were employed to label the RNA transcript. In the first case, T7 transcription was carried out in the presence of α-^{32}P-UTP leading to a "body" or internally labeled pre-miRNA. We included 5 μl of α-^{32}P-UTP (3000 Ci/mmol, GE Healthcare) to the reaction, which was otherwise performed as outlined above. In the second instance, transcription by T7 RNA polymerase was carried out without radioactive isotopes and the transcript was 5′-end labeled using γ-^{32}P-ATP. For this purpose, the cold transcript was dephosphorylated with alkaline phosphatase (20 U/μl, Roche) using 1 U per pmol RNA at 50 °C for 60 min. To facilitate the phenol/chloroform extraction, the dephosphorylation reaction was filled up to 300 μl with water and extracted once with phenol (pH 4.0)/chloroform/isoamyl alcohol (P:C:I = 25:24:1, Applichem) and once with chloroform/isoamyl alcohol (C:I = 24:1, Applichem) followed by ethanol precipitation, where the aqueous phase was supplemented with 1/10 volume of 3 M NaOAc pH 4.6 (Applichem) and 3 volumes of 100% ethanol (Merck). The pellet was washed with 1 ml 70% ethanol and resuspended in an appropriate volume of water to a final concentration of approximately 10 pmoles/μl. The 5′-end labeling was performed using 10 pmoles of dephosphorylated transcript, 1.5 μl γ-^{32}P-ATP (6000 Ci/mmol, Perkin-Elmer) and 0.1 U T4 polynucleotide kinase (10,000 U/ml, NEB) in a final volume of 10 μl. After

30 min at 37 °C the reaction was quenched by adding 1 μl 100 mM ATP. After 3 additional min at 37 °C the reaction was stopped by adding 11 μl of 2× STOP buffer. The 5′-end labeled transcript was PAGE-purified as described above.

2.1.4. Folding

To be used in processing assays, pre-miRNA transcripts were diluted to a concentration of 100 nM in RNAi buffer (30 mM Hepes, pH 7.4, 100 mM KCl, 5 mM $MgCl_2$, 10% glycerol). The solution was heated to 95 °C for 1 min and then slowly cooled to room temperature. To avoid repeated freeze-thaw cycles, we made 10 μl aliquots and stored them at −20 °C.

2.2. Processing of pre-miRNAs using cellular extracts

Since miRNAs can be cloned from any mammalian or vertebrate tissue, the miRNA processing machinery appears to be expressed in a ubiquitous fashion. Consequently, Dicer activity should be present in virtually any cellular extract. We used HeLa cytoplasmic extracts (S100) from Paragon Bioservices for our studies. These extracts contained approximately 12 mg/ml protein and were supplemented with 100 mM KCl, 2 mM $MgCl_2$, and 10% glycerol. We mixed 1 μl of the substrate (100 nM in RNAi buffer), 5 μl S100, 3 μl H_2O, and 1 μl of a 3× reaction mix to adjust the reaction conditions to final concentrations of 100 mM KCl, 5 mM $MgCl_2$, 0.5 mM DTT, 1 mM ATP, and 0.2 mM GTP. The final concentration of the substrate was 10 nM, but this can also be adjusted to lower or higher values according to needs. The reaction was set up on ice, incubated for up to 2 h at 30 °C, and stopped by the addition of 1 volume 2× STOP buffer. Samples were boiled for 1 min at 95 °C and separation occurred on a 17 cm × 23 cm × 0.4 mm, 15% denaturing polyacrylamide gel (Sequagel, National Diagnostics) at 30 W. The use of 0.4 mm thin gels allow sharp separation of very small loading volumes (2 μl). To further optimize resolution, the gel was pre-run at 30 W for 45–60 min. The gel was removed after the bromophenol blue marker reached the bottom and dried for 1 h at 80 °C (Model 583 gel dryer, Bio-Rad). Reaction products were detected by using Storage Phosphor screens (GE Healthcare) and visualized by Phosphorimaging on a Typhoon Trio (GE Healthcare). Fig. 2 shows the result of a typical Dicer-guided processing reaction in HeLa S100 cytoplasmic extracts.

This protocol can be applied to a variety of cellular extracts. For efficient lysis of cells or tissues, we used a lysis buffer containing 30 mM Hepes, pH 7.4, 100 mM KCl, 5 mM $MgCl_2$, 10% glycerol, 0.5 mM DTT, 0.1 mM AEBSF (a serine protease inhibitor), and 0.2% NP40. This allowed lysis of cells directly on the culture plate. To generate extracts from tissues and/or whole organs, samples were cut into small pieces and sonicated in lysis buffer using 6 × 20 s bursts at 90% intensity with a 1 min pause on ice. To remove cell debris, extracts were centrifuged at 4 °C, 13,000 rpm in a refrigerated table-top microcentrifuge

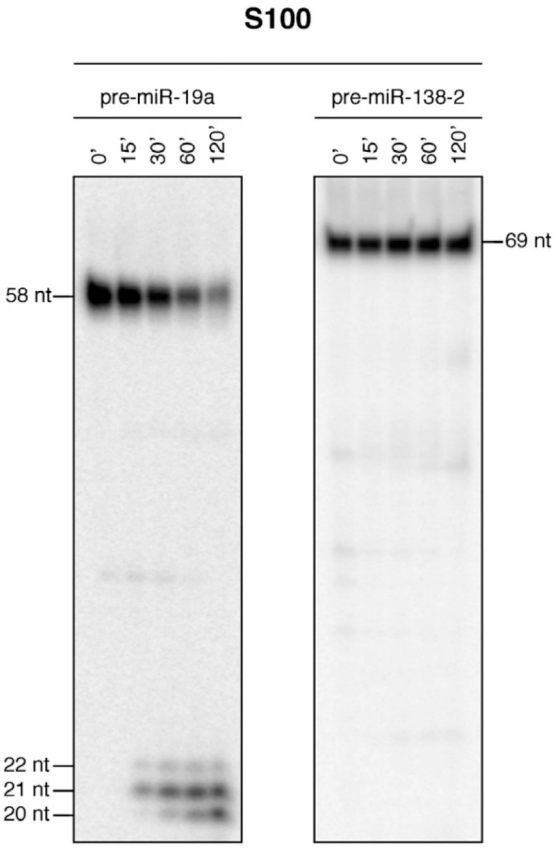

Fig. 2. Processing of pre-miR-19a and pre-miR-138–2 using HeLa S100 extracts. Processing was performed as described in Section 2.2. In this case, we employed precursor transcripts labeled at the 5′ end using γ-^{32}P-ATP. While pre-miR-19a is readily processed into the mature ~21-nt miRNA, HeLa S100 fails to cleave pre-miR-138–2 due to the presence of an inhibitory factor [22]. Note that miR-19a is encoded in the 3′ arm of the stem-loop precursor. The reaction products visible on the gel are actually the miR-19a* strand that is indicative of Dicer-mediated cleavage.

and the supernatant was transferred to a new tube. Protein concentration was determined by performing a Bradford assay (Bio-Rad). Extract concentrations were subsequently adjusted to approximately 5–10 mg/ml.

2.3. Processing of pre-miRNAs using recombinant Dicer enzyme

S100 HeLa cytoplasmic extracts are not able to process pre-miR-138–2. We therefore used recombinant Dicer enzyme (rDcr) to assess whether this particular precursor hairpin is not cleaved due to its structure or due to the action of an inhibitory factor. We employed a protocol established in the Filipowicz lab, whereby rDcr is proteolytically activated using proteinase K prior to cleavage of the pre-miRNA substrate [26]. We prepared a 2× reaction buffer (60 mM Tris–HCl, pH 6.8, 100 mM NaCl, 6 mM $MgCl_2$, 0.2% Triton X, 40% glycerol, and 2 mM DTT) that was used in processing studies as specified in [26]. For a typical reaction, we mixed 5 μl 2× rDcr buffer, 0.25 μl rDcr

enzyme (1 U/μl, Ambion), 1 μl substrate (100 nM in 1× lysis buffer), and 3.75 μl of H_2O to a final volume of 10 μl. Proteolytic activation of rDcr was performed before adding the substrate in 2× rDcr buffer by using 5 ng proteinase K (Sigma) for 1 U rDcr. The reaction was incubated for 10 min at 37 °C and then placed back on ice. The substrate was added and the reaction was incubated at 37 °C for up to 10 min and stopped by the addition of 1 volume 2× STOP-buffer. Separation of cleavage products was performed as outlined in Section 2.2. A typical autoradiograph is shown in Fig. 3.

2.4. Processing of pre-miRNAs using rDcr and cytoplasmic extracts

Since rDcr alone was able to cleave pre-miR-138–2, we presumed that an inhibitory factor was present in HeLa S100 extracts that abolishes processing of this particular precursor by endogenous Dicer. To verify this assumption, we repeated the previous processing reaction, but this time we included 3.75 μl S100 instead of H_2O. The result is shown in Fig. 4. While pre-miR-19a is still converted into mature miR-19a, rDcr fails to process pre-miR-138–2. We have thus generated a method whereby any extract/fraction/factor that is hypothesized to influence processing of precursor-miRNAs by Dicer can be analyzed by simply adding it to the processing reaction. Due to the high activity of rDcr enzyme, it may be necessary to pre-incubate the substrate with the respective sample in order to allow sufficient interaction. Modulation of pre-miRNA processing may also occur by chemical modification of the substrate such as RNA editing [27], which could require a longer pre-incubation time or even different buffer conditions that could in turn abolish cleavage of the RNA substrate by Dicer. In such a case, proteinase K should be added after the pre-incubation reaction, the RNA substrate phenol extracted, ethanol precipitated, and folded prior to use in the pre-miRNA processing assay.

This protocol can also be adapted for diluted factors/extracts. Here, the concentration of the substrate as well as the amount of rDcr can be adjusted to low levels, whereby a difference in rDcr processing may become more easily visible.

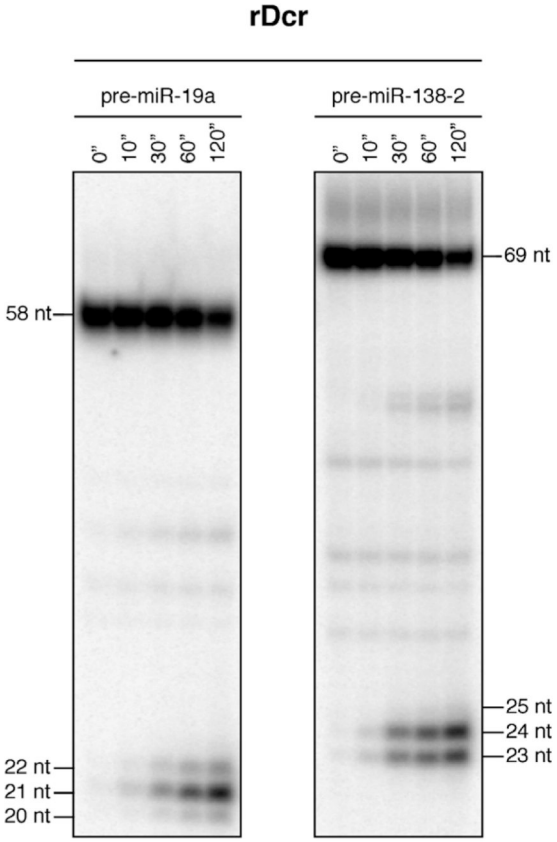

Fig. 3. Processing of pre-miR-19a and pre-miR-138–2 using recombinant Dicer (rDcr). 5′-end labeled pre-miR-19a and pre-miR-138–2 were used in rDcr processing reactions as outlined in Section 2.3. Due to the high activity of rDcr, time point intervals should be set much shorter. Note that the first reaction products appear after 10 s. In contrast to Fig. 1, pre-miR-138–2 is converted into mature miR-138, demonstrating that pre-miR-138–2 is a genuine substrate for Dicer.

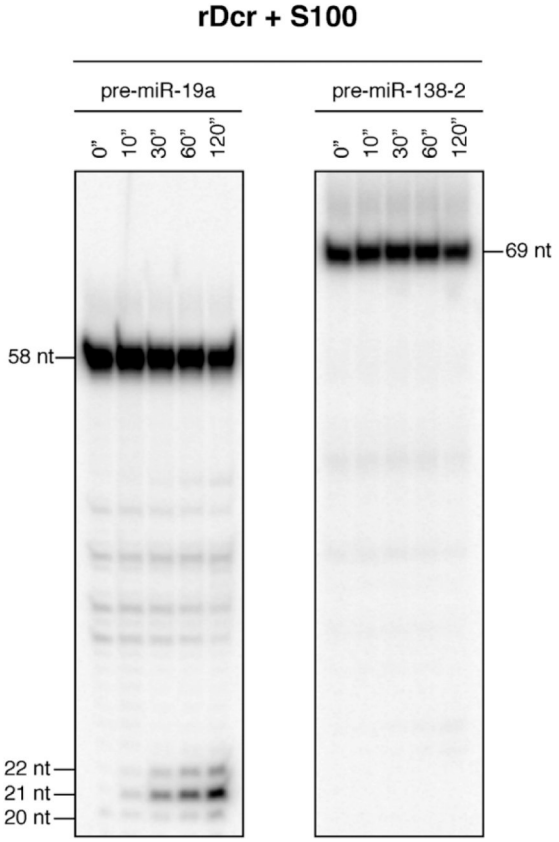

Fig. 4. Processing of pre-miR-19a and pre-miR-138–2 using recombinant Dicer in the presence of HeLa S100 extracts. The processing reaction displayed in Fig. 2 was repeated with the difference that HeLa S100 extracts were added to the reaction. Processing of pre-miR-19a remained largely unaffected, whereas cleavage of pre-miR-138–2 was completely abolished indicating the presence of an inhibitory factor for processing of this precursor.

3. Troubleshooting

3.1. The substrate

A prerequisite for efficient T7-mediated *in vitro* transcription is the presence of at least two guanosine residues after the core promoter sequence. Full T7 activity is only obtained if three guanosine residues are present. Since—as most pre-miRNAs—pre-miR-19a and pre-miR-138–2 do not start with "GG", not to mention "GGG", at the 5′ end, we had to exchange the first two nucleotides for "GG". Transcription of these two templates worked fine. However, similar templates encoding different pre-miRNAs did not provide satisfactory yields. An elegant way to circumvent such problems is described in Zhang et al. [28], where a hammerhead ribozyme is placed 5′ to the pre-miRNA sequence. Thus, the optimal three guanosine residues can be used, since the 5′ end of the pre-miRNA is established by autocatalytic cleavage of the hammerhead ribozyme.

3.2. The processing reaction

In some cases, nonspecific nucleases present in the extracts of various tissues or cell types may lead to a high background and could over-shadow specific cleavage products. This is especially true for "RNase-rich" tissues such as pancreas or liver. Here, dilutions of the extract may solve the problem. We have also observed that the best signal-to-noise ratio is obtained using 5′ end labeled substrates, since only cleavage products from nt N_1 are visible on the gel. Body-labeled pre-miRNA substrates result in much higher background, but on the other hand allow detection of any cleavage product from the substrate.

4. Concluding remarks

The techniques outlined above enabled us to offer the first conclusive biochemical evidence of post-transcriptional regulation of miRNA expression. These methods are currently employed to purify the inhibitory factor present in HeLa S100 extract using classical chromatography and the processing assay as a read-out for the presence of the inhibitor in the various fractions. We envision that these protocols can also be very helpful for both discovery and biochemical characterization of novel factors affecting processing of other pre-miRNAs.

References

[1] V. Ambros, Nature 431 (7006) (2004) 350–355.
[2] D.P. Bartel, Cell 116 (2) (2004) 281–297.
[3] S. Yekta, I.H. Shih, D.P. Bartel, Science 304 (5670) (2004) 594–596.
[4] R.S. Pillai et al., Science 309 (5740) (2005) 1573–1576.
[5] V.N. Kim, Nat. Rev. Mol. Cell Biol. (2005).
[6] X. Cai, C.H. Hagedorn, B.R. Cullen, RNA 10 (12) (2004) 1957–1966.
[7] Y. Lee et al., EMBO J. 23 (20) (2004) 4051–4060.
[8] G.M. Borchert, W. Lanier, B.L. Davidson, Nat. Struct. Mol. Biol. 13 (12) (2006) 1097–1101.
[9] A.M. Denli et al., Nature 432 (7014) (2004) 231–235.
[10] R.I. Gregory et al., Nature 432 (7014) (2004) 235–240.
[11] J. Han et al., Genes Dev. 18 (24) (2004) 3016–3027.
[12] M. Landthaler, A. Yalcin, T. Tuschl, Curr. Biol. 14 (23) (2004) 2162–2167.
[13] M.T. Bohnsack, K. Czaplinski, D. Gorlich, RNA 10 (2) (2004) 185–191.
[14] E. Lund et al., Science 303 (5654) (2004) 95–98.
[15] R. Yi et al., RNA (2004).
[16] E. Bernstein et al., Nature 409 (2001) 363–366.
[17] G. Hutvágner et al., Science 93 (2001) 834–838.
[18] R.F. Ketting et al., Genes Dev. 15 (20) (2001) 2654–2659.
[19] S.W. Knight, B.L. Bass, Science 2 (2001) 2.
[20] A. Khvorova, A. Reynolds, S.D. Jayasena, Cell 115 (2) (2003) 209–216.
[21] D.S. Schwarz et al., Cell 115 (2) (2003) 199–208.
[22] G. Obernosterer et al., RNA 12 (7) (2006) 1161–1167.
[23] E. van Rooij et al., Proc. Natl. Acad. Sci. USA 103 (48) (2006) 18255–18260.
[24] J.M. Thomson et al., Genes Dev. 20 (16) (2006) 2202–2207.
[25] S. Griffiths-Jones, Nucleic Acids Res. 32 (Database issue) (2004) D109–D111.
[26] H. Zhang et al., EMBO J. 21 (21) (2002) 5875–5885.
[27] W. Yang et al., Nat. Struct. Mol. Biol. 13 (1) (2006) 13–21.
[28] H. Zhang et al., Cell 118 (1) (2004) 57–68.

6.1. Chromatography

6.1.1. Purification of the inhibitory activity from HeLa extracts

The Lührmann lab, MPI Göttingen, generously provided cytoplasmic extracts prepared from HeLa cells according to the Dignam protocol (Dignam et al., 1983). The cytoplasmic fraction was supplemented to final concentrations of 100 mM KCl, 2 mM $MgCl_2$ and 10% glycerol, frozen it in liquid nitrogen and stored it at –80ºC. S100 extracts were prepared by ultracentrifugation for 1 h at 29,000 rpm at 4ºC using a Sorvall T-1250 rotor. The protein concentration of HeLa S100 extracts usually varied between 3-5 mg/ml. The purification of the inhibitory activity is schematically shown in Figure 6. All procedures were carried out at 4ºC. Column fractions were assayed for inhibition of pre-miR-138-2 processing by recombinant Dicer enzyme as described above. A total of 2,400 ml HeLa S100 extract (~4 mg/ml) were divided into 6× 400 ml fractions that were individually loaded onto a Heparin Sepharose 6 FF column (XK26, 100 ml bed volume, GE Healthcare) equilibrated in buffer BA100 (100 mM KCl, 30 mM Hepes pH 7.4, 5 mM $MgCl_2$, 10% glycerol, 0.5 mM DTT, 0.1 mM AEBSF). Elution occurred over 800 ml of a linear gradient in buffer BA1000 containing 1 M KCl. The 500 mM–660 mM fraction (6× ~120 ml) was supplemented with 35% ammonium sulfate (23.9 g), left for 15 min on ice, and centrifuged for 20 min at 16,000 rpm at 4ºC using a Sorvall SS34 rotor. The supernatant was collected and supplemented with 24.8 g ammonium sulfate (65%), again left for 15 min on ice and centrifuged for 20 min at 16,000 rpm at 4ºC. Three pellets (2×) were combined and dissolved in 100 ml buffer BB30 (30 mM KCl, 30 mM Hepes pH 6.0, 5 mM $MgCl_2$, 10% glycerol, 0.5 mM DTT, 0.1 mM AEBSF) and loaded onto a HiPrep 16/10 SP FF column (20 ml bed volume, GE Healthcare) equilibrated with buffer BB30. The column was developed with a gradient over 10× column volumes (CV) to buffer BB1000 containing 1 M KCl. The active pool (320 mM–490 mM) was dialyzed overnight against buffer BC100 (100 mM KCl, 30 mM Tris-HCl pH 8.0, 5 mM $MgCl_2$, 10% glycerol, 0.5 mM DTT, 0.1 mM AEBSF) and applied to a HiTrap Q XL sepharose column (5 ml bed volume, GE Healthcare) equilibrated in buffer BB100. Protein was eluted with a gradient over 10× CV to buffer BC1000 (1 M KCl). The active pool (110 mM–-280 mM KCl) was dialyzed overnight against buffer BD10 (10 mM KP_i pH 7.4, 10% glycerol, 0.5 mM DTT, 0.1 mM AEBSF) and applied to a Hydroxyapatite CHT-II column (1 ml bed volume, Biorad) equilibrated with buffer

BD10. The column was developed with a gradient over 10× CV to buffer BD500 (containing 500 mM KP_i). Fractions (250 mM–400 mM KP_i) from the two inividual column runs were pooled, dialyzed overnight against buffer BA100 and loaded onto a single HiTrap Blue HP column (1 ml bed volume, GE Healthcare) equilibrated with buffer BA100. Protein was eluted with a gradient over 10× CV to buffer BA2000. The active pool (1600 mM–1800 mM KCl) was dialyzed overnight against buffer BA100 containing only 3% glycerol and layered on top of a 12 ml linear 5% to 20% (w/w) glycerol gradient adjusted to 100 mM KCl, 30 mM Hepes pH 7.4, 5 mM $MgCl_2$, 0.5 mM DTT. Centrifugation was performed for 20 h at 40,000 rpm at 4ºC using a Sorvall TH641 rotor. Standard proteins (bovine serum albumine [BSA], 4.6 S; aldolase 7.3 S; catalase, 11.3 S) were run in a parallel gradient. Twenty fractions of 0.6 ml were collected sequentially from the top. 0.5 ml of each fraction was precipitated overnight with 0.5 ml trichloroacetic acid (TCA). The precipitates were dissolved in SDS-PAGE loading buffer, and samples were analyzed by 10% SDS-PAGE followed by silver staining. Protein bands present in the active fractions were excised and analyzed by mass spectrometry, together with a sample from the liquid fraction. The protein samples were reduced with DTT, alkylated by iodine acetamide and trypsinized. Peptides were separated by nano-HPLC chromatography and analyzed on a LTQ ion trap mass spectrometer. Mass data of all peptides were analyzed using the MASCOT software (Matrix Science).

6.1.2. Determination of the molecular weight of the inhibitory activity

To determine the molecular weight of the inhibitor, we performed size exclusion chromatography on a Superdex 200 column (Highload 16/60 column, GE Healthcare) using buffer BA100 as running buffer. The inhibitory activity was pre-purified on a HiPrep Heparin FF column (5 ml CV) followed by a HiTrap Blue HP column (1 ml CV) without dialysis in between or thereafter. For column calibration, standard proteins were used (blue dextran, exclusion; catalase, r_s = 5.2 nm, 250 kDa; aldolase, r_s = 4.8 nm, 158 kDa; bovine serum albumin, r_s = 3.6 nm, 66 kDa; RNase A, r_s = 1.6 nm, 13 kDa). The native molecular weight of the inhibitory protein was determined to be approximately 20 kDa.

6.1.3. StreptoTag purification of the inhibitor

The StreptoTag purification was performed as described in (Windbichler and Schroeder, 2006), using 200 pmol hybrid RNA immobilized on the column. The inhibitory activity was pre-purified using a HiTrap Blue HP column (see above).

6.2. Mammalian cell culture

HeLa cells were cultured at 37ºC, 95% humidity and 5% CO_2 using Dulbecco's Modified Eagle's Medium (DMEM) supplemented with 10% fetal bovine serum, 3 mM glutamine, 100 U/ml penicillin and 100 μg/ml streptomycin sulfate (all reagents were from Gibco) as a growth medium.

7. References

Aboobaker, A.A., Tomancak, P., Patel, N., Rubin, G.M., and Lai, E.C. (2005). Drosophila microRNAs exhibit diverse spatial expression patterns during embryonic development. Proceedings of the National Academy of Sciences of the United States of America *102*, 18017-18022.

Abrahante, J.E., Daul, A.L., Li, M., Volk, M.L., Tennessen, J.M., Miller, E.A., and Rougvie, A.E. (2003). The *Caenorhabditis elegans* hunchback-like gene *lin-57/hbl-1* controls developmental time and is regulated by microRNAs. Developmental cell *4*, 625-637.

Ambros, V. (2004). The functions of animal microRNAs. Nature *431*, 350-355.

Ameres, S.L., Martinez, J., and Schroeder, R. (2007). Molecular basis for target RNA recognition and cleavage by human RISC. Cell *130*, 101-112.

Aravin, A., Gaidatzis, D., Pfeffer, S., Lagos-Quintana, M., Landgraf, P., Iovino, N., Morris, P., Brownstein, M.J., Kuramochi-Miyagawa, S., Nakano, T.*, et al.* (2006). A novel class of small RNAs bind to MILI protein in mouse testes. Nature *442*, 203-207.

Aravin, A.A., Lagos-Quintana, M., Yalcin, A., Zavolan, M., Marks, D., Snyder, B., Gaasterland, T., Meyer, J., and Tuschl, T. (2003). The small RNA profile during *Drosophila melanogaster* development. Developmental cell *5*, 337-350.

Aravin, A.A., Sachidanandam, R., Girard, A., Fejes-Toth, K., and Hannon, G.J. (2007). Developmentally regulated piRNA clusters implicate MILI in transposon control. Science (New York, N.Y *316*, 744-747.

Bartel, D.P. (2004). MicroRNAs: genomics, biogenesis, mechanism, and function. Cell *116*, 281-297.

Bartel, D.P., and Chen, C.Z. (2004). Micromanagers of gene expression: the potentially widespread influence of metazoan microRNAs. Nat Rev Genet *5*, 396-400.

Baulcombe, D. (2004). RNA silencing in plants. Nature *431*, 356-363.

Berezikov, E., Guryev, V., van de Belt, J., Wienholds, E., Plasterk, R.H., and Cuppen, E. (2005). Phylogenetic shadowing and computational identification of human microRNA genes. Cell *120*, 21-24.

Bernstein, E., Caudy, A.A., Hammond, S.M., and Hannon, G.J. (2001). Role for a bidentate ribonuclease in the initiation step of RNA interference. Nature *409*, 363-366.

Bernstein, E., Kim, S.Y., Carmell, M.A., Murchison, E.P., Alcorn, H., Li, M.Z., Mills, A.A., Elledge, S.J., Anderson, K.V., and Hannon, G.J. (2003). Dicer is essential for mouse development. Nature genetics *35*, 215-217.

Betel, D., Sheridan, R., Marks, D.S., and Sander, C. (2007). Computational Analysis of Mouse piRNA Sequence and Biogenesis. PLoS computational biology *3*, e222.

Bhattacharyya, S.N., Habermacher, R., Martine, U., Closs, E.I., and Filipowicz, W. (2006). Relief of microRNA-mediated translational repression in human cells subjected to stress. Cell *125*, 1111-1124.

Bohmert, K., Camus, I., Bellini, C., Bouchez, D., Caboche, M., and Benning, C. (1998). AGO1 defines a novel locus of *Arabidopsis* controlling leaf development. The EMBO journal *17*, 170-180.

Bohnsack, M.T., Czaplinski, K., and Gorlich, D. (2004). Exportin 5 is a RanGTP-dependent dsRNA-binding protein that mediates nuclear export of pre-miRNAs. RNA (New York, N.Y *10*, 185-191.

Borchert, G.M., Lanier, W., and Davidson, B.L. (2006). RNA polymerase III transcribes human microRNAs. Nature structural & molecular biology *13*, 1097-1101.

Brennecke, J., Aravin, A.A., Stark, A., Dus, M., Kellis, M., Sachidanandam, R., and Hannon, G.J. (2007). Discrete small RNA-generating loci as master regulators of transposon activity in Drosophila. Cell *128*, 1089-1103.

Brennecke, J., and Cohen, S.M. (2003). Towards a complete description of the microRNA complement of animal genomes. Genome Biol *4*, 228.

Brennecke, J., Hipfner, D.R., Stark, A., Russell, R.B., and Cohen, S.M. (2003). *bantam* encodes a developmentally regulated microRNA that controls cell proliferation and regulates the proapoptotic gene *hid* in *Drosophila*. Cell *113*, 25-36.

Brennecke, J., Stark, A., Russell, R.B., and Cohen, S.M. (2005). Principles of microRNA-target recognition. PLoS Biol *3*, e85.

Buhler, M., Verdel, A., and Moazed, D. (2006). Tethering RITS to a nascent transcript initiates RNAi- and heterochromatin-dependent gene silencing. Cell *125*, 873-886.

Cai, X., Hagedorn, C.H., and Cullen, B.R. (2004). Human microRNAs are processed from capped, polyadenylated transcripts that can also function as mRNAs. RNA (New York, N.Y *10*, 1957-1966.

Calin, G.A., and Croce, C.M. (2006). MicroRNA signatures in human cancers. Nature reviews *6*, 857-866.

Calin, G.A., Liu, C.G., Sevignani, C., Ferracin, M., Felli, N., Dumitru, C.D., Shimizu, M., Cimmino, A., Zupo, S., Dono, M*., et al.* (2004a). MicroRNA profiling reveals distinct signatures in B cell chronic lymphocytic leukemias. Proceedings of the National Academy of Sciences of the United States of America *101*, 11755-11760.

Calin, G.A., Sevignani, C., Dumitru, C.D., Hyslop, T., Noch, E., Yendamuri, S., Shimizu, M., Rattan, S., Bullrich, F., Negrini, M., and Croce, C.M. (2004b). Human microRNA genes are frequently located at fragile sites and genomic regions involved in cancers. Proceedings of the National Academy of Sciences of the United States of America *101*, 2999-3004.

Carmell, M.A., Girard, A., van de Kant, H.J., Bourc'his, D., Bestor, T.H., de Rooij, D.G., and Hannon, G.J. (2007). MIWI2 is essential for spermatogenesis and repression of transposons in the mouse male germline. Developmental cell *12*, 503-514.

Carmell, M.A., Xuan, Z., Zhang, M.Q., and Hannon, G.J. (2002). The Argonaute family: tentacles that reach into RNAi, developmental control, stem cell maintenance, and tumorigenesis. Genes & development *16*, 2733-2742.

Carthew, R.W. (2006). Gene regulation by microRNAs. Current opinion in genetics & development *16*, 203-208.

Cerutti, L., Mian, N., and Bateman, A. (2000). Domains in gene silencing and cell differentiation proteins: the novel PAZ domain and redefinition of the piwi domain. Trends Biochem Sci *25*, 481-482.

Chalker, D.L., and Yao, M.C. (2001). Nongenic, bidirectional transcription precedes and may promote developmental DNA deletion in Tetrahymena thermophila. Genes & development *15*, 1287-1298.

Chen, J.F., Mandel, E.M., Thomson, J.M., Wu, Q., Callis, T.E., Hammond, S.M., Conlon, F.L., and Wang, D.Z. (2006). The role of microRNA-1 and microRNA-133 in skeletal muscle proliferation and differentiation. Nature genetics *38*, 228-233.

Chendrimada, T.P., Finn, K.J., Ji, X., Baillat, D., Gregory, R.I., Liebhaber, S.A., Pasquinelli, A.E., and Shiekhattar, R. (2007). MicroRNA silencing through RISC recruitment of eIF6. Nature *447*, 823-828.

Chendrimada, T.P., Gregory, R.I., Kumaraswamy, E., Norman, J., Cooch, N., Nishikura, K., and Shiekhattar, R. (2005). TRBP recruits the Dicer complex to Ago2 for microRNA processing and gene silencing. Nature.

Chiu, Y.L., and Rana, T.M. (2003). siRNA function in RNAi: a chemical modification analysis. RNA (New York, N.Y *9*, 1034-1048.

Ciafre, S.A., Galardi, S., Mangiola, A., Ferracin, M., Liu, C.G., Sabatino, G., Negrini, M., Maira, G., Croce, C.M., and Farace, M.G. (2005). Extensive modulation of a set of microRNAs in primary glioblastoma. Biochemical and biophysical research communications *334*, 1351-1358.

Conaco, C., Otto, S., Han, J.J., and Mandel, G. (2006). Reciprocal actions of REST and a microRNA promote neuronal identity. Proceedings of the National Academy of Sciences of the United States of America *103*, 2422-2427.

Cullen, B.R. (2006). Viruses and microRNAs. Nature genetics *38 Suppl*, S25-30.

Dietzl, G., Chen, D., Schnorrer, F., Su, K.C., Barinova, Y., Fellner, M., Gasser, B., Kinsey, K., Oppel, S., Scheiblauer, S.*, et al.* (2007). A genome-wide transgenic RNAi library for conditional gene inactivation in Drosophila. Nature *448*, 151-156.

Dignam, J.D., Lebovitz, R.M., and Roeder, R.G. (1983). Accurate transcription initiation by RNA polymerase II in a soluble extract from isolated mammalian nuclei. Nucleic acids research *11*, 1475-1489.

Doench, J.G., Petersen, C.P., and Sharp, P.A. (2003). siRNAs can function as miRNAs. Genes & development *17*, 438-442.

Doench, J.G., and Sharp, P.A. (2004). Specificity of microRNA target selection in translational repression. Genes & development *18*, 504-511.

Elbashir, S.M., Harborth, J., Lendeckel, W., Yalcin, A., Weber, K., and Tuschl, T. (2001a). Duplexes of 21-nucleotide RNAs mediate RNA interference in mammalian cell culture. Nature *411*, 494-498.

Elbashir, S.M., Lendeckel, W., and Tuschl, T. (2001b). RNA interference is mediated by 21 and 22 nt RNAs. Genes & development *15*, 188-200.

Elbashir, S.M., Martinez, J., Patkaniowska, A., Lendeckel, W., and Tuschl, T. (2001c). Functional anatomy of siRNAs for mediating efficient RNAi in *Drosophila melanogaster* embryo lysate. The EMBO journal *20*, 6877-6888.

Enright, A.J., John, B., Gaul, U., Tuschl, T., Sander, C., and Marks, D. (2003). MicroRNA targets in *Drosophila melanogaster*. Genome Biol, in press.

Filipowicz, W. (2005). RNAi: the nuts and bolts of the RISC machine. Cell *122*, 17-20.

Fire, A., Xu, S., Montgomery, M.K., Kostas, S.A., Driver, S.E., and Mello, C.C. (1998). Potent and specific genetic interference by double-stranded RNA in *Caenorhabditis elegans*. Nature *391*, 806-811.

Forstemann, K., Horwich, M.D., Wee, L., Tomari, Y., and Zamore, P.D. (2007). Drosophila microRNAs are sorted into functionally distinct argonaute complexes after production by dicer-1. Cell *130*, 287-297.

Forstemann, K., Tomari, Y., Du, T., Vagin, V.V., Denli, A.M., Bratu, D.P., Klattenhoff, C., Theurkauf, W.E., and Zamore, P.D. (2005). Normal microRNA Maturation and Germ-Line Stem Cell Maintenance Requires Loquacious, a Double-Stranded RNA-Binding Domain Protein. PLoS Biol *3*, e236.

Fukagawa, T., Nogami, M., Yoshikawa, M., Ikeno, M., Okazaki, T., Takami, Y., Nakayama, T., and Oshimura, M. (2004). Dicer is essential for formation of the heterochromatin structure in vertebrate cells. Nature cell biology *6*, 784-791.

Giraldez, A.J., Cinalli, R.M., Glasner, M.E., Enright, A.J., Thomson, M.J., Baskerville, S., Hammond, S.M., Bartel, D.P., and Schier, A.F. (2005). MicroRNAs Regulate Brain Morphogenesis in Zebrafish. Science (New York, N.Y.

Girard, A., Sachidanandam, R., Hannon, G.J., and Carmell, M.A. (2006). A germline-specific class of small RNAs binds mammalian Piwi proteins. Nature *442*, 199-202.

Gregory, R.I., Chendrimada, T.P., Cooch, N., and Shiekhattar, R. (2005). Human RISC couples microRNA biogenesis and posttranscriptional gene silencing. Cell *123*, 631-640.

Griffiths-Jones, S. (2004). The microRNA Registry. Nucleic acids research *32*, D109-111.

Grimaud, C., Bantignies, F., Pal-Bhadra, M., Ghana, P., Bhadra, U., and Cavalli, G. (2006). RNAi components are required for nuclear clustering of Polycomb group response elements. Cell *124*, 957-971.

Grivna, S.T., Beyret, E., Wang, Z., and Lin, H. (2006a). A novel class of small RNAs in mouse spermatogenic cells. Genes & development *20*, 1709-1714.

Grivna, S.T., Pyhtila, B., and Lin, H. (2006b). MIWI associates with translational machinery and PIWI-interacting RNAs (piRNAs) in regulating spermatogenesis. Proceedings of the National Academy of Sciences of the United States of America *103*, 13415-13420.

Grosshans, H., Johnson, T., Reinert, K.L., Gerstein, M., and Slack, F.J. (2005). The temporal patterning microRNA let-7 regulates several transcription factors at the larval to adult transition in C. elegans. Developmental cell *8*, 321-330.

Guil, S., and Caceres, J.F. (2007). The multifunctional RNA-binding protein hnRNP A1 is required for processing of miR-18a. Nature structural & molecular biology *14*, 591-596.

Gunawardane, L.S., Saito, K., Nishida, K.M., Miyoshi, K., Kawamura, Y., Nagami, T., Siomi, H., and Siomi, M.C. (2007). A slicer-mediated mechanism for repeat-associated siRNA 5' end formation in Drosophila. Science (New York, N.Y *315*, 1587-1590.

Haase, A.D., Jaskiewicz, L., Zhang, H., Laine, S., Sack, R., Gatignol, A., and Filipowicz, W. (2005). TRBP, a regulator of cellular PKR and HIV-1 virus expression, interacts with Dicer and functions in RNA silencing. EMBO reports *6*, 961-967.

Hagan, J.P., and Croce, C.M. (2007). MicroRNAs in carcinogenesis. Cytogenet Genome Res *118*, 252-259.

Haley, B., and Zamore, P.D. (2004). Kinetic analysis of the RNAi enzyme complex. Nature structural & molecular biology *11*, 599-606.

Hamilton, A.J., and Baulcombe, D.C. (1999). A species of small antisense RNA in posttranscriptional gene silencing in plants. Science (New York, N.Y *286*, 950-952.

Hammond, S.M., Boettcher, S., Caudy, A.A., Kobayashi, R., and Hannon, G.J. (2001). Argonaute2, a link between genetic and biochemical analyses of RNAi. Science (New York, N.Y *293*, 1146-1150.

Hanamura, A., Caceres, J.F., Mayeda, A., Franza, B.R., Jr., and Krainer, A.R. (1998). Regulated tissue-specific expression of antagonistic pre-mRNA splicing factors. RNA (New York, N.Y *4*, 430-444.

Hannon, G.J. (2002). RNA interference. Nature *418*, 244-251.

Hannon, G.J., and Rossi, J.J. (2004). Unlocking the potential of the human genome with RNA interference. Nature *431*, 371-378.

Hartig, J.V., Tomari, Y., and Forstemann, K. (2007). piRNAs--the ancient hunters of genome invaders. Genes & development *21*, 1707-1713.

He, L., and Hannon, G.J. (2004). MicroRNAs: small RNAs with a big role in gene regulation. Nat Rev Genet *5*, 522-531.

Houbaviy, H.B., Dennis, L., Jaenisch, R., and Sharp, P.A. (2005). Characterization of a highly variable eutherian microRNA gene. RNA (New York, N.Y *11*, 1245-1257.

Humphreys, D.T., Westman, B.J., Martin, D.I., and Preiss, T. (2005). MicroRNAs control translation initiation by inhibiting eukaryotic initiation factor 4E/cap and poly(A) tail function. Proceedings of the National Academy of Sciences of the United States of America *102*, 16961-16966.

Hutvágner, G., and Zamore, P.D. (2002). A microRNA in a multiple-turnover RNAi enzyme complex. Science (New York, N.Y *297*, 2056-2060.

Jackson, A.L., Burchard, J., Schelter, J., Chau, B.N., Cleary, M., Lim, L., and Linsley, P.S. (2006). Widespread siRNA "off-target" transcript silencing mediated by seed region sequence complementarity. RNA (New York, N.Y *12*, 1179-1187.

Jackson, R.J., and Standart, N. (2007). How do microRNAs regulate gene expression? Sci STKE *2007*, re1.

Jakymiw, A., Lian, S., Eystathioy, T., Li, S., Satoh, M., Hamel, J.C., Fritzler, M.J., and Chan, E.K. (2005). Disruption of GW bodies impairs mammalian RNA interference. Nature cell biology *7*, 1267-1274.

Jiang, F., Ye, X., Liu, X., Fincher, L., McKearin, D., and Liu, Q. (2005). Dicer-1 and R3D1-L catalyze microRNA maturation in Drosophila. Genes & development.

Kalmykova, A.I., Klenov, M.S., and Gvozdev, V.A. (2005). Argonaute protein PIWI controls mobilization of retrotransposons in the Drosophila male germline. Nucleic acids research *33*, 2052-2059.

Kanellopoulou, C., Muljo, S.A., Kung, A.L., Ganesan, S., Drapkin, R., Jenuwein, T., Livingston, D.M., and Rajewsky, K. (2005). Dicer-deficient mouse embryonic stem cells are defective in differentiation and centromeric silencing. Genes & development *19*, 489-501.

Kawahara, Y., Zinshteyn, B., Chendrimada, T.P., Shiekhattar, R., and Nishikura, K. (2007). RNA editing of the microRNA-151 precursor blocks cleavage by the Dicer-TRBP complex. EMBO reports *8*, 763-769.

Kawasaki, H., and Taira, K. (2004). Induction of DNA methylation and gene silencing by short interfering RNAs in human cells. Nature *431*, 211-217.

Ketting, R.F., Fischer, S.E., Bernstein, E., Sijen, T., Hannon, G.J., and Plasterk, R.H. (2001). Dicer functions in RNA interference and in synthesis of small RNA involved in developmental timing in C. elegans. Genes & development *15*, 2654-2659.

Khvorova, A., Reynolds, A., and Jayasena, S.D. (2003). Functional siRNAs and miRNAs exhibit strand bias. Cell *115*, 209-216.

Kim, K., Lee, Y.S., and Carthew, R.W. (2007). Conversion of pre-RISC to holo-RISC by Ago2 during assembly of RNAi complexes. RNA (New York, N.Y *13*, 22-29.

Kim, V.N. (2005). MicroRNA biogenesis: coordinated cropping and dicing. Nat Rev Mol Cell Biol.

Kim, V.N., and Nam, J.W. (2006). Genomics of microRNA. Trends Genet *22*, 165-173.

Kiriakidou, M., Tan, G.S., Lamprinaki, S., De Planell-Saguer, M., Nelson, P.T., and Mourelatos, Z. (2007). An mRNA m7G cap binding-like motif within human Ago2 represses translation. Cell *129*, 1141-1151.

Kloosterman, W.P., and Plasterk, R.H. (2006). The diverse functions of microRNAs in animal development and disease. Developmental cell *11*, 441-450.

Knight, S.W., and Bass, B.L. (2001). A Role for the RNase III Enzyme DCR-1 in RNA Interference and Germ Line Development in C. elegans. Science (New York, N.Y *2*, 2.

Kolb, F.A., Zhang, H., Jaronczyk, K., Tahbaz, N., Hobman, T.C., and Filipowicz, W. (2005). Human dicer: purification, properties, and interaction with PAZ PIWI domain proteins. Methods Enzymol *392*, 316-336.

Krek, A., Grun, D., Poy, M.N., Wolf, R., Rosenberg, L., Epstein, E.J., MacMenamin, P., da Piedade, I., Gunsalus, K.C., Stoffel, M., and Rajewsky, N. (2005). Combinatorial microRNA target predictions. Nature genetics *37*, 495-500.

Lagos-Quintana, M., Rauhut, R., Lendeckel, W., and Tuschl, T. (2001). Identification of novel genes coding for small expressed RNAs. Science (New York, N.Y *294*, 853-858.

Lagos-Quintana, M., Rauhut, R., Meyer, J., Borkhardt, A., and Tuschl, T. (2003). New microRNAs from mouse and human. RNA (New York, N.Y *9*, 175-179.

Lagos-Quintana, M., Rauhut, R., Yalcin, A., Meyer, J., Lendeckel, W., and Tuschl, T. (2002). Identification of Tissue-Specific MicroRNAs from Mouse. Curr Biol *12*, 735-739.

Lai, E.C., Burks, C., and Posakony, J.W. (1998). The K box, a conserved 3' UTR sequence motif, negatively regulates accumulation of enhancer of split complex transcripts. Development (Cambridge, England) *125*, 4077-4088.

Lai, E.C., Tam, B., and Rubin, G.M. (2005). Pervasive regulation of Drosophila Notch target genes by GY-box-, Brd-box-, and K-box-class microRNAs. Genes & development *19*, 1067-1080.

Lau, N.C., Lim, L.P., Weinstein, E.G., and Bartel, D.P. (2001). An abundant class of tiny RNAs with probable regulatory roles in *Caenorhabditis elegans*. Science (New York, N.Y *294*, 858-862.

Lee, R.C., Feinbaum, R.L., and Ambros, V. (1993). The C. elegans heterochronic gene lin-4 encodes small RNAs with antisense complementarity to lin-14. Cell *75*, 843-854.

Lee, Y., Jeon, K., Lee, J.T., Kim, S., and Kim, V.N. (2002). MicroRNA maturation: stepwise processing and subcellular localization. The EMBO journal *21*, 4663-4670.

Lee, Y., Kim, M., Han, J., Yeom, K.H., Lee, S., Baek, S.H., and Kim, V.N. (2004a). MicroRNA genes are transcribed by RNA polymerase II. The EMBO journal *23*, 4051-4060.

Lee, Y.S., Nakahara, K., Pham, J.W., Kim, K., He, Z., Sontheimer, E.J., and Carthew, R.W. (2004b). Distinct roles for Drosophila Dicer-1 and Dicer-2 in the siRNA/miRNA silencing pathways. Cell *117*, 69-81.

Lei, E.P., and Corces, V.G. (2006). RNA interference machinery influences the nuclear organization of a chromatin insulator. Nature genetics *38*, 936-941.

Leuschner, P.J., Ameres, S.L., Kueng, S., and Martinez, J. (2006). Cleavage of the siRNA passenger strand during RISC assembly in human cells. EMBO reports.

Lewis, B.P., Burge, C.B., and Bartel, D.P. (2005). Conserved seed pairing, often flanked by adenosines, indicates that thousands of human genes are microRNA targets. Cell *120*, 15-20.

Lewis, B.P., Shih, I.H., Jones-Rhoades, M.W., Bartel, D.P., and Burge, C.B. (2003). Prediction of mammalian microRNA targets. Cell *115*, 787-798.

Lim, L.P., Glasner, M.E., Yekta, S., Burge, C.B., and Bartel, D.P. (2003a). Vertebrate microRNA genes. Science (New York, N.Y *299*, 1540.

Lim, L.P., Lau, N.C., Weinstein, E.G., Abdelhakim, A., Yekta, S., Rhoades, M.W., Burge, C.B., and Bartel, D.P. (2003b). The microRNAs of *Caenorhabditis elegans*. Genes & development *17*, 991-1008.

Lin, S.Y., Johnson, S.M., Abraham, M., Vella, M.C., Pasquinelli, A., Gamberi, C., Gottlieb, E., and Slack, F.J. (2003). The *C. elegans* hunchback homolog, *hbl-1*, controls temporal patterning and is a probable microRNA target. Developmental cell *4*, 639-650.

Liu, J., Carmell, M.A., Rivas, F.V., Marsden, C.G., Thomson, J.M., Song, J.J., Hammond, S.M., Joshua-Tor, L., and Hannon, G.J. (2004). Argonaute2 Is the Catalytic Engine of Mammalian RNAi. Science (New York, N.Y.

Liu, J., Valencia-Sanchez, M.A., Hannon, G.J., and Parker, R. (2005). MicroRNA-dependent localization of targeted mRNAs to mammalian P-bodies. Nature cell biology *7*, 719-723.

Lu, J., Getz, G., Miska, E.A., Alvarez-Saavedra, E., Lamb, J., Peck, D., Sweet-Cordero, A., Ebert, B.L., Mak, R.H., Ferrando, A.A.*, et al.* (2005). MicroRNA expression profiles classify human cancers. Nature *435*, 834-838.

Lund, E., Guttinger, S., Calado, A., Dahlberg, J.E., and Kutay, U. (2004). Nuclear export of microRNA precursors. Science (New York, N.Y *303*, 95-98.

Manche, L., Green, S.R., Schmedt, C., and Mathews, M.B. (1992). Interactions between double-stranded RNA regulators and the protein kinase DAI. Mol Cell Biol *12*, 5238-5248.

Maniataki, E., and Mourelatos, Z. (2005). A human, ATP-independent, RISC assembly machine fueled by pre-miRNA. Genes & development *19*, 2979-2990.

Maroney, P.A., Yu, Y., Fisher, J., and Nilsen, T.W. (2006). Evidence that microRNAs are associated with translating messenger RNAs in human cells. Nature structural & molecular biology *13*, 1102-1107.

Martinez, J., Patkaniowska, A., Urlaub, H., Lührmann, R., and Tuschl, T. (2002a). Single-stranded antisense siRNAs guide target RNA cleavage in RNAi. Cell *110*, 563-574.

Martinez, J., and Tuschl, T. (2004). RISC is a 5' phosphomonoester-producing RNA endonuclease. Genes & development *18*, 975-980.

Martinez, L.A., Naguibneva, I., Lehrmann, H., Vervisch, A., Tchenio, T., Lozano, G., and Harel-Bellan, A. (2002b). Synthetic small inhibiting RNAs: efficient tools to inactivate oncogenic mutations and restore p53 pathways. Proceedings of the National Academy of Sciences of the United States of America *99*, 14849-14854.

Matranga, C., Tomari, Y., Shin, C., Bartel, D.P., and Zamore, P.D. (2005). Passenger-strand cleavage facilitates assembly of siRNA into Ago2-containing RNAi enzyme complexes. Cell *123*, 607-620.

Matzke, M.A., and Birchler, J.A. (2005). RNAi-mediated pathways in the nucleus. Nat Rev Genet *6*, 24-35.

Meister, G., Landthaler, M., Patkaniowska, A., Dorsett, Y., Teng, G., and Tuschl, T. (2004). Human Argonaute2 mediates RNA cleavage targeted by miRNAs and siRNAs. Molecular cell *15*, 185-197.

Mette, M.F., Aufsatz, W., van der Winden, J., Matzke, M.A., and Matzke, A.J.M. (2000). Transcriptional silencing and promoter methylation triggered by double-stranded RNA. The EMBO journal *19*, 5194-5201.

Miyoshi, K., Tsukumo, H., Nagami, T., Siomi, H., and Siomi, M.C. (2005). Slicer function of Drosophila Argonautes and its involvement in RISC formation. Genes & development *19*, 2837-2848.

Mochizuki, K., Fine, N.A., Fujisawa, T., and Gorovsky, M.A. (2002). Analysis of a piwi-related gene implicates small RNAs in genome rearrangement in tetrahymena. Cell *110*, 689-699.

Mochizuki, K., and Gorovsky, M.A. (2004). Conjugation-specific small RNAs in Tetrahymena have predicted properties of scan (scn) RNAs involved in genome rearrangement. Genes & development *18*, 2068-2073.

Mochizuki, K., and Gorovsky, M.A. (2005). A Dicer-like protein in Tetrahymena has distinct functions in genome rearrangement, chromosome segregation, and meiotic prophase. Genes & development *19*, 77-89.

Motamedi, M.R., Verdel, A., Colmenares, S.U., Gerber, S.A., Gygi, S.P., and Moazed, D. (2004). Two RNAi Complexes, RITS and RDRC, Physically Interact and Localize to Noncoding Centromeric RNAs. Cell *119*, 789-802.

Murchison, E.P., and Hannon, G.J. (2004). miRNAs on the move: miRNA biogenesis and the RNAi machinery. Curr Opin Cell Biol *16*, 223-229.

Naguibneva, I., Ameyar-Zazoua, M., Polesskaya, A., Ait-Si-Ali, S., Groisman, R., Souidi, M., Cuvellier, S., and Harel-Bellan, A. (2006). The microRNA miR-181 targets the homeobox protein Hox-A11 during mammalian myoblast differentiation. Nature cell biology *8*, 278-284.

Napoli, C., Lemieux, C., and Jorgensen, R. (1990). Introduction of a Chimeric Chalcone Synthase Gene into Petunia Results in Reversible Co-Suppression of Homologous Genes in trans. Plant Cell *2*, 279-289.

Noma, K., Sugiyama, T., Cam, H., Verdel, A., Zofall, M., Jia, S., Moazed, D., and Grewal, S.I. (2004). RITS acts in cis to promote RNA interference-mediated transcriptional and post-transcriptional silencing. Nature genetics *36*, 1174-1180.

Nottrott, S., Simard, M.J., and Richter, J.D. (2006). Human let-7a miRNA blocks protein production on actively translating polyribosomes. Nature structural & molecular biology *13*, 1108-1114.

Novina, C.D., and Sharp, P.A. (2004). The RNAi revolution. Nature *430*, 161-164.

Obernosterer, G., Leuschner, P.J., Alenius, M., and Martinez, J. (2006). Post-transcriptional regulation of microRNA expression. RNA (New York, N.Y *12*, 1161-1167.

Okamura, K., Hagen, J.W., Duan, H., Tyler, D.M., and Lai, E.C. (2007). The mirtron pathway generates microRNA-class regulatory RNAs in Drosophila. Cell *130*, 89-100.

Olsen, P.H., and Ambros, V. (1999). The lin-4 regulatory RNA controls developmental timing in Caenorhabditis elegans by blocking LIN-14 protein synthesis after the initiation of translation. Dev Biol *216*, 671-680.

Parker, J.S., Roe, S.M., and Barford, D. (2004). Crystal structure of a PIWI protein suggests mechanisms for siRNA recognition and slicer activity. The EMBO journal *23*, 4727-4737.

Pasquinelli, A.E., Reinhart, B.J., Slack, F., Martindale, M.Q., Kuroda, M.I., Maller, B., Hayward, D.C., Ball, E.E., Degnan, B., Muller, P.*, et al.* (2000). Conservation of the sequence and temporal expression of let-7 heterochronic regulatory RNA. Nature *408*, 86-89.

Peters, L., and Meister, G. (2007). Argonaute proteins: mediators of RNA silencing. Molecular cell *26*, 611-623.

Petersen, C.P., Bordeleau, M.E., Pelletier, J., and Sharp, P.A. (2006). Short RNAs repress translation after initiation in mammalian cells. Molecular cell *21*, 533-542.

Pfeffer, S., Zavolan, M., Grasser, F.A., Chien, M., Russo, J.J., Ju, J., John, B., Enright, A.J., Marks, D., Sander, C., and Tuschl, T. (2004). Identification of virus-encoded microRNAs. Science (New York, N.Y *304*, 734-736.

Pham, J.W., Pellino, J.L., Lee, Y.S., Carthew, R.W., and Sontheimer, E.J. (2004). A Dicer-2-dependent 80s complex cleaves targeted mRNAs during RNAi in Drosophila. Cell *117*, 83-94.

Pillai, R.S., Bhattacharyya, S.N., Artus, C.G., Zoller, T., Cougot, N., Basyuk, E., Bertrand, E., and Filipowicz, W. (2005). Inhibition of translational initiation by Let-7 MicroRNA in human cells. Science (New York, N.Y *309*, 1573-1576.

Pillai, R.S., Bhattacharyya, S.N., and Filipowicz, W. (2007). Repression of protein synthesis by miRNAs: how many mechanisms? Trends in cell biology *17*, 118-126.

Poy, M.N., Eliasson, L., Krutzfeldt, J., Kuwajima, S., Ma, X., Macdonald, P.E., Pfeffer, S., Tuschl, T., Rajewsky, N., Rorsman, P., and Stoffel, M. (2004). A pancreatic islet-specific microRNA regulates insulin secretion. Nature *432*, 226-230.

Provost, P., Dishart, D., Doucet, J., Frendewey, D., Samuelsson, B., and Radmark, O. (2002). Ribonuclease activity and RNA binding of recombinant human Dicer. The EMBO journal *21*, 5864-5874.

Rand, T.A., Petersen, S., Du, F., and Wang, X. (2005). Argonaute2 cleaves the anti-guide strand of siRNA during RISC activation. Cell *123*, 621-629.

Rehmsmeier, M., Steffen, P., Hochsmann, M., and Giegerich, R. (2004). Fast and effective prediction of microRNA/target duplexes. RNA (New York, N.Y *10*, 1507-1517.

Reinhart, B.J., Slack, F.J., Basson, M., Pasquinelli, A.E., Bettinger, J.C., Rougvie, A.E., Horvitz, H.R., and Ruvkun, G. (2000). The 21-nucleotide let-7 RNA regulates developmental timing in Caenorhabditis elegans. Nature *403*, 901-906.

Reinhart, B.J., Weinstein, E.G., Rhoades, M.W., Bartel, B., and Bartel, D.P. (2002). MicroRNAs in plants. Genes & development *16*, 1616-1626.

Reynolds, A., Leake, D., Boese, Q., Scaringe, S., Marshall, W.S., and Khvorova, A. (2004). Rational siRNA design for RNA interference. Nat Biotechnol *22*, 326-330.

Ritchie, W., Legendre, M., and Gautheret, D. (2007). RNA stem-loops: to be or not to be cleaved by RNAse III. RNA (New York, N.Y *13*, 457-462.

Rivas, F.V., Tolia, N.H., Song, J.J., Aragon, J.P., Liu, J., Hannon, G.J., and Joshua-Tor, L. (2005). Purified Argonaute2 and an siRNA form recombinant human RISC. Nature structural & molecular biology *12*, 340-349.

Robb, G.B., and Rana, T.M. (2007). RNA helicase A interacts with RISC in human cells and functions in RISC loading. Molecular cell *26*, 523-537.

Saito, K., Nishida, K.M., Mori, T., Kawamura, Y., Miyoshi, K., Nagami, T., Siomi, H., and Siomi, M.C. (2006). Specific association of Piwi with rasiRNAs derived from retrotransposon and heterochromatic regions in the Drosophila genome. Genes & development *20*, 2214-2222.

Sarot, E., Payen-Groschene, G., Bucheton, A., and Pelisson, A. (2004). Evidence for a piwi-dependent RNA silencing of the gypsy endogenous retrovirus by the Drosophila melanogaster flamenco gene. Genetics *166*, 1313-1321.

Schratt, G.M., Tuebing, F., Nigh, E.A., Kane, C.G., Sabatini, M.E., Kiebler, M., and Greenberg, M.E. (2006). A brain-specific microRNA regulates dendritic spine development. Nature *439*, 283-289.

Schwarz, D.S., Tomari, Y., and Zamore, P.D. (2004). The RNA-induced silencing complex is a Mg2+-dependent endonuclease. Curr Biol *14*, 787-791.

Sen, G.L., and Blau, H.M. (2005). Argonaute 2/RISC resides in sites of mammalian mRNA decay known as cytoplasmic bodies. Nature cell biology *7*, 633-636.

Siegel, L.M., and Monty, K.J. (1966). Determination of molecular weights and frictional ratios of proteins in impure systems by use of gel filtration and density gradient centrifugation. Application to crude preparations of sulfite and hydroxylamine reductases. Biochimica et biophysica acta *112*, 346-362.

Sokol, N.S., and Ambros, V. (2005). Mesodermally expressed Drosophila microRNA-1 is regulated by Twist and is required in muscles during larval growth. Genes & development *19*, 2343-2354.

Song, J.J., Smith, S.K., Hannon, G.J., and Joshua-Tor, L. (2004). Crystal Structure of Argonaute and Its Implications for RISC Slicer Activity. Science (New York, N.Y.

Stark, G.R., Kerr, I.M., Williams, B.R., Silverman, R.H., and Schreiber, R.D. (1998). How cells respond to interferons. Annu Rev Biochem *67*, 227-264.

Tahbaz, N., Kolb, F.A., Zhang, H., Jaronczyk, K., Filipowicz, W., and Hobman, T.C. (2004). Characterization of the interactions between mammalian PAZ PIWI domain proteins and Dicer. EMBO reports *5*, 189-194.

Takamizawa, J., Konishi, H., Yanagisawa, K., Tomida, S., Osada, H., Endoh, H., Harano, T., Yatabe, Y., Nagino, M., Nimura, Y*., et al.* (2004). Reduced expression of the let-7 microRNAs in human lung cancers in association with shortened postoperative survival. Cancer research *64*, 3753-3756.

Taverna, S.D., Coyne, R.S., and Allis, C.D. (2002). Methylation of histone h3 at lysine 9 targets programmed DNA elimination in tetrahymena. Cell *110*, 701-711.

Teleman, A.A., Maitra, S., and Cohen, S.M. (2006). Drosophila lacking microRNA miR-278 are defective in energy homeostasis. Genes & development *20*, 417-422.

Thomson, J.M., Newman, M., Parker, J.S., Morin-Kensicki, E.M., Wright, T., and Hammond, S.M. (2006). Extensive post-transcriptional regulation of microRNAs and its implications for cancer. Genes & development *20*, 2202-2207.

Tomari, Y., Du, T., and Zamore, P.D. (2007). Sorting of Drosophila small silencing RNAs. Cell *130*, 299-308.

Tomari, Y., Matranga, C., Haley, B., Martinez, N., and Zamore, P.D. (2004). A protein sensor for siRNA asymmetry. Science (New York, N.Y *306*, 1377-1380.

Tomari, Y., and Zamore, P.D. (2005). Perspective: machines for RNAi. Genes & development *19*, 517-529.

Tuddenham, L., Wheeler, G., Ntounia-Fousara, S., Waters, J., Hajihosseini, M.K., Clark, I., and Dalmay, T. (2006). The cartilage specific microRNA-140 targets histone deacetylase 4 in mouse cells. FEBS letters *580*, 4214-4217.

Vagin, V.V., Sigova, A., Li, C., Seitz, H., Gvozdev, V., and Zamore, P.D. (2006). A distinct small RNA pathway silences selfish genetic elements in the germline. Science (New York, N.Y *313*, 320-324.

Valencia-Sanchez, M.A., Liu, J., Hannon, G.J., and Parker, R. (2006). Control of translation and mRNA degradation by miRNAs and siRNAs. Genes & development *20*, 515-524.

van der Krol, A.R., Mur, L.A., Beld, M., Mol, J.N., and Stuitje, A.R. (1990). Flavonoid genes in petunia: addition of a limited number of gene copies may lead to a suppression of gene expression. Plant Cell *2*, 291-299.

van Rooij, E., Sutherland, L.B., Liu, N., Williams, A.H., McAnally, J., Gerard, R.D., Richardson, J.A., and Olson, E.N. (2006). A signature pattern of stress-responsive microRNAs that can evoke cardiac hypertrophy and heart failure. Proceedings of the National Academy of Sciences of the United States of America *103*, 18255-18260.

Verdel, A., Jia, S., Gerber, S., Sugiyama, T., Gygi, S., Grewal, S.I., and Moazed, D. (2004). RNAi-mediated targeting of heterochromatin by the RITS complex. Science (New York, N.Y *303*, 672-676.

Vo, N., Klein, M.E., Varlamova, O., Keller, D.M., Yamamoto, T., Goodman, R.H., and Impey, S. (2005). A cAMP-response element binding protein-induced microRNA regulates neuronal morphogenesis. Proceedings of the National Academy of Sciences of the United States of America *102*, 16426-16431.

Volinia, S., Calin, G.A., Liu, C.G., Ambs, S., Cimmino, A., Petrocca, F., Visone, R., Iorio, M., Roldo, C., Ferracin, M*., et al.* (2006). A microRNA expression signature of human solid tumors defines cancer gene targets. Proceedings of the National Academy of Sciences of the United States of America *103*, 2257-2261.

Volpe, T.A., Kidner, C., Hall, I.M., Teng, G., Grewal, S.I., and Martienssen, R.A. (2002). Regulation of heterochromatic silencing and histone H3 lysine-9 methylation by RNAi. Science (New York, N.Y *297*, 1833-1837.

Wassenegger, M., Heimes, S., Riedel, L., and Sanger, H.L. (1994). RNA-directed de novo methylation of genomic sequences in plants. Cell *76*, 567-576.

Watanabe, T., Totoki, Y., Sasaki, H., Minami, N., and Imai, H. (2007). Analysis of Small RNA Profiles During Development. Methods Enzymol *427C*, 155-169.

Wightman, B., Ha, I., and Ruvkun, G. (1993). Posttranscriptional regulation of the heterochronic gene *lin-14* by *lin-4* mediates temporal pattern formation in *C. elegans*. Cell *75*, 855-862.

Windbichler, N., and Schroeder, R. (2006). Isolation of specific RNA-binding proteins using the streptomycin-binding RNA aptamer. Nature protocols *1*, 637-640.

Wintersberger, U. (1990). Ribonucleases H of retroviral and cellular origin. Pharmacology & therapeutics *48*, 259-280.

Yanaihara, N., Caplen, N., Bowman, E., Seike, M., Kumamoto, K., Yi, M., Stephens, R.M., Okamoto, A., Yokota, J., Tanaka, T*., et al.* (2006). Unique microRNA molecular profiles in lung cancer diagnosis and prognosis. Cancer cell *9*, 189-198.

Yang, W., Chendrimada, T.P., Wang, Q., Higuchi, M., Seeburg, P.H., Shiekhattar, R., and Nishikura, K. (2006). Modulation of microRNA processing and expression through RNA editing by ADAR deaminases. Nature structural & molecular biology *13*, 13-21.

Yao, M.C., Fuller, P., and Xi, X. (2003). Programmed DNA deletion as an RNA-guided system of genome defense. Science (New York, N.Y *300*, 1581-1584.

Yekta, S., Shih, I.H., and Bartel, D.P. (2004). MicroRNA-directed cleavage of HOXB8 mRNA. Science (New York, N.Y *304*, 594-596.

Yigit, E., Batista, P.J., Bei, Y., Pang, K.M., Chen, C.C., Tolia, N.H., Joshua-Tor, L., Mitani, S., Simard, M.J., and Mello, C.C. (2006). Analysis of the C. elegans Argonaute family reveals that distinct Argonautes act sequentially during RNAi. Cell *127*, 747-757.

Zhang, H., Kolb, F.A., Jaskiewicz, L., Westhof, E., and Filipowicz, W. (2004). Single processing center models for human Dicer and bacterial RNase III. Cell *118*, 57-68.

Zhao, Y., Samal, E., and Srivastava, D. (2005). Serum response factor regulates a muscle-specific microRNA that targets Hand2 during cardiogenesis. Nature *436*, 214-220.

Zhou, X., Ruan, J., Wang, G., and Zhang, W. (2007). Characterization and identification of microRNA core promoters in four model species. PLoS computational biology *3*, e37.

8. Abbreviations

ADAR	Adenosine deaminases acting on RNA
b	base(s)
bp	basepair(s)
BSA	bovine serum albumine
CV	column volume
DNA	deoxyribonucleic acid
dsRBD	double stranded RNA binding domain
dsRNA	double-stranded RNA
min	minute(s)
miRISC	miRNA-associated RISC
miRNA	microRNA
mRNA	messenger RNA
Mw	molecular weight
ncRNA	non-coding RNA
nt	nucleotide(s)
p-bodies	processing bodies
PCR	polymerase chain reaction
pRNAs	PIWI-associated RNAs
RISC	RNA induced silencing complex
RITS	RNA-Induced Initiation of Transcriptional gene Silencing
RLC	RISC loading complex
RNA	ribonucleic acid
RNAi	RNA interference
rpm	revolutions per minute
r_s	Stoke's radius
siRNA	short interfering RNA
siRISC	siRNA-associated RISC
ssRNA	single stranded RNA
TCA	trichloroacetic acid
UTR	untranslated region

9. Acknowledgements

First, I would like to thank my supervisor Javier Martinez for giving me the opportunity to work as the first PhD student in his laboratory, for his assistance, constant support and encouragement throughout my projects. I learned a lot during these three years, not only at the bench, but also the famous "soft skills" in order to succeed in the scientific field. The time was terrific and passed flying.

I also want to thank the Boehringer Ingelheim Fonds for supporting and funding my research that went far beyond just paying my salaries. Thank you for covering my travel expenses to international meetings, for organizing great seminars and workshops, from which I could profit a lot, and for giving me the feeling, to be part of a scientific family.

I want to thank everyone in the Martinez lab for providing and maintaining such a great and stimulating atmosphere. Gregor and Stefan, lab members from the first day, too, who plunged into the "cold water" of a lab that still had to be established back then. Dubravka and Katrin, for breaking the sonic Y-chromosome barrier in our lab and for all the fun; Jutta, for keeping our mess organized in the lab and providing a great infrastructure; Christoph, who switched from the IMP, for fruitful and hilarious discussions; Anne, who spent a summer internship in our lab and contributed considerably to the miR-138 project; Jana, the second diploma student under my supervision, for continuing the projects during the time I was writing this thesis; Andrea, for repeatedly providing jamón ibérico to our lab.

I would also like to acknowledge Heiko Manninga and the Lührmann lab in Göttingen, for generously providing huge amounts of HeLa cytoplasmic extracts that allowed our chromatographic purifications attempts.

A very big thank you goes to my family for their constant and unconditional support in any imaginable way throughout now nearly 28 years.

And finally I want to thank my wife Barbara, who was always at my side these three years, for her constant support, her understanding, her unswerving belief in me and for filling my life with love and joy.

10. Curriculum Vitae

Philipp Leuschner
Institute of Molecular Biotechnology
Dr.-Bohr-Gasse 3-5
1030 Vienna, Austria

fon: +43 1 79044 4858
fax: +43 1 79044 110
http://www.imba.oeaw.ac.at
philipp.leuschner@imba.oeaw.ac.at

Education

- **IMBA, Institute of Molecular Biotechnology** — Vienna, Austria
  PhD student, Molecular Biology — *since Oct. 2004*

- **University of Vienna** — Vienna, Austria
  M.Sc. with distinction, Genetics — *Oct. 1998 – Oct. 2003*
  - Thesis: *Balance Between Renewal And Differentiation Of Erythroid Cells: Role Of The Glucocorticoid Receptor*
  - Minors: Theoretical Chemistry, Biochemistry

- **Bundesgymnasium Oberschützen** — Oberschützen, Austria
  Matura with distinction — *Sep. 1990 – Jun. 1998*

Research And Professional Experience

- **IMBA, Institute of Molecular Biotechnology** — Vienna, Austria
  Graduate School Student — *since Oct. 2004*
  - Regulation of microRNA-biogenesis and -expression:
    (a) We have discovered that differential, context-dependent processing of the miR-138-2 precursor hairpin confers tissue- and developmental stage-specific expression of the mature miR-138 to the otherwise ubiquitously transcribed *mi*R-*138-2* gene.
    (b) We are currently investigating the factor responsible for the context-dependent processing of pre-miR-138-2 by classical chromatography and mass spectrometry. Structure/function analyses revealed that an internal loop of the precursor RNA hairpin is responsible for its recognition by the factor.
  - miRNA function:
    (a) In collaboration with Hartmut Beug's lab at the IMP Vienna, we have conducted a miRNA expression profiling and identified miRNAs that are regulated during epithelial-to-mesenchymal transition as a correlate of metastasis.
    (b) We are generating transgenic mice to investigate the role of miR-138 in neuronal plasticity and fetal liver hematopoiesis.
  - Assembly of RISC:
    We demonstrated that passenger strand cleavage is a crucial step for its release during the assembly phase of RISC on an siRNA duplex.

- **IMP, Institute of Pathology** — Vienna, Austria
  Undergraduate School Student — *Jun. 2002 – Jun. 2003*
  Regulation of Erythroid Cell Differentiation:
  In the laboratory of Dr. Hartmut Beug I was investigating the role of the glucocorticoid receptor in the fate decision of erythroblasts to either undergo terminal differentiation or to self-renew. I was working with transgenic mice and primary erythroblasts isolated from fetal liver or adult spleen.

Publications

Leuschner PJ, Martinez J, *In vitro analysis of microRNA processing using recombinant Dicer and cytoplasmic extracts of HeLa cells.* Methods. 2007 Oct;43(2):105-9

Nielsen AF, Leuschner PJ, Martinez J., *Not miR-ly a splicing factor: hnRNP A1 succumbs to microRNA temptation.* Nat Struct Mol Biol. 2007 Jul;14(7):572-3. Review.

Obernosterer G*, Leuschner PJ*, Alenius M*, Martinez J., *Post-transcriptional regulation of microRNA expression.* RNA. 2006 Jul;12(7):1161-7.

Leuschner PJ, Ameres SL, Kueng S, Martinez J., *Cleavage of the siRNA passenger strand during RISC assembly in human cells.* EMBO Rep. 2006 Mar;7(3):314-20

Leuschner PJ, Obernosterer G, Martinez J., *MicroRNAs: Loquacious speaks out.* Curr Biol. 2005 Aug 9;15(15):R603-5. Review.

* equal contribution

Conference Contributions

Leuschner P, Obernosterer G, Alenius M, Martinez J, *How to restrict microRNA expression to specific tissues.* Keystone Symposia, Keystone, CO, USA, Feb 2007 (poster).

A New Twist In microRNA-Biogenesis: Processing makes a difference.
Fourth International Boston RNAi meeting, Waltham, MA, USA, May 2006.
Poster abstract selected for oral presentation.

Post-transcriptional regulation of tissue specific miRNA expression.
Cold Spring Harbor Laboratories Conference on RNAi, Cold Spring Harbor, NY, USA, Oct 2005.
Poster abstract selected for oral presentation.

Leuschner P, Obernosterer G, Martinez J, *Post-transcriptional regulation of tissue specific miRNA expression.* IMP-IMBA Spring Conference, Vienna, Austria, May 2005 (poster).

Teaching

Advanced Cell Biology, University of Vienna, 2007
Advanced Cell Biology, University of Vienna, 2006

Awards And Scholarships

Boehringer Ingelheim Fonds PhD Scholarship, Oct. 2005 – Oct. 2007
Validation and characterization of miRNA-dependent regulation of gene expression.

Interests

Sports: Rock climbing and mountaineering
Music: Jazz (Puschnig, Muthspiel)